## TNO innovation for life

**TNO report**

**TNO 2015 R10160 | Final report**

# Corrosion in Dutch geothermal systems

| | |
|---|---|
| Date | 15 Mar 2016 |
| Author(s) | J.G. Veldkamp, T.V. Goldberg, P.M.M.C. Bressers, F. Wilschut |
| Copy no | |
| No. of copies | |
| Number of pages | 105 (incl. appendices) |
| Number of appendices | 3 |
| Sponsor | Energie combinatie Middenmeer ECW, GeoPower Oudcamp VOF, Green Well Westland BV, A.C. Hartman BV, IF Technology, Aardwarmte de Lier, Nature's Heat, Aardwarmte Vogelaer VOF, Kwekerij de Wieringermeer, Pieter Wijnen Egchel BV, Twan Wijnen Egchel BV, A+G van den Bosch BV, Gebr. Duijvestijn |
| Project name | IPC Geothermie 2.0 - part I: Corrosion |
| Project number | 060.06962 |

**RESTRICTED**

# Summary

Ensuring that the integrity of geothermal installations is sustained is one of the biggest concerns in the geothermal industry. In geothermal installations steel is used as construction material. It is a well-known fact that corrosion can degrade steel. Corrosion can occur when steel in geothermal installations comes in contact with brine (formation water). This can result in the gradual degradation of metal, or, in the case of pitting corrosion, extremely fast degradation. Corrosion can occur hand in hand with scaling in case corrosion products enhance the precipitation of different minerals. Corrosion that threatens the integrity of the doublet system can increase the risk of leakage of the produced or injected brine to other aquifers as well. It can also result in increased cost due to non-availability of the sustainable energy production and expensive repair work. This report describes the causes and effects of corrosion (and scaling) within geothermal installations, as well as means to identify and prevent corrosion. This report aims to support the establishment of a Well Integrity Management program for geothermal wells by answering the following questions:

- Can corrosion of unprotected steel be expected?
- Is it reasonable to expect that conditions exist where corrosion in geothermal wells is limited by natural protection mechanisms like oil films or iron carbonate scaling?
- At which locations in a geothermal well can the corrosion rate be expected to be relatively high and / or low?
- In which ways can the corrosion rate be lowered, either by design, or by the application of inhibitors?
- If corrosion should be expected, which monitoring techniques are available / effective / achievable / applicable?

**Theory of corrosion**
The most relevant types of corrosion are general or **uniform corrosion** (including galvanic), **localised corrosion**, **erosion corrosion** and **environmentally induced cracking.** Localised corrosion includes pitting, crevice corrosion and filiform corrosion. Causes of corrosion are the presence of **oxidizing elements** in the formation water like oxygen, carbon dioxide[1], hydrogen sulphide, chloride, ammonia, sulphate and hydrogen ions. Carbon dioxide is the most important oxidizing element for the Dutch doublets. Galvanic corrosion takes place when two metals with different potentials are in contact with each other and with formation water. Erosion corrosion takes place at high flow rates and/or fines.

**Assessment of corrosion potential**
The most relevant parameters for assessing the corrosion potential of an installation are the **formation water and gas chemistry** (and, related, the pH, TDS), **temperature** and **pressure,** and **steel or alloy type**. Water and gas chemistry samples are routinely measured after drilling has finished.

---

[1] Technically, hydrogen ions (protons) formed by the dissolution of $CO_2$ in the water are the oxidizing elements

Formation water chemistry may vary drastically on short distance due to varying geological circumstances. There is a general tendency of increasing salinity with depth. The gas chemistry is extremely important, as dissolved $CO_2$ is the most important oxidizing element. Other oxidizing elements such as $O_2$ and $H_2S$ are in principle absent in Dutch doublets. $H_2S$ has not been detected yet in Dutch geothermal installations. Oxygen ($O_2$) is not present in the produced anaerobic brine and oxygen entrance into the system can normally be avoided. $CO_2$ concentrations measured in geothermal wells at varying locations along the installation vary strongly. Partly this is due to varying sampling strategies. The majority of $CO_2$ concentrations measured in geothermal wells is significantly higher than those measured in gas fields, giving rise to higher $CO_2$ corrosion risk in geothermal wells, when compared to gas wells. This may be due to inherent differences between free and dissolved gas. It is strongly suggested to develop standardized brine and gas sampling methods to increase the reliability and accuracy of the measurements. Generally, there is a positive correlation between temperature and corrosion rate in the temperature range that is relevant for the current Dutch doublets. Pourbaix diagrams predict the stable phases (solid or in solution), for varying pH and electric potential for a given mixture of chemical compounds (e.g., iron in water, or iron and carbon dioxide in water), at a given temperature. The alloy type also strongly influences the corrosion potential.
For casings, usually low grade carbon steel types, also known as 'mild steel', are used, like K55, N80, L80 and P110. They are more susceptible to general corrosion than high grade steel types like stainless steel, chrome steel and nickel alloys, but the latter are far more expensive and can be susceptible for pitting. The material choice is a trade-off between cost and durability.

**Corrosion prediction models**
Corrosion prediction models have been developed mainly by the oil and gas industry for several decades. Two major different types exist, empirical and mechanistic models. **Empirical models** are based on interpolations and regressions of laboratory and field measurements and have limited theoretical background. These models cannot be used for extrapolation beyond the limits of the data they were based on. **Mechanistic models** have a strong theoretical approach and describe the underlying (electro-)chemical reactions and transport processes. The underlying chemical processes, as well as the interaction with scaling, are very complex and still not completely understood. Further differences between the models relate to the way that different processes are taken into account, like the effects of protective scaling, oil and water wetting, multi-phase flow etc. As most models were developed for the oil and gas industry, where oil or gas is the dominant phase, their applicability to geothermal is limited, and the results always uncertain.

**Corrosion prevention**
Various corrosion prevention measurements can be taken. **Naturally occurring inhibitors** like oil and oily substances may form a barrier between the steel and the oxidizing agent. Synthetic inhibitors can be grouped into those that form impermeable films, those that form bonds with oxidizing agents and those that displace those agents. **Anodic inhibitors** act by forming a protective oxide film on the surface of the metal. **Cathodic inhibitors** act by either slowing the cathodic reaction itself or selectively precipitating on the area on the steel where the reduction takes place.

Many different types (and brands) of inhibitors exist, each with its own applicability window in terms of brine composition, salinity, temperature and acidity. The dose is usually best determined experimentally. Application of the inhibitor is best executed in such a way that the entire system is covered. This could mean that it is applied at the bottom of the production well. Scales sometimes form by precipitation of minerals from the brine, possibly in combination with corrosion, like for instance the formation of the iron carbonate siderite. This type of scales can be either protective or non-protective. **Passive cathodic protection** safeguards the steel by putting it in electrical contact with a lower nobility material, like zinc. In such a way, zinc is corroded rather than the more noble casing steel. With **active cathodic protection**, an anode is placed close to the steel surface that needs to be protected and an external voltage is applied between the iron substrate and the anode in order to create an electrochemical reaction at the anode, but protecting the iron. **Galvanic corrosion** can be prevented by avoiding electrical contact of dissimilar metals by electrically separating them with an insulating material or by physically insulating the environment from the metal surface. Smart operating strategies and good maintenance ((e.g. the use of oxygen scavengers) can be applied to keep the system oxygen free.

**Corrosion monitoring and measurements**
General and $CO_2$ corrosion is likely to have a higher rate in (parts of) the production well where the temperature is higher, the pH lower and free $CO_2$ is possible present. Corrosion in the wells is difficult to detect visually, or monitor continuously (uniform corrosion along the casing segments, crevice corrosion at irregularities such as connectors etc., and top-of-line corrosion above the fluid level). Corrosion can eventually cause leaks in the casing. This will then result in changed pressures and temperatures. Pressure and temperature is monitored continuously at the surface. Various wireline tools exist that can measure the integrity of the casing, like caliper, ultrasonic tools and electro-magnetic. Corrosion coupons can be applied in the surface system (or even downhole) to measure the corrosion rate. One should note however that tests executed at surface conditions may give different results compared to tests at subsurface conditions (temperature, changed chemistry due to degassing, etc.). Corrosion experiments can be conducted at surface level on site by using bypasses. Laboratory experiments can be conducted if care is taken to mimic the in situ circumstances (pressure, temperature, chemistry, time).

**Examples of corrosion control methods abroad**
Experience with corrosion prevention abroad shows that successful mitigation of corrosion starts with good design and execution combined with long-lasting monitoring in the surface system (and the laboratory). The corrosion rate may change quickly in the course of time due to the formation of protective scales, especially in the first days or weeks. Scales may either be protective, or not, depending on the formation process. This behaviour can change in time.
Good results have been achieved in France using fiberglass and coated completions, in combination with downhole inhibitor addition. This implies that corrosion prevention should already be accommodated during the well design phase. While degassing may be beneficial from a technical and/or financial point of view (if the gas contains a major component of natural gas), it changes the brine composition. This may have undesired effects in the injection well, especially scaling. Some German authors therefore advise against degassing.

Good results have also been achieved by dosing corrosion inhibitor. The selection and dosing of the best inhibitor is often a matter of trial-and-error.

The most important conclusions of the project are that:

- Uniform and crevice corrosion of unprotected steel should be expected due to the occurrence of $CO_2$ in most doublets.
- Rough estimates of the uniform $CO_2$ corrosion that do not take inhibition into account are up to several mm per year. It should be noted that the estimated corrosion rate is based on models that were not validated for geothermal service. The calculated rates are therefore very uncertain as long as field data are unavailable.
- Corrosion in some geothermal wells will be limited by the occurrence of natural oil. It is unknown whether the oil water ratio will remain constant over time. Precipitation of iron carbonates may also offer 'natural' protection against corrosion. The degree of protection depends on many operational factors.
- The corrosion risk is highest in the production well. If the brine is degassed, the corrosion risk in the surface system and the injection well is reduced.
- Inhibitors can significantly reduce the corrosion rate. They can be applied downhole to offer full protection of the system. The dosing should be determined experimentally. The dosing may change during the operational lifetime. The choice of the correct inhibitor depends on operational parameters like brine composition, pH and temperature.

# Contents

# 1    Introduction

## 1.1    Background

Ensuring that the integrity of geothermal installations is sustained is one of the biggest concerns in the geothermal industry. In geothermal installations steel is used as material for casing, pipes, valves etc. It is well known that corrosion can degrade steel. Corrosion can occur when steel parts of geothermal installations are in contact with brine (formation waters) and results in the gradual degradation of metal, or, in the case of pitting corrosion, extremely fast degradation. Corrosion often can occur simultaneously with scaling because corrosion products can enhance precipitation. Corrosion that threatens the integrity of the doublet system can increase the risk of leakage of the produced or injected brine to other aquifers as well as result in increased cost due to non-availability of the sustainable energy production and expensive repair work. This report describes the causes and effects of corrosion (and scaling) within geothermal installations, as well as means to identify and prevent corrosion.

In the fall of 2013, a consortium consisting of a number of geothermal operators and IF Technology started a government funded project ('Innovatie Prestatie Contract' or IPC) to investigate ways to improve the operation of geothermal doublets. The project was focused around two major topics: corrosion (related to well integrity) and optimizing injection temperatures. As part of the project, TNO carried out a literature study and performed analyses based on available data (directed and supported by the consortium) on corrosion in geothermal installations. This report documents the results of that study. A report on optimizing injection temperatures will be published separately.

Prior to and during the project, discussions were held with representatives of the stakeholders, in particular DAGO and ECW. These discussions improved TNO's understanding of the operation of geothermal installations, and thereby to optimize the scope of the project. The following paragraphs describe the outcome of the discussions.

Operators of geothermal systems in the Netherlands employ an HSE[2] management system to ensure that risks are properly addressed and controlled. A major point of concern for the management of HSE risks is that no fluid or gas may be released uncontrolled from the closed installation.

Steel casings and installations are commonly used in geothermal systems. In the wells these steel constructions are part of the barriers that prevent uncontrolled release. Apart from the steel, the barrier also consists of cement that is applied behind the casing steel. Multiple barriers are always present in a geothermal well at critical locations, to ensure the well integrity in case of failure of one of the barriers and to make certain that the installation remains fluid- and gas-tight.

---

[2] Health, Safety and Environment, in Dutch 'Veiligheid, Gezondheid en Milieu' (VGM)

After a geothermal well has been realised, the barriers must remain intact during the entire exploitation phase. Therefore, the condition of the barriers that safeguard the well integrity must be monitored. This implies, among other things, monitoring of the steel parts of the barriers. As steel can be corroded, a review of corrosion must be part of the entire well integrity program. The monitoring is part of the HSE management system as well.

The development of geothermal systems in the Netherlands has only started relatively recently. This sustainable way of energy production may well play an important role in the national energy supply in the coming decades. At a national level, arrangements with respect to knowledge sharing, (management of) research projects and setup of best practices and industry standards, among other topics, were agreed upon in the Geothermal Acceleration Plan ('Versnellingsplan Aardwarmte'). The first systems were realised safely by employing knowledge and experience from the oil and gas industry, and the geothermal industry in France and Germany. Despite the use of the best available knowledge and experience, the successful deployment of geothermal systems in the Netherlands demands significant innovation.

The implementation of a well integrity monitoring program requires more knowledge about corrosion of steel parts in the geothermal well. Therefore, the operators of the geothermal wells took the initiative of asking TNO to answer a number of corrosion related questions, given the operating conditions of the wells and the applied steel grades. All of these questions are addressed in this report:

- Can corrosion of unprotected steel be expected?
- Is it reasonable to expect that conditions exist where corrosion in geothermal wells is limited by natural protection mechanisms like oil films or iron carbonate scaling?
- At which locations in a geothermal well can the corrosion rate be expected to be relatively high and / or low?
- In which ways can the corrosion rate be lowered, either by design, or by the application of inhibitors?
- If corrosion should be expected, which monitoring techniques are available / effective / achievable / applicable?

Geothermal installations are subject to the Dutch Mining Law. Possible answers to the above mentioned questions are relevant for the preparation of an integral monitoring program for well integrity, aiming, among other things, at compliance to the Mining Law.

Additional information required for such a monitoring program is outside the scope of the research carried out by TNO. This can for instance be acquired by carrying out a well integrity assessment according to OGP draft 116530-2 (or comparable) (IOGP 2012). Using this standard, more specific follow-up questions can be answered, such as:

- What are the optimally applicable barrier options for new well designs?
- Which barriers are required during the exploration and exploitation phases?
- Which barriers have been applied, and what is their baseline measurement?
- Which components do the barriers comprise, apart from steel?

- Which circumstances may influence the condition of materials other than steel?
- Which condition of the composing parts of the barriers is still acceptable for the functional preservation of the barrier?
- In which way can the condition of the materials, other than steel, be monitored?
- What are the options for protecting and fixing corroded barriers?

In the course of 2015, these questions will be addressed with DAGO (Dutch Association Geothermal Operators). At the end of 2015, the results of this research will be used for the deployment of a draft well integrity management program. This program will become part of the HSE management system of the geothermal well operators after testing and certification.

The guideline for the HSE management system is that the remaining risks are limited to a level which is reasonably practically applicable (ALARP[3]). This principle will also be applied to the well integrity program.

## 1.2 Scope

Corrosion can, in principle, occur along the entire installation. It is especially important at locations where a single barrier is separating the produced water from the subsurface, which is along the casing. This report is limited to corrosion of steel within the well, between reservoir depth and the well head. The reason is that this part of the installation is:

- (together with the cement) the major barrier between the produced water and the environment;
- susceptible to corrosion;
- poorly accessible;
- difficult and expensive to replace when it has failed.

Hence, the report does not deal with:

- the ESP. The pump is constructed of relatively more corrosion resistant material and therefore less prone to corrosion;
- the production liner. This part of the installation, from which the pump is hanging. Both can be inspected and replaced relatively easily when necessary. Because the bubble point is expected below the ESP, two-phase flow will occur in the production string;
- the surface installation. Like the ESP, it is often constructed using high-end steel and synthetic materials (for instance in valves or between flanges) which are both more corrosion resistant, and can also relatively easily replaced;
- well screens. The screens may consist of a combination of a perforated mild steel core, wrapped with stainless steel. The mild steel, often L80 or the like, is susceptible to corrosion. Corrosion of the screens does not threaten the well integrity as complete removal of the screen by corrosion would technically result in an open hole completion.

---

[3] As Low As Reasonably Practicable

- External corrosion of steel casings is not described (either cemented or not). This type of corrosion is well known and published, and comparable to the corrosion taking place in the oil and gas industry. It is considered to have much lower rates than corrosion in the geothermal industry and therefore less important.
- Corrosion of cement and other non-steel materials (casing liner hangers, packers) is not described either.
- Other failure mechanisms than corrosion such as for instance described in the Standard Handbook of Petroleum and Natural Gas Engineering (Chapter 4 Drilling and Completion, p437 'Causes of casing troubles').

# 2 Theory of corrosion

## 2.1 Corrosion types

An exhaustive classification of corrosion types is given by Sully and Taylor (1987). The most relevant ones for the geothermal industry are addressed by Libowitz and Whittingham (1979), subdivided by the extent and texture of the corroded metals. Different causes may result in the same effect. **General** or **uniform corrosion** is distributed uniformly along an extended area on the metal surface, causing the metal thickness to decrease with time. **Localised corrosion** on the other hand is localised, causing (initially) microscopically small holes (**pitting**) that can extend deep into the metal. The particular danger of pitting corrosion is that it may not be detected easily as the total amount of material loss is small, and yet it may lead to very fast local degradation of the installation and leakage. **Crevice corrosion** is similar to pitting, however it forms within installation crevices like for instance between adjacent parts of casing and coupling (it has been observed in some Dutch installations). It covers a larger area than pitting corrosion. A further type of localised corrosion is **filiform corrosion**. It occurs as worm-like passages underneath coatings. **Erosion corrosion**, a subtype of **mechanical** corrosion, typically occurs at bends, joints and other obstructions in the installation. Increased turbulence caused by irregularities along the pipe inner surface (e.g. caused by pitting etc.) can lead to high erosion rates. It usually exhibits a directional pattern with the direction of flow. Erosion corrosion is mitigated by low flow velocities (laminar flow) and smooth surfaces. **Environmentally induced cracking,** including **stress corrosion cracking** which occurs in the form of cracks that result in the embrittlement of the metal. Due to the often small size of the cracks this type of corrosion can also remain undetected. Intergranular and selective corrosion are other types of corrosion that are considered less relevant.

The most likely forms of corrosion that will probably be encountered in Dutch installations are general corrosion (along the inside of the casing pipes), and under certain circumstances crevice corrosion around crevices present between adjacant parts of casing and coupling.

Table 2.1   ASM classification of corrosion types (Sully and Taylor, 1987). Photos from sources: Mundhenk et al. 2013, Ginzel and Kanters 2002, http://www.cqj.dk; Roberts 2008, Wikipedia.

| corrosion type | description | subtypes | photo |
|---|---|---|---|
| general | corrosive attack dominated by uniform thinning | - atmospheric<br>- galvanic<br>- stray-current<br>- general biological<br>- molten salt<br>- in liquid metals<br>- high – temperature |  |
| localized | high rates of metal penetration at specific sites | - pitting |  |
|  |  | - filiform |  |
|  |  | - crevice |  |
|  |  | - localized biological |  |
| mechanically assisted | corrosion with a mechanical component | - erosion<br>- fretting<br>- cavitation and water drop impingement<br>- fatigue |  |
| environmentally induced cracking | cracking produced by corrosion, in the presence of stress | - stress – corrosion cracking (SCC)<br>- hydrogen damage<br>- liquid metal embrittlement<br>- solid metal induced embrittlement |  |
| metallurgically influenced | affected by alloy chemistry & heat treatment | - intergranular<br>- dealloying |  |
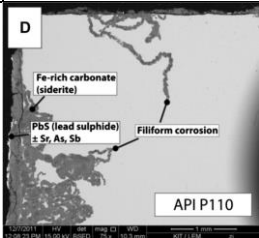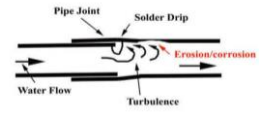
## 2.2      Causes of corrosion in geothermal installations

This section describes the processes and factors that contribute to corrosion.

### 2.2.1    *Oxidizing elements in the formation water*

One of the most prominent causes of corrosion is the presence of oxidizing corrosive elements in formation waters. The corrosion is driven by electrochemical reactions between the metal of the geothermal installation and constituents in the formation waters. Seven key species are known to be most detrimental to geothermal installations: **oxygen** ($O_2$), **carbon dioxide** ($CO_2$), **hydrogen sulphide** ($H_2S$), **chloride** ($Cl^-$), **ammonia** ($NH_3$), **sulphate** ($SO_4^{2-}$) and acidity as $H^+$ (hydrogen) ions (Mundhenk et al., 2013). Other oxidizing species that should be considered are Nickel (Ni), Copper (Cu) and lead (Pb). Generally low grade steel types are prone to corrosion by the active species in the formation water, although species that enhance pitting like $Cl^-$ and $H_2S$ are more dangerous for stainless steel (localized corrosion). In a chlorine rich environment, localized corrosion is strongly enhanced when crevices are already present. Water chemistry dependent corrosion can lead to uniform, pitting, erosion and stress cracking corrosion.

The most problematic gasses in this respect to corrosion are oxygen, carbon dioxide and hydrogen sulphide. In themselves, gasses do not constitute a corrosion problem, only when they are dissolved in the brine they can either oxidize or lead to pitting. By far the most corrosive gas is **oxygen**. Oxygen is in principle considered to be absent in geothermal installations which are considered to be closed. However, oxygen may enter the system:

-   when the installation is opened for maintenance (e.g., changing filters) or inspection;
-   during shutdown by diffusion of oxygen through synthetic material (e.g., gaskets);
-   during leakage (e.g. seals, gaskets), if oxygen containing water enters the system;
-   when oxygen-containing gas or fluid is entered in the system. This can for instance occur during nitrogen blanketing, dilution of chemicals with oxygen-containing water, dosing of chemicals (inhibitor or HCl), $CO_2$ dosing. On site produced nitrogen is virtually devoid of oxygen, but this is not necessarily the case for certain $CO_2$ usages like pH control.

The use of oxygen scavengers and proper nitrogen ('blanketing') can prevent this effectively from happening.

At an equal concentration **carbon dioxide** is less corrosive to steel than oxygen (Figure 2.1) but it is far more prominent in Dutch geothermal installations than oxygen. Whereas dry $CO_2$ is, in itself, not corrosive, $CO_2$ in combination with water creates an acidic environment that causes corrosion of steel (Zhang and Kermen, 2013, see eq. 1). Dissolution of carbon dioxide in the formation water leads to formation of hydrogen ions (protons), and carbonic acid ($HCO_3^-$). Dissociation of carbonic acid to carbonate ($CO_3^{2-}$) at the steel/electrolyte interface yields even more protons.
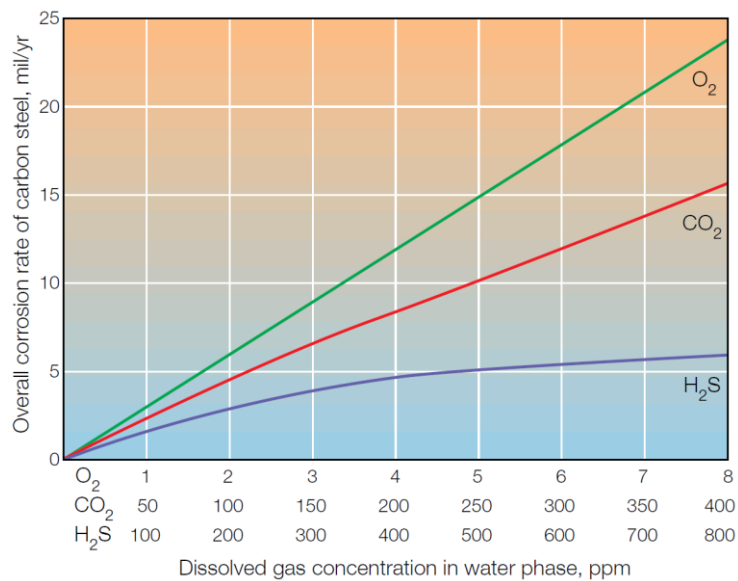
Figure 2.1 'Comparison of corrosion rates of steel. Measurements of the corrosion rates of a carbon steel exposed to different concentrations of $O_2$, $CO_2$ and $H_2S$ gases dissolved in water show that $O_2$ is about 80 times more corrosive than $CO_2$ and 400 times more corrosive than $H_2S$' (derived from Brondel et al. 1994). Note that 1 mil = 0.0254 mm and 25 mil/yr ≈ 0.6 mm/yr. Test conditions 25°C, 5-7 day exposure, 2-5 g/l NaCl, $HCO_3$ alkalinity < 50 mg/l.

$$CO_2 + H_2O \rightarrow H^+ + HCO_3^-$$                                     Eq. 1

As a consequence of this reaction, the pH of the formation water decreases. Metal Fe is not a stable phase across the entire pH range (appendix A). The production of hydrogen ions will potentially remove Fe from the metal surface (eq. 2). In the presence of $CO_2$, an anodic reaction takes place at the steel/liquid interface and iron atoms are oxidized to cations (Fe(II)). Contemporaneously, a cathodic reaction (eq. 3) takes place and protons are reduced forming bicarbonate ions ($HCO_3^-$). Generally speaking, an increase in $CO_2$ increases the corrosion rate in aqueous solutions by increasing the rate of hydrogen evolution (Nesic, 2007).

$$Fe^0\ (solid) + 2H^+ \rightarrow Fe^{2+} + H_2$$                           Eq. 2

$$Fe^0\ (solid) + CO_2 + H_2O \rightarrow Fe^{2+} + 2HCO_3^- + H_2$$          Eq. 3
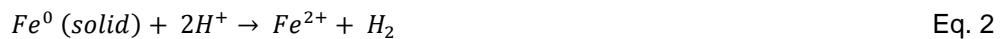
Indeed, Alt-Epping et al. (2013) state that 'any sign of an increase in the hydrogen concentration in the fluid should be taken as a strong indicator of corrosion within the system'. An increased hydrogen content should be measureable when degassing a brine sample and analysing the gas composition.

**Hydrogen sulphide**, when dissolved in water, is known as hydrosulfuric acid. This is a weak acid that induces corrosion. Hydrogen sulphide can be present in the formation waters but it can also be formed by sulphate reducing bacteria (if present in the geothermal installation). Higher concentrations of $H_2S$ compared to $CO_2$ are required to achieve equal corrosion rates (given identical conditions). At the same time a protective scaling layer, consisting of iron sulphide (FeS), can form on the metal surface. FeS is the Fe-rich end member of the pyrrhotite $Fe_{(1-x)}S$ group. It is amorphous and can convert to pyrite.

$$H_2S \rightarrow H^+ + HS^-$$

$$Fe^{2+} + H_2S \rightarrow FeS + 2H^+ \hspace{3cm} \text{Eq. 4}$$
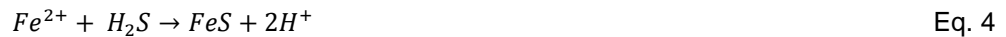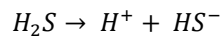
An additional problem with hydrogen sulphide is sulphide stress. Although hydrogen sulphide does not participate directly in sulphide stress cracking, it promotes the diffusion of hydrogen atoms into the base metal and embrittles the crystal structure (NACE, 2002). This is also called "hydrogen induced cracking". This type of corrosion frequently leads to pitting. Hard metals are in particular prone to sulphide stress cracking (Drijver, 2014).

**Chloride** and other salts are further corrosion factors in geothermal installations. The concentration of chloride in formation waters varies in different geothermal doublets. The main effect of chloride is the local breakdown of oxide films that protect the metal surface (Gräfen and Kuron, 1996). Next, the chloride facilitates dissolution of iron, leading to a solution of iron chloride and finally formation of a precipitation salt film. The formation of metal chlorides on the metal/film interface leads to expansive stress and rupture of the oxide film (Mundhenk et al., 2013). This is the main risk for stainless steel type materials.

High concentrations of lead, nickel and copper or other dissolved metals in formation waters more noble than iron, can also be oxidising to the metal surfaces and thus corrode them (e.g. Gräfen and Kuron, 1996). Particularly the Slochteren formation waters tend to be rich in lead (Schmidt 2000, Schmidt et al. 2000). Due to the more noble character of the lead ions will oxidize iron and use the electrons to form metallic lead. This type of reaction is often referred to as an exchange reaction. The more noble metal (lead) is deposited, the lesser noble metal (iron) is dissolved (Eq. 6), which will lead to both iron corrosion and lead scaling (Bressers, 2014).

$$Fe\ (solid) + Pb^{2+} \rightarrow Fe^{2+} + Pb\ (solid) \hspace{2cm} \text{Eq. 5}$$

An example of lead deposit on low grade steel is given in Figure 2.2. Hartog and Jonkers (2002) observed lead deposits exceeding 10 mm in thickness on steel casings in Dutch natural gas systems. When in contact with air the metallic lead deposits can also convert to secondary lead minerals. Lead corrosion is generally prone to low grade steel.
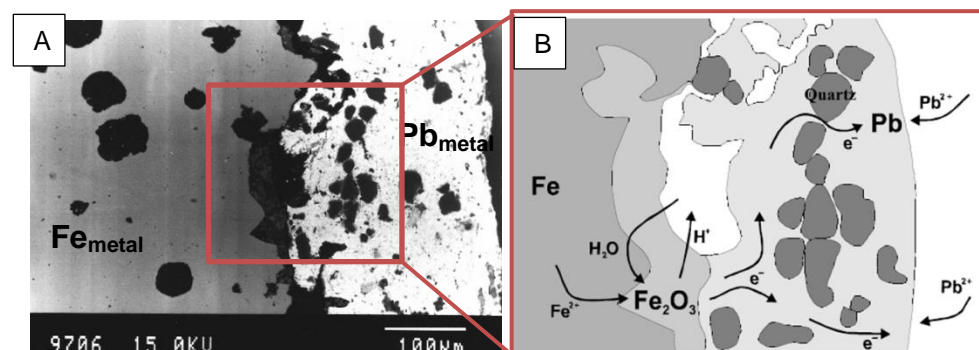


Figure 2.2 (A) SEM cross-section photograph showing elemental lead on an iron surface; (B) Schematic detail drawing of the situation and the electrochemical reaction in A (derived from Hartog and Jonkers, 2002).

2.2.2    *Galvanic corrosion*

Galvanic corrosion takes place when two dissimilar metals are in electrical contact with each other and the same electrolyte (in this case formation water). The dissimilarity of the metals is directed by their equilibrium potential (Me(0) to Me+ reaction). Figure 2.3 shows the galvanic series (in sea water at 25°C and 1 bar), which expresses the nobility of various metals. The x-axis shows the so-called open-circuit potentials (in Volts) of the metals that were measured in reference to a saturated calomel electrode[4]. The most noble metals (such as gold and platinum) are listed in the lower left corner, and the least noble (magnesium, zinc) in the top right corner. The graph shows that for these conditions there is a large difference between the often used stainless steel 316 (~ −0.1V) and low alloy steel (−0.6V). One should note that this plot is not representing the situation for the Dutch geothermal installations as the temperature, pressure and electrolyte composition are different from seawater, and dissolved oxygen is generally absent. Therefore, Figure 2.3 does not necessarily apply and should be seen only as an example.
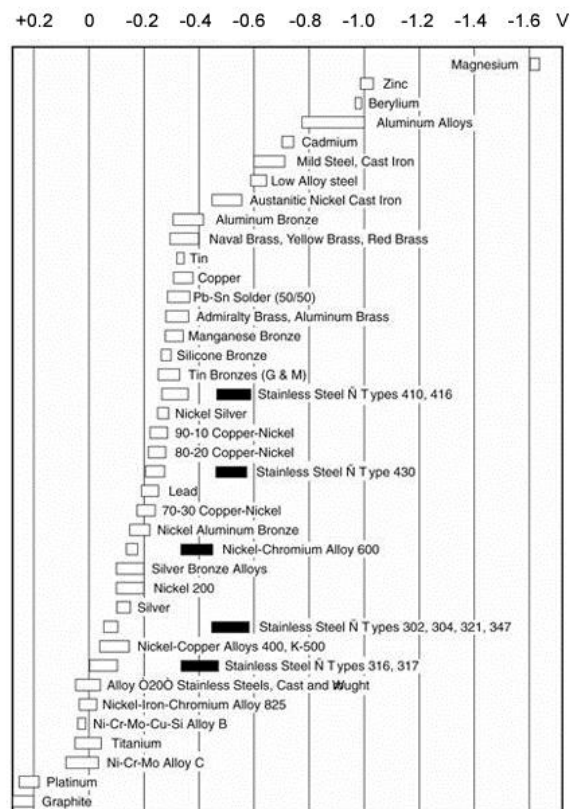


Figure 2.3 Galvanic series for the situation in sea water at 25°C for different metals. Left hand side: most noble, cathodic. Right hand side: least noble, anodic (derived from intechopen.com website).

When two dissimilar metals are electrically connected to each other the equilibrium potential will depend on the ratio between the surface areas of the two metals in contact and the size of each surface (Figure 2.4 – left part).
When the metals are in contact they will be forced to be at the same equilibrium

---

[4] A saturated Calomel Electrode (SCE) is an often used type of reference electrode for chloride containing aqueous electrolytes

potential. This will cause electrons to be transported along the interface between the two metals. This effect is called galvanic element formation. It will make one of the metals more positively, and the other more negatively polarised than their individual equilibrium potentials (Bressers, 2014). During galvanic corrosion the more noble metal will be the interface at which electroactive species will be reduced (for instance oxygen to water or protons to hydrogen), while the less noble metal is oxidized and thus corroded. In practical applications one generally assumes that potential differences less than ~ 0.15V will not be effective (Roberge, 2000) and that therefore metals which are neighbours in the galvanic series can be used in a direct electrical contact.
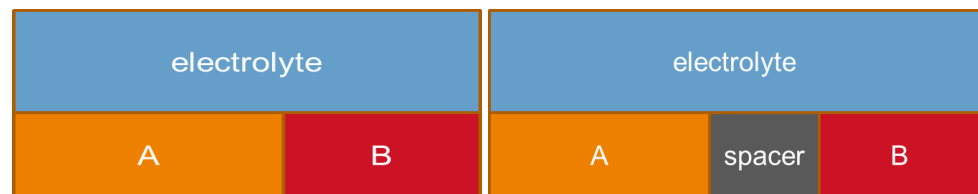


Figure 2.4  Left - Situation in which two different types of metal are used in direct electrical contact; Right - Situation where two different installation materials are in contact with the formation water (electrolyte), but not with each other (derived from Bressers, 2014).

When two metals are electrically disconnected, for instance by the use of a non-conducting spacer (Figure 2.4, right), both materials will be in an independent equilibrium with the electrolyte. The equilibrium potential will in this case depend on the material itself (composition and morphology) and the interaction with the electrochemical active species in the electrolyte (Bressers, 2014). Thus, the equilibrium potential (= open-circuit potential) of interfaces A - electrolyte and B - electrolyte can be at different values. In other words, galvanic corrosion will not take place. The possibility that corrosion occurs will then only depend on the metal and the electrolyte (formation water composition), but not on the difference in open circuit potential between metals A and B.

Pitting corrosion may result from galvanic corrosion. Lead deposition can also be triggered by galvanic corrosion in the absence of oxygen (Equations 5 and 6), as $Pb^{2+}$ can be reduced on the negatively polarized metal. As a consequence metallic lead would deposit on the noble metal while the least noble metal, in this case the low grade steel, will be positively polarized and therefore corrode (Bressers, 2014). Whereas lead is formed on stainless steel, it does not hold, so eventually grains of lead will be encountered in the installation (Erik Ham pers. comm.).

2.2.3     *Erosion corrosion*

Flow velocity can play a role in the corrosion process (Figure 2.5), particularly when solid fragments are present in the formation water that can file away the metal surfaces, leading to erosion corrosion (Nesic, 2007).

Erosion corrosion is caused by continuous fluid flow, which removes any protective scales or other inhibitors from the metal surface. The flow regime is equally important. During multiphase flow (e.g. water-gas-oil) the flow patterns can interchange between stratified, slug and annular flow. The different flow patterns lead to differential surface wetting mechanisms that drive corrosion (Nesic, 2007). It is generally desirable to reduce the fluid velocity and promote laminar flow. Increased pipe diameters are useful in this context[5]. Flow accelerated corrosion can also remove protective scale and inhibitor films leading to localised corrosion attack (Nesic, 2007; Banas et al., 2007, see Figure 2.5). Chawla and Gupta (2010) show that the corrosion rate of carbon steel in seawater increases from 0.16 to 0.34 and 1.19 mm/yr when the velocity is increased from 0.3 to 1.2 and 8.2 m/s. Changes in pipe inner diameter can initiate disturbed turbulent flow, thereby enhancing the possibility of erosion corrosion (Figure 2.6).
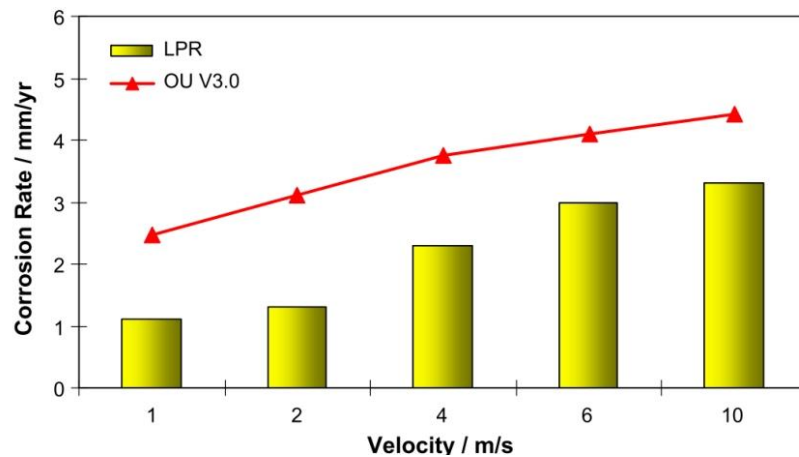


Figure 2.5 Modelled (OU V3.0) and measured (LPR) corrosion rates with increasing flow velocity at 20°C and 1 bar, in absence of iron carbonate scales. Steel grade X-65, electrolyte 1 mass% NaCl (derived from Nesic 2007).

---

[5] e.g. www.corrosion-doctors.org
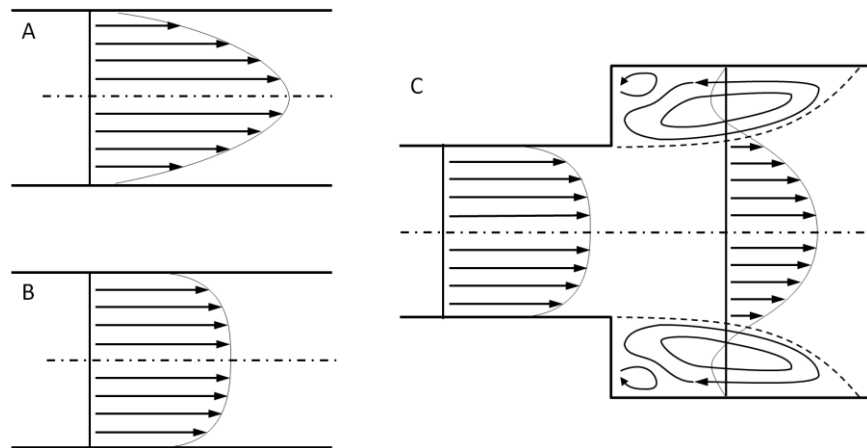
Figure 2.6 'Single phase pipe flow. (a) Developed laminar flow, showing parabolic velocity profile. (b) Developed turbulent flow, showing logarithmic velocity profile with large gradient near the wall (nondisturbed flow). (c) Disturbed turbulent flow with separation, recirculation and reattachment, showing complex velocity field' (derived from Heitz 1991, cited in Postlethwaite and Nesic 2000). The erosion corrosion potential is enhanced after a change in pipe diameter at C.

### 2.2.4 Other causes of corrosion

Microbial activity that operates both under oxic and anoxic conditions can create corrosive environments. For example, sulphate reducing bacteria produce $H_2S$ which induces pH reduction. Other types of bacteria 'can promote corrosion by creating differential oxygen cells on steel in aerated waters' (Jones, 1988).

# 3 Assessment of corrosion potential

## 3.1 Relevant parameters

Each geothermal doublet and installation is unique. To be able to assess the possibility and grade of corrosion in geothermal installations, it is important to acquire data on the following parameters:

- formation water and gas chemistry;
- temperature;
- steel/alloy type.

It is in principle possible to deduct whether formation brine induced corrosion may take place and which elements can cause it, provided sufficient knowledge is available regarding the installation components and their concentrations of the formation waters, pH, temperature and preferably the open circuit potentials.

## 3.2 Formation water chemistry and gas composition

Both formation water chemistry and gas compositions are routinely collected during oil and gas exploration and production (Figure 3.1, Figure 3.2). Hence, many data are already available to the geothermal industry through the Oil & Gas data portal www.nlog.nl. For the geothermal industry, similar samples are taken and analysed (Table 3.1, Table 3.2).

### 3.2.1 Brine chemistry

There is a clear trend of increasing salinity with depth. For Germany, a similar trend was observed by Wolfgramm et al. (2011). Furthermore, locally collected formation water chemistry and gas composition data are by now available for nearly all doublets. The data shown below (Table 3.1, Table 3.2 and Figure 3.1, Figure 3.2) indicate that there is a wide spread in data values, even between samples from the same location (although not visible from the graphs shown here).
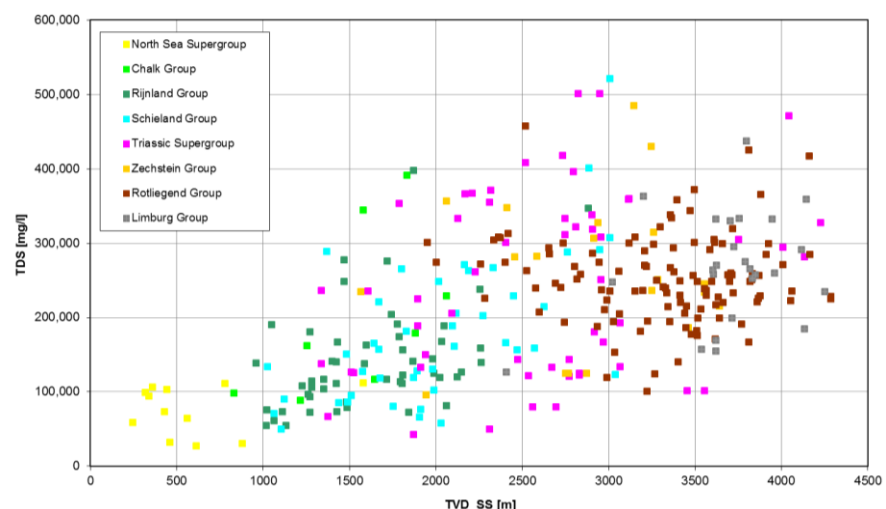


Figure 3.1 Formation water analysis results showing general increase of TDS with depth, and large scatter (source: www.NLOG.nl).

| | Cl | | | | SO$_4$ | | | | HCO$_3$ | | | | Fe | | | |
|---|---|---|---|---|---|---|---|---|---|---|---|---|---|---|---|---|
| | n | min | avg | max | n | min | avg | max | n | min | avg | max | n | min | avg | max |
| KN/SL | 24 | 46 | 63182 | 85000 | 23 | 54 | 221 | 2469 | 18 | 35 | 150 | 260 | 22 | 1 | 34 | 111 |
| RO | 26 | 86000 | 131669 | 160000 | 15 | 185 | 438 | 610 | 21 | 14 | 301 | 670 | 34 | 26 | 139 | 730 |
| DC | 1 | 48000 | 48000 | 48000 | 1 | 15 | 15 | 15 | 1 | 360 | 360 | 360 | 1 | 29 | 29 | 29 |
| | Ca | | | | K | | | | Pb | | | | Na | | | |
| | n | min | avg | max | n | min | avg | max | n | min | avg | max | n | min | avg | max |
| KN/SL | 25 | 4 | 4849 | 8300 | 24 | 177 | 10698 | 92818 | 0 | -1 | -1 | -1 | 25 | 41 | 29914 | 40000 |
| RO | 34 | 7200 | 9953 | 16600 | 34 | 650 | 1406 | 2400 | 1 | 4 | 4 | 4 | 34 | 43000 | 64088 | 87000 |
| DC | 1 | 3580 | 3580 | 3580 | 1 | 1600 | 1600 | 1600 | 0 | -1 | -1 | -1 | 1 | 23800 | 23800 | 23800 |

Table 3.1   Minimum and maximum concentrations of some key elements and compounds in the formation water of Dutch geothermal wells. Concentrations are given in ppm. DC = Carboniferous, RO = Rotliegend, KN/SL = Jurassic / Cretaceous. Source: Dutch geothermal wells (not public). Note that in the Netherlands only one doublet exists in DC and three in RO, so the amount of data for those formations is limited.

| | n | CH$_4$ | | | CO$_2$ | | | N$_2$ | | | O$_2$ | | |
|---|---|---|---|---|---|---|---|---|---|---|---|---|---|
| | | Min | avg | max | min | avg | max | min | avg | max | min | avg | max |
| KN/SL | 25 | 39.3 | 82.6 | 95.8 | 0.0 | 11.0 | 56.7 | 0.4 | 3.0 | 13.4 | 0.00 | 0.23 | 0.51 |
| RO | 12 | 22.8 | 55.9 | 75.1 | 7.2 | 25.4 | 43.5 | 3.0 | 12.5 | 38.6 | 0.07 | 0.09 | 0.12 |
| DC | 3 | 2.9 | 4.1 | 5.6 | 36.6 | 53.2 | 74.8 | 6.8 | 32.0 | 57.6 | - | - | - |

Table 3.2   Minimum, average and maximum concentrations of major gas components in the formation water of Dutch geothermal wells. Concentrations are given in mole%. All available samples used. Stratigraphic codes as in Table 3.1. Source: Dutch geothermal wells (not public).

Not surprisingly, the results shown in Figure 3.1, Table 3.1 and Table 3.2 emphasize the fact that even within a single reservoir unit and at comparable depth the compositions of both brine and gas widely vary. This has to do with the original composition, the depositional and burial history (compaction, diagenesis), present depth (pressure and temperature conditions), the presence of faults, and the geochemistry of overlying, underlying and adjacent (as diapirs) rocks, like for instance Carboniferous coal layers and Zechstein salt (Verweij, 2006).

### 3.2.2   Gas composition

Figure 3.2 shows gas composition data (CH$_4$ and CO$_2$). It is based on 'free' gas composition data collected in Dutch gas fields (www.NLOG.nl), doublet gas composition data collected by TNO from various reports by (mostly) Panterra, GPC IP, KIWA and BWG, and recent dissolved gas data by GPC IP et al. (2015). Most doublet samples were taken at surface level. In principle bottom-hole samples are preferred over surface samples as they are considered to be more representative of the reservoir gas composition, but the former are also more expensive. In between reservoir and surface level, pressure and temperature change. This may lead to various processes that change the chemical equilibrium (unmixing, degassing, precipitation). As such, the surface level measurements may not always be representative for the subsurface situation.

The scatter of the various data points in Figure 3.2 is remarkable. Most data from the Dutch gas fields and most of those measured by GPC et al. (2015) have CH$_4$ contents exceeding 80% and CO$_2$ below 5% (Figure 3.2 lower right corner).

A number of data points from Rotliegend gas fields have lower $CH_4$ and higher $CO_2$ contents ($CH_4 + CO_2 > 90\%$). Those are possibly related to the presence of intrusions. Most data measured by other companies (blue dots), however, display lower $CH_4$ and higher $CO_2$ contents. The measured gas composition for multiple samples taken from the same well or doublet is also found to be variable. This indicates that:

- the $CO_2$ gas content of some of the doublet brines is higher than that found in gas fields *or;*
- the sampling and measuring has been erroneous (if, for instance, part of the $CH_4$ is lost during sampling, the relative $CO_2$ content is automatically increased, etc.) *or;*
- the measurement accuracy of the surface samples is low.

A combination of all three is also possible. Given the fact that for nearly all doublets the $CO_2$ content is high, it is concluded that indeed the $CO_2$ content of dissolved gas is higher than that of free gas. For some measurements with high $CO_2$ content shown in Figure 3.2 it is a known fact that the sample was contaminated or not usable for other reasons (e.g., taken before the hole was circulated clean, etc.). Hence, it is extremely important that a quality assessment is done for each gas sample. A factor of 2 or 3 difference in the determination of the $CO_2$ content (e.g., 20% or 30% w.r.t. 10%) automatically leads to an over-estimation of the $CO_2$ partial pressure with a factor of 2 or 3. There is a strong link between the $CO_2$ partial pressure and the corrosion risk (see paragraph 4.1).
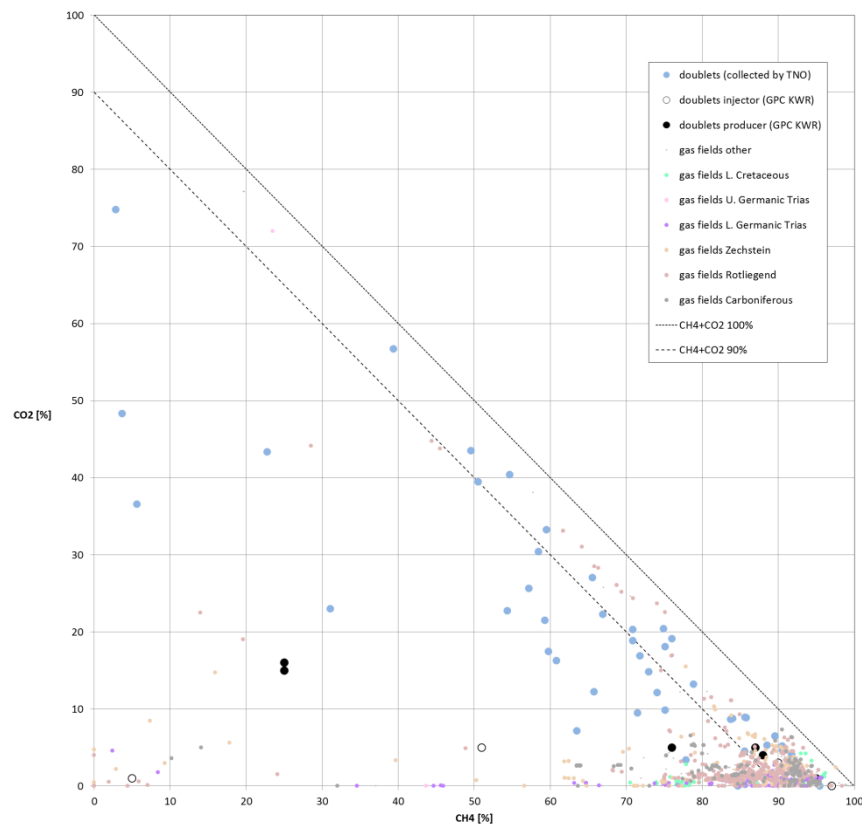


Figure 3.2 Relative amounts of $CH_4$ and $CO_2$ in Dutch gas fields (small dots), gas composition measurements collected by TNO from various sources (blue dots), and GPC / KWR

measurements. The majority of the non-gas field data are surface samples. For reasons of confidentiality, doublet labels have been omitted.

From a theoretical point of view, it is unlikely that the gas composition of free gas in a gas cap is equal to that of dissolved gas in the water leg. Given the better solubility of $CO_2$ in water, the $CH_4$ content of the free gas is considered to be higher than that of the dissolved gas. This would mean that the $CO_2$ content of the doublet brines is probably higher than about 0-5%, as is confirmed by the blue dots of Figure 3.2. If this is the case, the use of gas compositions measured in gas fields as prediction for nearby doublets is limited. This also means that the $CO_2$ partial pressures in doublets are relatively high (also see 3.2.4: CO2 partial pressure), and the corrosion risk is increased with respect to the situation where the $CO_2$ content is ~5% maximum.

An additional problem, especially with the interpretation of the gas samples, is that they were taken under a wide range of temperature and pressure conditions, and using varying sampling strategies, e.g. bottom hole or surface, before or after flashing, etc. Sometimes, the exact sampling location and conditions are unclear. Degassing or partial degassing of the brine will result in an erronous estimate of the gas content and / or composition.

A conclusion that must be drawn from the wide spread in observed formation water analysis results is that it is impossible to predict the corrosional behaviour of a doublet on the basis of the average brine and gas composition for a single reservoir rock unit only.

A standard sampling procedure is also important. In the Netherlands, not imperative standard exists for sampling reservoir brine and gas, like for instance API Recommended Practice 45 (Sampling Oil Field Waters). RP45 may be a good basis for a Dutch sampling standard - it is already being used in the Netherlands by some consultants. As it is developed for oil and gas fields, it should be adapted and extended to suit all needs for measuring and monitoring corrosion. Similarly, in Germany the sampling procedures are sometimes described in high level of detail (e.g. Regenspurg et al. 2013).

$H_2S$ is (currently) not encountered in Dutch doublets. It is found in a number of Dutch gas fields of Zechstein age only. Some oil and gas operators who produce gas from the Slochteren Formation plug their wells back after the Slochteren has been exhausted, in order to produce some gas from the less favourable Zechstein. Those gas wells are completed using L80 13Cr, which is basically L80 with between 12 and 14% or Chromium.

Given the $CO_2$ partial pressure, the degree of corrosion is highly dependent on the steel type. For example, the following $CO_2$ pressure limits are assumed by NACE (1999) for carbon steel in the absence of $H_2S$:

- $CO_2$ pressure  <  0.2 bar:                    no risk of corrosion
- 0.2 bar            <  $CO_2$ pressure  <  2 bar:  corrosion may occur
- $CO_2$ pressure  >  2 bar:                      corrosion will likely occur

Of course, this is only a very rough estimate which is strongly influenced by other parameter values. $CO_2$ acts in two ways – it increases the amount of hydrogen

formed on the cathode and forms the carbonate-oxide films on the surface of the metal (El-Lateef et al. 2012). The corrosion rate is then determined by whichever of the two processes performs the most efficiently. For higher grade steel types, particularly Cr, Ni and Mo-rich steels, the $CO_2$ tolerance is higher (Figure 3.3). Note that the NACE (1999) upper limit for 'no risk of corrosion' more or less corresponds to the upper limit for the recommended use of carbon steels J-55 and N-80, L-80 and C-75-2, and 85SS and 90SS (for varying $H_2S$ partial pressures, see Figure 3.3).
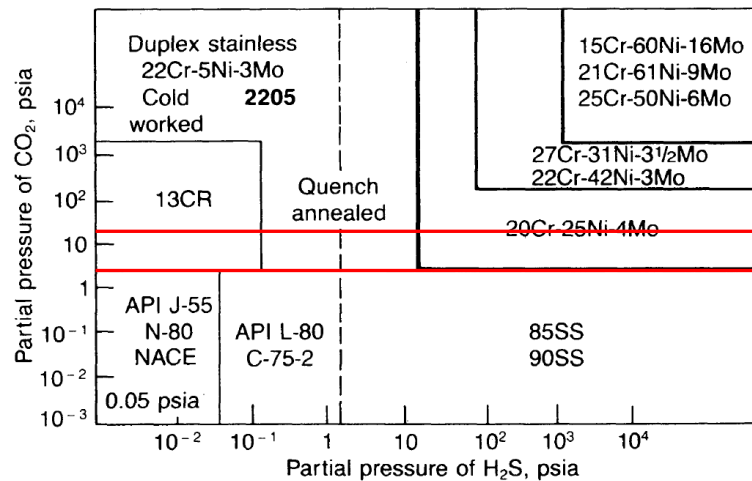


Figure 3.3 Selection guide for steel types considering $CO_2$ and $H_2S$ concentrations (derived from Schillmoller, 1989). Red lines correspond to the NACE $P_{CO2}$ 0.2 and 2 bar limits (2.9 and 29.0 psia respectively).

A conclusion is that determination of the $CO_2$ pressure is necessary for an assessment of the risk of $CO_2$ corrosion,. As $CO_2$ pressures cannot be measured directly and *in situ*, they must be calculated from surface measurements.
Two important factors for determining the $CO_2$ pressure, the bubble point pressure and the $CO_2$ partial pressure, are explained below.

3.2.3    *Bubble point pressure*
In a liquid containing dissolved gas, the bubble point pressure is the pressure at which the first gaseous bubble is formed when de-pressurizing. It depends on the chemical composition of the brine and the kind of gas. The ESP (electric submersible pump) in a production well is usually positioned below the bubble point pressure depth. This avoids the formation of bubbles in the brine at ESP depth which would decrease the pump efficiency and lifetime. Although routinely measured from samples under laboratory conditions, the bubble point pressure of a reservoir brine is often difficult to determine because the composition of a brine sample often deviates from the composition in the reservoir. This is due to a wide variety of changing conditions from reservoir to sample point, like differences in temperature, pressure (and hence solubility) and flow rate. On the way up, the chemistry of the brine usually changes due to precipitation of minerals or preferential movement of one or more components. Some components of the gas may move more easily than others through the reservoir. The solubility of the various gas components is also different, and may change due to changing conditions (P, T).

A way to measure the bubble point *in situ* is as follows. During production, water passes the ESP. The pressure above the ESP decreases upward to the wellhead pressure which is maintained between the ESP production string and the casing. Gas escapes from the water between the production string and the casing, thereby slowly increasing the pressure until bubble point (unless the annulus is continuously being degassed). Initially the speed of the pressure build-up is quick, but it decreases when the bubble point pressure approaches.

It is therefore important to realize how and where the sample was taken and measured when considering the importance of the amount of dissolved $CO_2$ in the brine for corrosion.

3.2.4    *$CO_2$ partial pressure*
In a mixture of different gases, each individual gas has a partial pressure which is the hypothetical pressure of that individual gas if it alone occupied the volume of the mixture, at the same temperature. The total pressure of an ideal gas mixture is the sum of the partial pressures of each individual gas in the mixture. The partial pressure of an individual gas equals the mole fraction of the gas times the total pressure of the gas mixture. Typical gas mixtures found in Dutch doublets do not behave like an ideal gas. Hence, a correction should be applied using a compressiblity factor Z (Figure 3.4). For instance, a gas mixture having 70% $CH_4$, 3% $C_2H_6$, 25% $CO_2$ and 2% $N_2$ at 200 bar and 88 °C has a $CO_2$ z-factor of about 0.57. Instead of a 50 bar $CO_2$ partial pressure, this yields 71 bar.

For doublets, the $CO_2$ partial pressure is only relevant if there is a gas phase, which is in contact with fluid (formation water). Here, the bubble point plays an important role. Below the bubble point pressure (i.e. at lower pressure, and therefore at shallow depth in the well), the $CO_2$ partial pressure is calculated from the $CO_2$ fraction in the gas, and the gas mixture pressure. If gas is not present over the entire length of the well, for instance below the bubble point depth / pressure, the $CO_2$ partial pressure is calculated using the last (lowest in depth) partial pressure where gas is present. Usually, the assumption of a linear pressure change with depth is sufficient.

With a higher $CO_2$ partial pressure, the concentration of $H_2CO_3$ increases, whereby, as is assumed by many authors, the speed of the redox half-reaction $2H_2CO_3 + 2e \rightarrow H_2 + 2HCO_3^-$ (see Table 4.2) increases. If, however, the conditions for the formation of iron carbonate are favourable, a higher $CO_2$ partial pressure in combination with a high pH can also lead to an increased formation of protective scales (Nesic, 2007).

Sander (2014) states that 'many atmospheric chemicals occur in the gas phase as well as in liquid cloud droplets [..]. Therefore, it is necessary to understand the distribution between the phases. According to Henry's Law for ideal gases[6], the equilibrium ratio between the abundances in the gas phase and in the aqueous phase is constant for a dilute solution':

$$k = \frac{p_x}{c_x}$$
Eq. 1

where:

- k Henry's law constant (note that sometimes the inverse of k is used);
- $p_x$ partial pressure of gas x in equilibrium with a solution containing some of the gas (MPa);
- $c_x$ the concentration of gas *x* in the liquid solution (mol/L, mol/kg or mole fraction).

The form of the equilibrium constant shows that the concentration of a solute gas in a solution is directly proportional to the partial pressure of that gas above the solution. In order to calculate the corrosion the dissolved $CO_2$ should be used, which is equal to $P_{CO2}$ / k. The Henry constant is strongly temperature dependent, but since the temperature drop from reservoir to surface installation is very limited, a single value of the Henry constant may be used for a single installation.
A relationship between temperature and the Henry constant was derived by Carroll et al. (1991) for pressures up to 10 bar (in order to satisfy the conditions for an ideal gas – apparently this does not hold for reservoir pressures). The findings by Carroll et al. (1991) are confirmed for ambient temperatures by Sander (2014) (Figure 3.5).

The solubility of $CO_2$ depends on pressure, temperature and salinity. It can be calculated using models, like for instance the improved model by Duan (2006). An example is given in Figure 3.6. The solubility is at minimum level around 100°C at higher pressures (250 bar and up), but further decreases with temperature at lower pressures.

---

[6] An ideal gas is a theoretical gas in which all collisions between molecules are fully elastic,, and forces between molecules negligible. The ideal gas concept is useful because it obeys Boyle's ideal gas law. Under high pressure, the distance between the molecules decreases, thereby violating the assumption that they do not interact. Henry's Law only applies for ideal solutions and for solutions where the liquid solvent does not react chemically with the gas being dissolved.
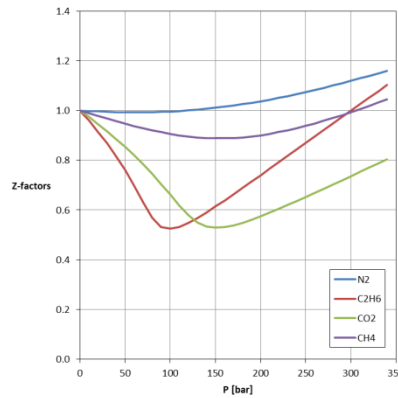
Figure 3.4 Z-factors for four major gas components @88 °C. A Z-factor of 1 indicates the gas behaves like an ideal gas. $CO_2$ and $C_2H_6$ deviate strongly from the ideal behaviour in the 0-100 °C range so the ideal gas law does not apply.
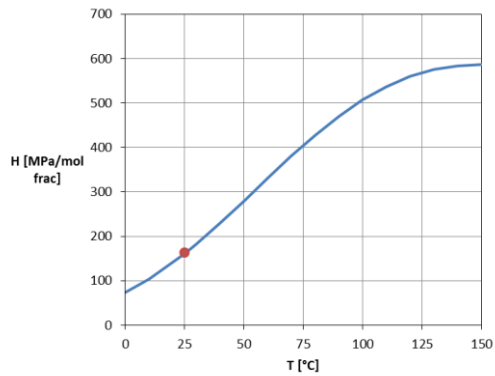


Figure 3.5 Relation between temperature and Henry's constant based on the regression by Carroll et al. (1991) for 0 < T < 150°C and pressures up to 1 MPa = 10 bar. Red dot from Sander (2014).
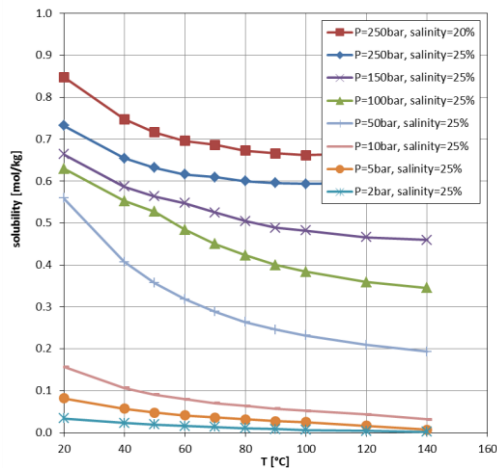


Figure 3.6 $CO_2$ solubility in formation brine as a function of temperature at various pressures and salinities according to the Duan (2006) model. For example, at a high value of 30 wt% $CO_2$ and an average gas density of 1.1 kg/m³ (which is the average value of all doublets), this comes to approximately 0.33 grams of $CO_2$ per liter brine, which is below the maximum solubility at most pressures. So, the $CO_2$ present at concentrations recorded in the brines of the Dutch doublets can be considered to be solvable.

From the point of view of $CO_2$, various regions in the production well with different $CO_2$ characteristics can be differentiated. From top to bottom these are:

- Above the fluid level in the annulus between the casing and the production tubing, $H_2O$ and $CO_2$ condense on the cold casing. There will be a corrosive mixture of $H_2O$ and $CO_2$ present (supposing the annulus is kept oxygen free). Dissolution of $CO_2$ in $H_2O$ will lower the pH, which enhances corrosion and possibly iron carbonate film formation (Nyborg 2010). This effect is known as 'top of line corrosion'. Prediction of top of line corrosion is difficult, and requires detailed fluid flow simulation, including heat transfer through the pipe walls (Nyborg 2010). A nitrogen blanket should be used to keep the oxygen away.
- Above the bubble point outside the production tubing, and below the fluid level, the pressure linearly decreases to the pressure maintained in the surface system. $CO_2$ will be present both in solution and in the gas phase. The $CO_2$ partial pressure can be calculated from the $CO_2$ content of the gas and the pressure.
- Inside the production tubing between the ESP and the surface installation, the pressure linearly decreases to the pressure that is maintained in the surface installation. If the surface installation pressure is lower than the bubble point pressure, the partial $CO_2$ pressure is calculated in a similar fashion as for the annulus (but with a different pressure gradient). If the pressure is kept above bubble point, the partial pressure is calculated in the standard way.
- Below the bubble point (which is usually located some distance above the ESP) all $CO_2$ is dissolved (as long a the solution is not fully saturatured – see Figure 3.6). If the pressures are high, like at larger depths in the well, the gas mixture does not behave like an ideal gas anymore. The correction of the $CO_2$ partial pressure can be calculated using Boyle's law, and the compressibility factor Z (Figure 3.4). The Z-factor for a gas component depends on pressure and temperature. For an ideal gas, Z = 1. For $CO_2$, the Z-factor varies between 0.4 and 1.0 and is lowest between 100 and 200 bar. For natural gas, the Z-factor is much closer to 1 (and the effect of increased pressure less). The effect of increased pressure on partial pressure is disproportionally larger for $CO_2$. Henry's law and the gas composition data (% $CO_2$, gas density etc.) can then be used to calculate the bubble point pressure and the partial $CO_2$ pressure. Calculation results using Henry's Law are supported by preliminary PHREEQC calculations.

**Sulfide stress cracking** starts at as low as 0.5 psi $H_2S$. However, this is only for low grade metals (NACE, 2002; Drijver, 2015) like API J-55, N-80 and API L-80. Higher grade metals containing chromium (Cr), nickel (Ni) and/or molybdenum (Mo) can resist far higher $H_2S$ concentrations (Figure 3.3). Sulfide stress cracking is also highly temperature dependant. The maximum SSC susceptibility of an API casing steel (containing carbon and manganese) is at room temperature. It strongly decreases with increasing temperature (Kane and Cayard, 1998).

When planning new geothermal doublets high $CO_2$ and $H_2S$ concentrations can be avoided by consulting gas and water composition maps and databases. $H_2S$ has only been observed in Dutch Zechstein reservoirs, which are currently not targeted for geothermal applications. The concentration $H_2S$ in all measured gas samples that were made available in this project was below the detection limit. Hence, $H_2S$ is not considered a risk for the operation of geothermal doublets.

**Oxygen** is obviously is highly corrosive. It is not described in detail in this paragraph because it is considered to be well avoidable using nitrogen blankets and oxygen scavengers. After the installation has been open to the atmosphere, e.g. for maintenance or filter replacement, it is advised to perform a nitrogen flush.

3.2.5    *Sampling*
It is evident from the available measurements in geothermal wells that both sampling and measurement should be carried out cautiously. The in situ gas content and composition, and pH are difficult to measure. Especially an incorrectly measured $CO_2$ content and/or pH may lead to an incorrect assessment of the corrosion potential.

For a correct assessment of the pH, care should be taken that the sampled brine is not contaminated with drilling mud. A contaminated brine may for instance have increased pH, incorrect $HCO_3^-$, incorrect ionic balance, different Ec, increased calcium etc. content due to various mud additives. When a well has not been cleaned sufficiently, the filters will quickly clog with mud. As samples are often taken quickly after the drilling has finished, many of the samples will be contaminated and therefore unusable or at least less useful.

As water is being degassed and $CO_2$ is removed from the brine, the pH will increase. Therefore the pH, measured after degassing or above bubble point, is not representative of the pH of the brine in the reservoir, and along the production casing. If the gas composition of the degassed sample (taken after the hole has been circulated clean), the gas-water ratio, and the chemical composition of the brine (which needs to be in ionic balance) are all measured correctly (including the remaining $CO_2$ / $HCO_3^-$ in the brine), it is possible to calculate the $CO_2$ partial pressure and pH at reservoir level using software like PHREEQC. Calculations carried out by Wasch (2014; data not included in the report) show that $CO_2$ partial pressures for a number of Dutch doublets at low installation pressures (< 9 bar) are below 5 bar, but in the order of tens of bars for some doublets at reservoir pressure. Similarly, the pH of the flashed brine may usually be around 6, but clearly the pH at reservoir level is much lower (3-5) due to the solution of $CO_2$.

3.3      **Temperature**

Generally, a higher temperature enhances corrosion rates (Figure 3.7, Figure 3.8). However, as temperature increases the chance of precipitation will increase, as the solubility product is reduced (note that this observation is valid for carbonates by not for many other minerals, like for instance aluminium-silicates). The precipitation of minerals could have the opposite effect on corrosion. In addition, higher temperatures also result in less dissolved $CO_2$ (Kampman et al. 2014). This is called the carbonate/temperature dissolution effect. A reduction of $CO_2$ would increase the pH and diminish corrosion. The peak temperature for corrosion tends to be between 60 and 80°C (Nesic, 2007, also see Figure 4.2). Again, this is case specific and needs to be defined for each geothermal doublet. El-Lateef et al. (2012) state that *'the rate of corrosion of steel below 60°C in solutions that do not contain $O_2$, is controlled by the kinetics of the evolution of $H_2$, which is in turn determined by the homogeneous and /or heterogeneous formation of $H_2CO_3$. Within*

*the temperature range 60-100°C, corrosion rate is controlled by the stage in which the layers of siderite undergo chemical dissolution and become permeable. Since the solubility of the corrosion, products and the protective properties of the deposits depend on the pH. This means, pH of the media largely determines the rate of corrosion i.e. a decrease in pH leads to an increase in corrosion rate'.*
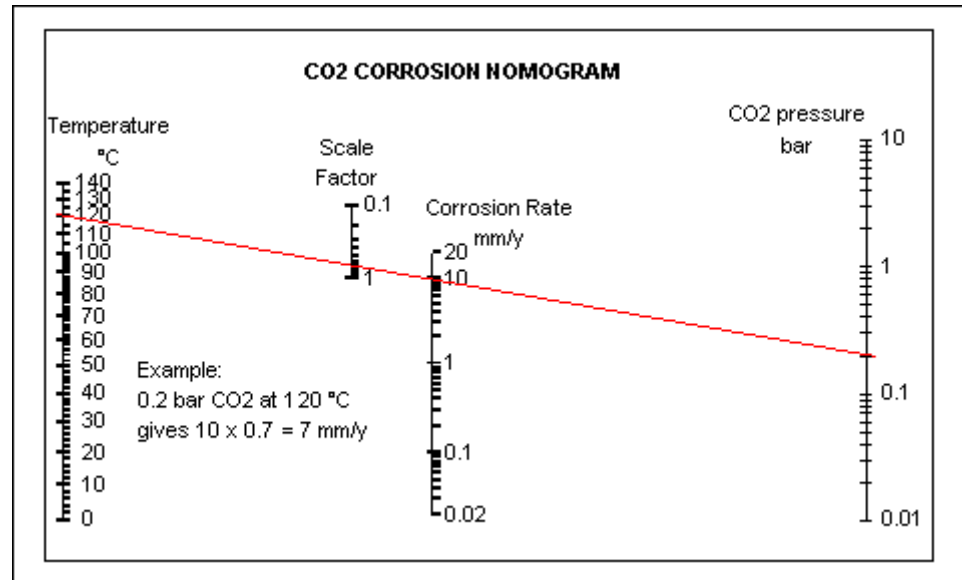


Figure 3.7 Simple corrosion nomogram taking into account both $CO_2$ pressure and temperature (derived from De Waard website http://cdewaard.home.xs4all.nl/). For a temperature of 120°C and a $CO_2$ partial pressure of 0.2 bar, corrosion rate is 7 mm/yr (given the scale factor of about 0.7).
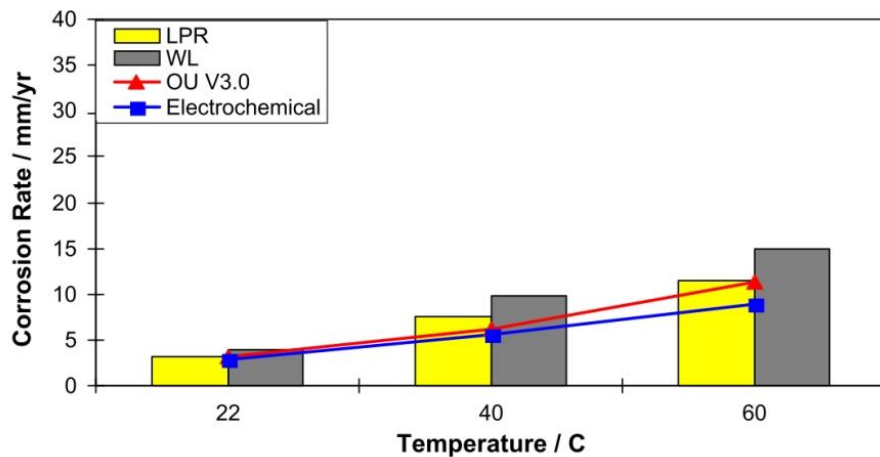


Figure 3.8 Predicted (red) and experimentally measured (blue) corrosion rates as effect of rising temperature at pH 4 and 1 bar pressure (derived from Nesic, 2007). Steel type and electrolyte as for Figure 2.5.

## 3.4 Open circuit potential - corrosion potential due to redox reactions

(Electro)chemical corrosion underlies one or more redox reactions. Pourbaix diagrams (Pourbaix, 1974) show the possible stable equilibrium phases at a given potential and pH. Pourbaix diagrams are based on thermodynamic calculations and do therefore not account for kinetics. This means that a Pourbaix diagram shows what in principle can occur, but not if it really occurs or how fast it will occur. In the

example of Fe (Figure 3.9), the Pourbaix diagram shows that Fe metal is stable at particular pH and $E_h$ conditions. Above a certain potential Fe can, depending on the pH of the electrolyte, precipitate as an Fe (oxyhydr)oxide or dissolve in solution as $Fe^{2+}$. The Pourbaix diagram will indicate how an element (here Fe) will react for a specific pH, potential at a given temperature. By looking at the Pourbaix diagrams for all elements in the geothermal system (steel and formation water) one can determine whether the elements are likely to undergo redox reactions that could lead to corrosion. A more detailed description of the interpretation of Pourbaix diagrams is given in Appendix A.
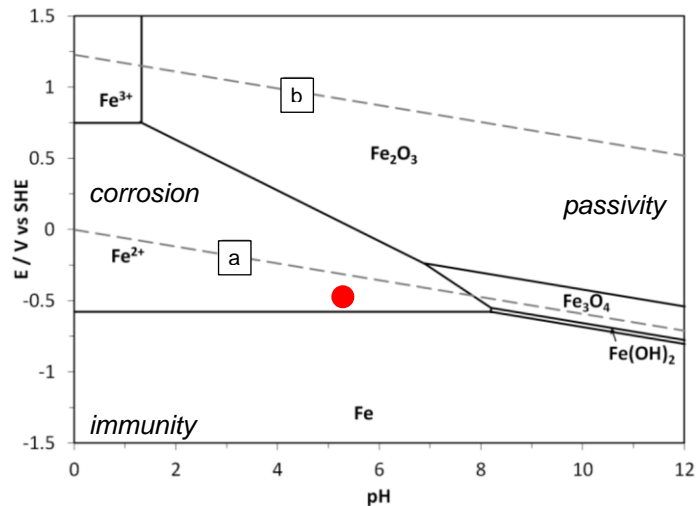


Figure 3.9  Simplified Pourbaix diagram for 10 ppm Fe in aqueous solution at 25°C. X-axis = pH, Y-axis = $E_h$ (redox potential, relative to SHE) (slightly modified after Tanupabrungsun et al. 2012)

The red dot in Figure 3.9 is an example case that describes a (hypothetical) condition in geothermal installations. It lies above the stability line for Fe, and below the water reduction line marked 'a'. The (casing) Fe in this case is not stable and will convert to $Fe^{2+}$, which is an indication of corrosion. It also evident that corrosion is less likely at a higher pH. The concentration of Fe in solution also plays a role, as it changes the equilibrium potential. The standard equilibrium potentials are given in Figure 3.10. This sequence indicates the oxidizing strength of the ions. The species on the left hand side of the plot have a strong oxidizing strength which means that they are thermodynamically able to oxidize the species on the right of them (Bressers, 2014). Note that if oxygen would be present in the formation water it would easily oxidize most metals. According to the Pourbaix diagrams copper, lead, nickel, water (protons) and cadmium, if dissolved in the brine, would be able to oxidize iron. While Figure 3.9 is valid for Fe at 25°C, Tanupabrungsun et al. (2012) present diagrams for the Fe-$CO_2$-$H_2O$ system and a wide range of temperatures, which are applicable to many Dutch geothermal doublets.
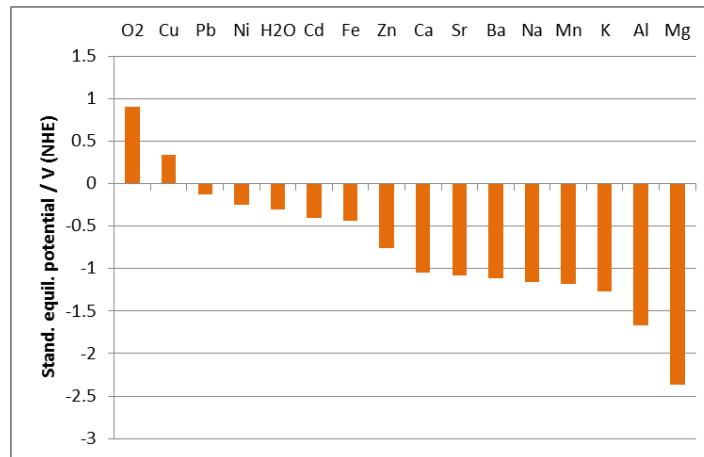
Figure 3.10    Standard equilibrium potentials for the ions observed in an average Slochteren
               Formation Dutch geothermal brine (derived from Bressers, 2014). pH between 4 and 7.
               Water bar based on the situation at pH = 5. Oxygen is added to show the strength of
               this oxidizing agent. The standard equilibrium potentials are based on thermodynamics
               and do not account for kinetics.

The species to the right of Fe in the graph are the reducing agents (Zn, Ca, Sr, Ba,
Na, Mn, K, Al, Mg). According to the Pourbaix diagrams, their reduction potentials
are greater than the reduction potential of water. Therefore these elements are only
stable in their oxidized form and can be neglected as being electrochemically
active.

Figure 3.11 shows the temperature dependence of the redox potentials for the most
electrochemically active species for the example above (Bressers, 2014). Stability is
not only a function of the pH and the voltage but depends also on the concentration
of free metal ions and on the presence of oxidizing agents in the electrolyte. The
graph shows which ions are able to oxidize iron. So Cu ions are thermodynamically
able to oxidize Fe(s)

The redox potentials were calculated using the Nernst equation: (see Appendix B
for a detailed explanation):

$$E = E_0 - \frac{RT}{nF}\ln\left(\frac{a_{red}}{a_{ox}}\right)$$                              Eq. 2

with:

- *E*     half-cell potential at the temperature of interest;
- *E_o*    standard equilibrium potential;
- *R*     universal gas constant: $R = 8.314\,472(15)$ J K$^{-1}$ mol$^{-1}$;
- *T*     absolute temperature (K);
- *a*     chemical activity for the relevant species or concentration;
- *F*     Faraday constant: $F = 96485$ C mol$^{-1}$ ;
- *n*     number of electrons transferred in the half-reaction.

A hypothetical brine composition derived from a number of Rotliegend formation
water samples was used as an example. It is evident that within the temperature
range of 0 to 100°C the redox potentials do not change significantly.
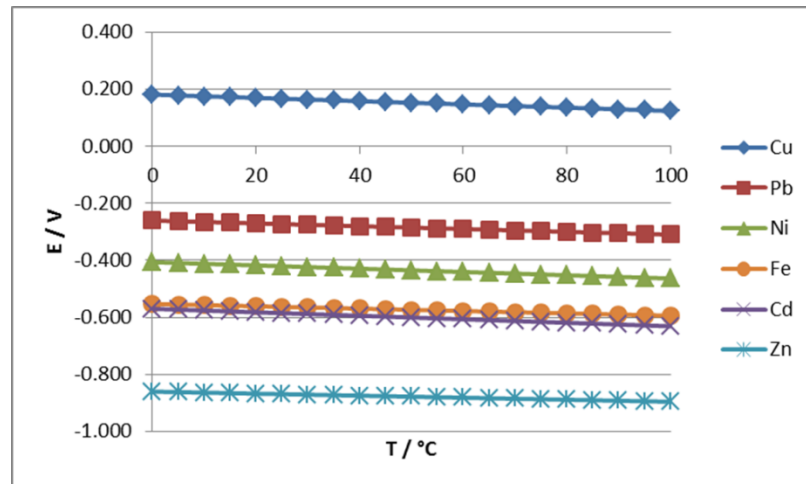
Figure 3.11    Temperature dependence of the redox potentials, calculated using the maximum
            measured concentrations in the geothermal brines of the Rotliegend doublets (derived
            from Bressers, 2014). pH between 4 and 7.

## 3.5    Alloy type

The amount of different steel grades is sheer endless. Steel is produced in large
variety of chemical compositions and post-treatments which give the material the
desired properties for the purpose of use. Various classification schemes for steel
grades exist.

This section does not go into all steel varieties as this would be beyond the scope of
the project. Instead it limits itself to the commonly applied major kinds 'mild steel'
a.k.a. 'carbon steel', and stainless steel. Some field and laboratory experiences with
different steel grades are described in chapter 7.

The most commonly used steel types for well constructions are listed below, in
sequence of increasing corrosion resistance (Zhang, 2013);

- **Carbon steel.**
  By definition, all steel is a mixture of iron and carbon. Steel to which no alloy
  elements have been added is called carbon steel or C-steel. Carbon steel
  contains less than 2.1% carbon in their chemical composition and is used where
  moderate strength is needed in a non-corrosive environment. This type of steel
  is commonly used for downhole constructions with standard steel grades such
  as K55, N80, L80, P110 amongst carbon steel pipes. K55 and N80 are the most
  basic steel grades with no additional corrosion resistant material present in their
  composition. Furthermore, any heat treatment on these grades of tubulars is
  optional. Other carbon steel grades such as L80 and P110 contains corrosion
  resistant material such as manganese and nickel, and undergo some form of
  heat treatment during the manufacturing phase. Tubulars of this grade are
  extremely vulnerable to (atmospheric) corrosion. K55 grade carbon steel casing
  is often used as surface casing, while L80 is the most commonly used casing
  material in the Netherlands under normal circumstances. While carbon steel is
  the most commonly used type of steel for casings other more corrosion
  resistant steel types might be used in well constructions.
- **Martensitic stainless / corrosion resistant steel.**
  Contains at least 11.5% chromium such as Cr13 and Cr17 steel. Most gas wells

in the Netherlands are completed with L80 13 Cr tubing in order to limit maintenance and, if necessary, to be able to produce from the Zechstein. Martensitic steels are not very corrosion resistant and are susceptible to sulphide stress cracking, which makes them ineffective in H2S environments. On the other hand, they are extremely resistant to chloride stress cracking (CSC).

- **Super martensitic stainless steel.**
  Contains less carbon and more nickel and molybdenum, and is more resistant to corrosion than normal martensitic Cr13 steel.

- **Ferritic-austenitic steel alloy**.
  Also known as duplex steel, this type of steel contains chromium, manganese, nickel, vanadium and molybdenum. As the name suggests, it is a mixture of austenitic and ferritic steel. It is much stronger than austenitic steel, and is also more resistive to corrosion pitting and stress cracking than regular austenitic steel. The overall corrosion resistance is also better than that of regular austenitic steel. They are characterised by low carbon content, high chromium (at least 20%) and molybdenum content (3-5%), and low nickel content (less than 5%) compared to austenitic steel. Cr22 is the most frequently used duplex steel in the oil industry. Superduplex steel (Cr25) contains significantly more nickel and molybdenum.

## 3.6    **Susceptibility to pitting corrosion**

Susceptibility to pitting corrosion can be estimated according to the Pitting Resistance Equivalent Number (PREN) of the metal in the respective geothermal installation and by determining the open circuit potential (OCP) and the critical pitting potential (Ep) or the repassivation potential (Er).

Certain elements within the steels and alloys make the metal particularly resistant to corrosion. These main elements are Cr, Mo, N, Si, and W (Frankel, 2003). The PREN is calculated from the weight fractions of these elements in the steel. The most commonly used version of the formula is:

$$PREN = Cr + 3.3Mo + 16N \qquad \text{Eq. 3}$$

To prevent pitting with seawater a minimum PREN of 32 is required at 20°C. However, higher temperatures and salinity have more impact on corrosion. In this case the PREN values will need to be higher. Salinities are often higher than seawater in formation waters commonly encountered in the Netherlands at relevant depths. Therefore, PREN values of steels and alloys given in Table 3.3 provide only a ranking of the metals and do not conclusively state whether pitting corrosion will occur.

| Stainless steels (RVS) | | Alloys | |
| --- | --- | --- | --- |
| **Type** | **PREN** | **Type** | **PREN** |
| 304 | 19 | 316L | 25 |
| 316 | 26 | 318LN | 35 |
| SAF 2304 | 26 | 904L | 36 |
| LDX 2101 | 26 | 625 | 52 |
| 317 | 30 | Ti gr. 2 | 54 |
| 2205 | 35 | | |
| 904L | 36 | | |
| SAF 2507 | 43 | | |
| 254 SMO | 43 | | |
| 654 SMO | 56 | | |
| DSS 2205 | ~35 | | |
| SDSS 2507 | ~42 | | |
| Hyperduplex 3207 | ~50 | | |

Table 3.3 PREN values for several stainless steels and alloys (Drijver, 2014, Mundhenk et al. 2013, Popoola et al. 2013).

The prediction of pitting in a geothermal doublet is possible by determining the open circuit potential (OCP) and the critical pitting potential. The following is generally accepted (Pohjanne et al., 2008):

OCP ≤ Ep: no risk of pitting corrosion

OCP ≈ Ep: pitting corrosion may occur

OCP ≥ Ep: pitting corrosion will occur

Some authors advise to apply the difference between the OCP and the repassivation potential (Er) for determining pitting stability (Blasco-Tamarit et al., 2008). OCP, Ep and Er are specific for each brine/metal combination and are temperature dependent (Mundhenk et al., 2014). Therefore, we rely on experiments to determine these values for each specific case of parameters. It is possible to make a rough estimate of the OCP and Ep without conducting experiments by consulting previous experiments with identical metal, identical pH and a similar water composition. The OCP can also be directly measured in the geothermal installation (above ground).

# 4    Corrosion prediction models

Many different models are used in the oil- and gas industry to predict the uniform corrosion rate. Except uniform corrosion, some models also predict (the risk of) 'localized attack' or pitting corrosion. An excellent overview is given by Nyborg (2010). The main characteristics of the models are listed in Table 4.1.

| Model | DW | NO | HY | CO | CA | KS | MU | EC | PR | TU | UL | CP | OL | SW |
|---|---|---|---|---|---|---|---|---|---|---|---|---|---|---|
| Lab data, **F**ield data model, **M**echanistic model | L | L | M | F | L | M | M | L | L | M | F | L | M | L |
| Scale effect formation water* | N | M | N | W | W | M | M | W | S | S | | M | W | W |
| Scale effect condensed water* | W | M | W | W | W | M | M | W | S | S | | M | M | W |
| Effect of pH on corrosion rate* | W | M | W | M | W | M | M | W | S | S | S | M | W | W |
| Risk for localized attack | | | | Y | | Y | | | Y | | Y | | | |
| Oil wetting effect crude oil* | S | N | M | M | N | N | S | S | S | N | S | M | N | N |
| Oil wetting effect condensate* | N | N | N | M | N | N | M | M | M | N | S | M | N | N |
| CaCO₃ correction for pH | | | | Y | | | Y | | | | | | Y | |
| Effect of organic acid on corrosion | | | Y | Y | Y | | Y | Y | Y | | | Y | | |
| Top of line corrosion | Y | | Y | | | | Y | Y | | | Y | | | |
| Effect of H₂S on corrosion rate* | N | N | W | N | N | N | M | S | S | N | W | N | S | N |
| Multiphase flow calculation** | N | P | M | P | N | N | P | M | P | P | M | M | N | N |
| Max. temperature limit °C | 140 | 150 | 150 | 150 | 140 | 150 | 100 | 140 | | 115 | | 150 | 120 | 120 |
| Max. CO₂ partial pressure bar | 10 | 10 | 20 | 20 | 10 | 20 | 20 | 20 | 70 | 17 | | 10 | 20 | |
| **O**pen, **C**ommercial, **P**roprietary | O | O | P | O | O | O | P | C | C | P | P | P | C | P |

\* S - strong effect, M - moderate effect, W - weak effect, N - no effect
\*\* P - point calculation, M - multiphase profile calculation, N - no multiphase flow calculation

Table 4.1    Major factors in CO₂ corrosion prediction models. The maximum CO₂ partial pressures are limited to 10 or 20 bar. The 'PR' model (Honeywell Predict) is based on the DW model (De Waard and Milliam) which is limited to 10 bar. Hence, the claimed 70 bar limit for PR may be exaggerated (Nyborg pers. comm.). NORSOK M-506 (NO) and MultiCorp (MU, in a limited version named FreeCorp) are freely available and can be found on the Internet. Five out of fourteen models are mechanistic. Derived from Nyborg (2010).

The models can be grouped in three classes with respect to their approach (Nesic, 2007:

- Mechanistic models have a strong theoretical approach and describe the underlying (electro-)chemical reactions and transport processes. If this kind of model is calibrated well to experimental (laboratory and / or field) data, it is possible to interpolate as well as extrapolate results. However, even after decades of research, the underlying chemical processes, as well as the interaction with scaling, are still not completely understood.
- Empirical models have little or no theoretical background. Most constants used in these models do not have a physical meaning, unlike those in mechanistic models. In case this kind of models is used within the limits for which experimental data are available, they can make reliable predictions. Extrapolation is precarious.
- Semi-empirical models can be positioned between mechanistic and empirical models.

Figure 4.1 shows how $CO_2$ corrosion can be predicted, taking all relevant mechanisms into account (IFE, 2009). Only a few of the models discussed by Nyborg (2010) are capable of dealing with all mechanisms. In practice, the major differences in the predictive force of these models can be attributed to the way in which the effects of protective scales and oil wetting are taken into account in the prediction (Nyborg, 2010). *'Some of the models have a very strong effect of oil wetting for some flow conditions, while other models do not consider oil wetting effects at all. Some models include strong effects of protective iron carbonate films especially at high pH or high temperature. These models rely on easy formation of protective corrosion films and absence of localized attack, while the models with weak effects of protective corrosion films assume that the films have only limited protectiveness or that there is a high risk for localized attack'* (Nyborg, 2010).
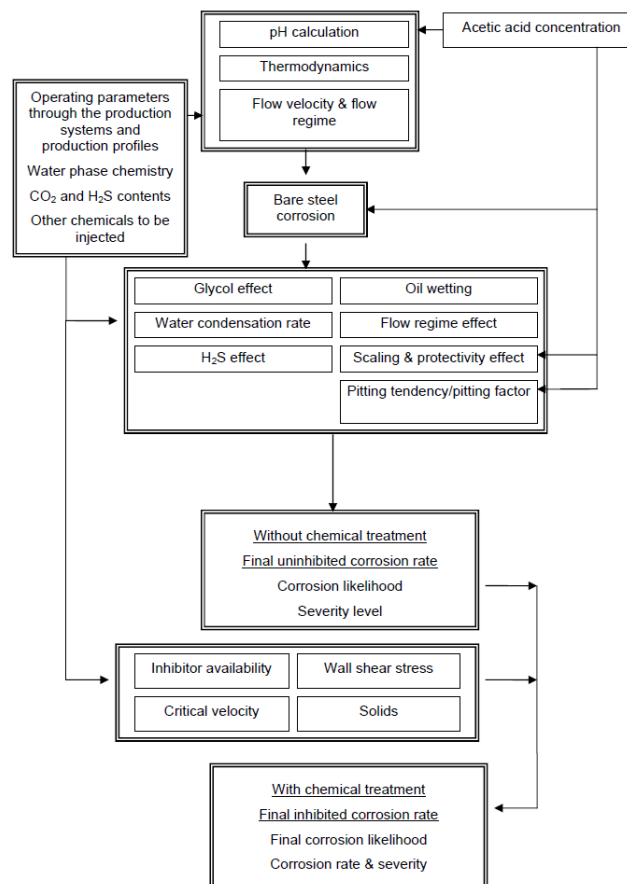


Figure 4.1  Example of the prediction of $CO_2$ corrosion, including all relevant mechanisms (derived from IFE 2009).

Most of the models were developed for the oil and gas industry. The effect of water wetting[7] is very important. Unlike geothermal wells, the major liquid produced is oil or gas rather than water. Therefore, for these models it is very important for corrosion prediction to know if and how the co-produced water is able to reach the casing steel. If enough oil is present to prevent the water from reaching the casing, no (brine-induced) corrosion will take place. The process of water wetting is very difficult to predict.

---

[7] Wetting is the ability of a liquid to maintain contact with a solid surface

One of the major $CO_2$ corrosion prediction models, NORSOK, which is developed by the joint Norwegian petroleum industry, therefore supposes that water wetting will always occur. A major conclusion of the model comparison study by Nyborg is that, after years of intense research, the prediction of $CO_2$ corrosion is still uncertain. Olsen (2003) states that in the oil and gas industry a tendency exists to move away from the use of prediction models in favour of focusing on the proper use of inhibitors and extensive monitoring. A successful operation therefore mostly depends on the proper use of inhibitors. Olsen further states that no universally standard exists for the prediction of $CO_2$ corrosion.

## 4.1    Empirical models

Most models consider the effects of oxygen, carbon dioxide, hydrogen sulfide, pH and temperature on corrosion rate, within the for the oil and gas industry relevant limits (Figure 4.1). Hence, the laboratory experiments on which the models listed in Table 4.1 are based, were calibrated to these parameters. Water is subordinate to oil and gas, which is in contrast to geothermal applications. Salinity and the composition of the formation water (e.g. the presence of metal ions – see Figure 3.10) largely lack in this list. De Waard is the author of Shell's De Waard – Milliams model which has long been the most widely used $CO_2$ corrosion prediction model (De Waard and Milliam, 1975). According to De Waard the experiments which underly these models are carried out using fresh water with dissolved $CO_2$, to which a little salt is added so the conductivity of the water will not be an issue (pers. comm. De Waard). Nesic (2007) presumes that 'probably one of the most influential parameters affecting $CO_2$ corrosion is the water chemistry'. Table 4.2 (from Nesic, 2007) lists some major occurring reactions in oil and gas fields but is not exhaustive (for instance, gypsum and calcite reactions are not listed). Nesic also poses that the specification of the water can be simple if only condensed water is co-produced with gas, or 'very complex with numerous species found' for formation water being co-produced with crude oil. A proper understanding of the chemical composition of the formation water is an important condition for being able to predict $CO_2$ corrosion, especially if the concentration is high (>10 wt%) because in that case the 'infinite dilution theory' does not hold – a correction should be applied for the fact that the solution is not ideal. For relatively low salinity (a few wt%) this can be achieved by using the concept of 'ionic strength'[8]. This is for instance used by the NORSOK M-506 model for calculation of the pH. This model accepts a maximum salinity of 175 g/l (NORSOK, 2005), which is roughly close to the average value for Dutch geothermal wells. This indicates that, from the point of salinity, the average Dutch geothermal system is already close to the application limit of the NORSOK model.

---

[8] Ionic strength is the concentration of all ions in solution It is equal to the sum of the molality of each type of ion present multiplied by the square of its charge: $I=\Sigma m_i z_i^2$ (source: Oxford Dictionary of Chemistry). One of the main characteristics of a solution with dissolved ions is the ionic strength.

| | Reaction | Equilibrium constant |
|---|---|---|
| Dissolution of carbondioxide | $CO_2(g) \Longleftrightarrow CO_2$ | $K_{sol} = C_{CO_2}/P_{CO_2}$ |
| Water dissociation | $H_2O \overset{K_{f,wa}}{\underset{K_{b,wa}}{\Longleftrightarrow}} H^+ + OH^-$ | $K_{wa} = C_{H^+}C_{OH^-}$ |
| Carbondioxide hydration | $CO_2 + H_2O \overset{K_{f,hy}}{\underset{K_{b,hy}}{\Longleftrightarrow}} H_2CO_3$ | $K_{hy} = C_{H_2CO_3}/C_{CO_2}$ |
| Carbonic acid dissociation | $H_2CO_3 \overset{K_{f,ca}}{\underset{K_{b,ca}}{\Longleftrightarrow}} H^+ + HCO_3^-$ | $K_{ca} = C_{H^+}C_{HCO_3^-}/C_{H_2CO_3}$ |
| Bicarbonate anion dissociation | $HCO_3^- \overset{K_{f,bi}}{\underset{K_{b,bi}}{\Longleftrightarrow}} H^+ + CO_3^{2-}$ | $K_{bi} = C_{H^+}C_{CO_3^{2-}}/C_{HCO_3^-}$ |
| Acetic acid dissociation | $HAc \overset{K_{f,ac}}{\underset{K_{b,ac}}{\Longleftrightarrow}} H^+ + Ac^-$ | $K_{HAc} = C_{H^+}C_{Ac^-}/C_{HAc}$ |
| Hydrogen sulphate anion dissociation | $HSO_4^- \overset{K_{f,HSO_4^-}}{\underset{K_{b,HSO_4^-}}{\Longleftrightarrow}} H^+ + SO_4^{2-}$ | $K_{HSO_4^-} = C_{H^+}C_{SO_4^{2-}}/C_{HSO_4^-}$ |

Values for various constants are readily available elsewhere [17].

Table 4.2   Some chemical reactions typical for the formation water in oil- and gas fields, and their equilibrium constants (derived from Nesic, 2007).

It is very important to know to which range of parameters the models have been calibrated. Most models described in Nyborg (2010) were calibrated to a $CO_2$ partial pressure of 10 - 20 bar. As was already pointed out in paragraph 3.2.4, a higher $CO_2$ partial pressure typically leads to a higher corrosion rate. This is illustrated by Figure 4.2.
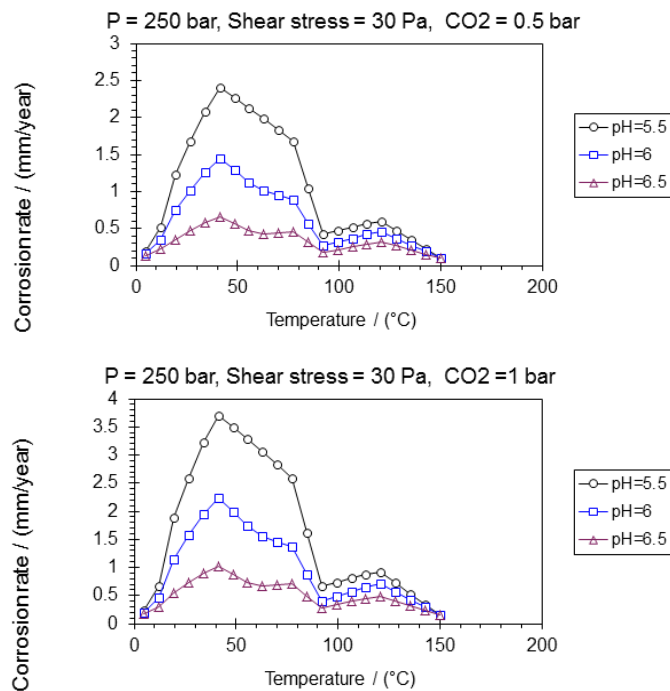


Figure 4.2   NORSOK M-506 corrosion rate in a relevant temperature range at varying pH levels, at 250 bar reservoir pressure and 0.5 (upper) and 1.0 (lower) bar $CO_2$ partial pressure. The correlation with both pH and temperature is large. Note the different ranges of the y-axis.

T = 100 °C, Shear stress = 30 Pa,  CO2 = 3 mole%
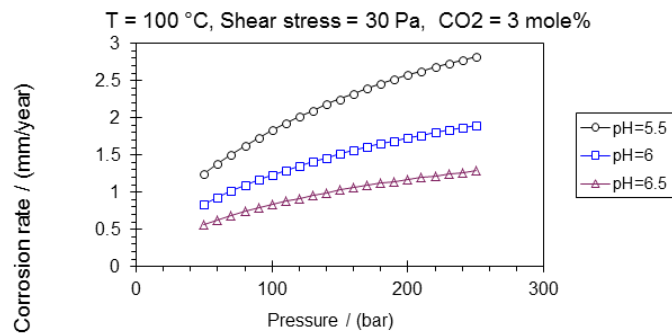
Figure 4.3 NORSOK M-506 corrosion rate in a relevant pressure (depth) range at varying pH
levels, at 100°C temperature and 3 mole% $CO_2$. There is a strong positive correlation
of corrosion rate and pressure (depth).

Figure 4.2 shows a general output graph of the NORSOK M-506 model. Note that
the results of this graph cannot easily be translated to the Dutch situation, given the
widely varying $CO_2$ content of the measured gases. The increase in corrosion rate
between 10 and 50°C is supposed to be due to the fact that corrosion enhancing
processes – electrochemical, chemical, transport - have a positive correlation with
increasing temperature, while protective scales are not precipitating. The strong
decrease of corrosion rate from 80°C onward is probably caused by the formation
of protective scale (although the NORSOK software does not allow the chemical
composition of the brine to be specified, and hence the amount and nature of the
protective scale can hardly be estimated). An increased pH decreases the solubility
of $FeCO_3$, and enhances the formation of protective scale. Therefore 'pH
stabilisation' (increase) may be an attractive option for decreasing the corrosion
rate. An increase of the pH will on the other hand lead to decreased solubility of iron
carbonate, increased precipitation and higher scaling tendency (Nesic 2007).
Therefore, it may well prove less useful for the Dutch formation water systems with
high salinity.

Figure 4.3 is a similar graph, but has pressure (depth) as horizontal axis. The
corrosion risk strongly increases with pressure (depth), so the conclusion is that the
corrosion risk is higher at larger depth.

More recently, models are being developed that predict corrosion rates in pipelines
used for $CO_2$ transport (CCS, EOR). The major differences with the corrosion
models known from the oil and gas industry are:

- Because of the higher $CO_2$ pressure, the pH is lower. Therefore, the solubility of
the corrosion products is higher, and the formation of protective scales is
inhibited. The potential corrosion rate is higher.
- Oxygen plays an important role
- If the $CO_2$ contains $SO_2$ and $NO_x$, these components may dissolve in the water
phase, thereby lowering the pH further.

In this kind of systems, $CO_2$ is not one of the dissolved components, but the main
component in which water can dissolve. Although 'dry' $CO_2$ in itself is not corrosive,
the potential corrosion rate increases if the $CO_2$ is not pure but, for instance,
contains water (Dugstad et al. 2011: *'free water can give both corrosion and hydrate
formation.*

*There is no consensus on what the actual target for the maximum water concentration should be. [..] Presently, the corrosion rate in a pipeline suffering from accidental water ingress cannot be estimated accurately due to lack of corrosion data'*). In the DYNAMIS project (Dugstad et al. 2011) it is stated that the concentration $H_2O$ (dissolved in $CO_2$) should not exceed 500 ppm. This has to do with the requirements concerning the purity of $CO_2$ for various applications. For storage this is >90% while for EOR >95%). It is clear that these $CO_2$ contents are not relevant to geothermal projects.

The electro-chemistry of the solution of mild steel in $CO_2$ is largely understood and modelled. Nesic (2007) concludes however that although *'understanding internal corrosion [..] has come a long way over the past few decades' [..] 'some mayor challenges [lie] ahead'*. This is illustrated by Figure 4.4. It shows that, for this specific test case, there is a wide spread in predicted (uniform) corrosion rates. The measured corrosion rate is lower than predicted by most models in the deeper subsurface. The high measured rate in the shallow subsurface is not reflected in most models either. Note that most models predict uniform corrosion, as localised attack, being associated with the formation of particularly protective scales, is difficult to predict.
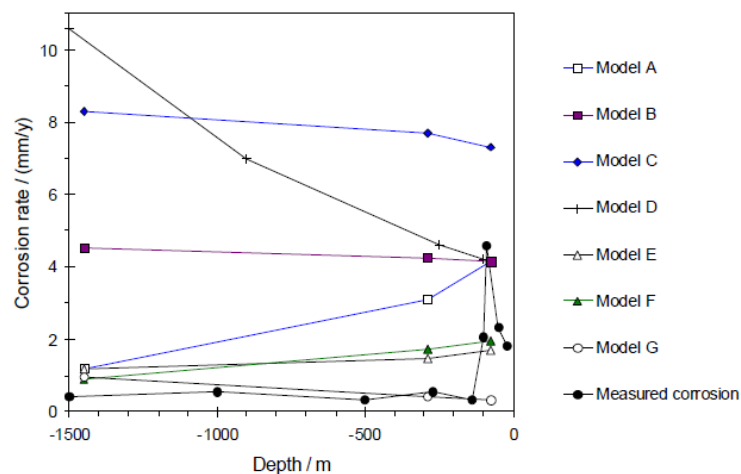


Figure 4.4  Modelled and measured corrosion rates at various depth in a test oil well (derived from Nyborg 2010). Especially at large depth, the modeled rates show a large spread.

In general, one should note that the oil and gas industry corrosion models have not been calibrated for use in geothermal systems, and that the effects of natural inhibitors and/or protective scales can not really be taken into account. Hence, the application of these models to the geothermal industry is very uncertain and the calculated corrosion rates should at best be considered to be indicative.

## 4.2    Mechanistic models

Alt-Epping et al. (2013) described a strongly mechanistic approach to corrosion, fitted to a geothermal system in Bad Blumau (Austria). This approach is very different from most of the corrosion prediction models known from the oil and gas industry that were described above. The FLOTRAN flow and transport model (Lichtner, 2007) uses abundant field data to 'determine whether there are chemical

fingerprints detectable at the surface, which could indicate that corrosion is commencing at some point within the production or injection wells'.

The Bad Blumau doublet produces water of 120°C from a depth of about 2800 meters at a rate of about 80 m³/hr. The reservoir consists of Palaeozoic carbonate rocks. The reservoir brine contains elevated concentrations of dissolved $CO_2$ (0.4 molal, 95% of the gas, with minor nitrogen and methane) which is removed from the brine during degassing, thereby causing carbonate precipitation. The pH is just about 5.7 (reservoir level), and about 7 after degassing. The TDS is very low, around 20,000 mg/l. The inhibitor used to prevent scaling is a polyphosphate-type one which is injected at a depth of 500 meters, which is below the bubble point.

The result of the FLOTRAN approach followed by Alt-Epping et al. is a number of modelled concentration profiles along the entire well trajectory, for key indicators like minerals, elements and pH (Figure 4.5). As they included models runs with and without possible corrosion, and with and without carbonate inhibition, the installation of monitoring probes at a number of key locations in the surface system, and comparison of the monitored values with the modelled values, will enable to make predictions about possible subsurface corrosion. From Figure 4.5 it can for instance be concluded that an increased concentration of $Fe^{2+}$ near surface level will be indicative of corrosion in the production well. A high corrosion rate may result in siderite saturation. Similarly, the model predicts a shift from dolomite and calcite dominated scales to various iron carbonates if inhibitors are used.
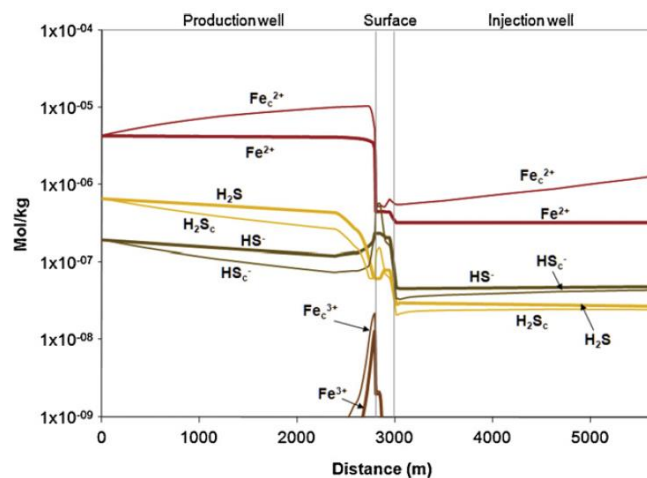


Figure 4.5  Profiles of the Fe and $S^{2-}$ speciation through the production and injection wells with and without corrosion of the borehole casing. Labels with subscript c indicate profiles with corrosion (derived from Alt-Epping et al. 2013).
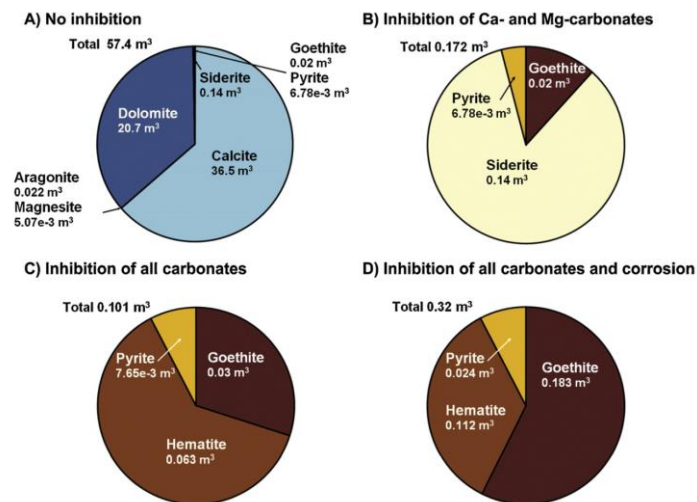
Figure 4.6 Computed integrated mineral volumes (m³) forming within the production well between the point of $CO_2$ gas separation and the head of the well, after 2 years of operation. Shown are different inhibition scenarios and the effect of corrosion (derived from Alt-Epping et al. 2013).

The last conclusion drawn by Alt-Epping et al., well worth mentioning here, is that *'chemical monitoring of geothermal systems should involve regular sampling and analysis of the fluid composition in addition to the mineral scales'*. Given the utmost importance of the field data used, this makes the model difficult to apply elsewhere without re-calibration. However, the approach seems promising.

# 5 Corrosion prevention measures

Degassing is probably the most efficient way to impede corrosion in the Dutch doublets. However, the expulsion of $CO_2$ increases the pH, thereby possibly leading to scaling, and it will not protect the production well and the part of the installation before the degasser. Therefore, other methods for corrosion protection need to be addressed.

## 5.1 Natural inhibitors

Crude oil, like for instance produced at the Pijnacker-Nootdorp and, to a lesser extent, the Honselersdijk production locations, is an effective natural inhibitor in a production well, comparable with the way inhibitors like tannic acids work. It is known that measured corrosion rates do not match those of laboratory experiments if crude oil is present in the produced water. Oil forms a passivating film on the casing surface and thereby prevents water from getting into contact with steel (decreasing the 'wettability'). A second effect oil has is that certain components, like saturates, aromatics, resins, asphaltenes, nitrogen and sulphur contribute to inhibition, but little is known about its precise nature and effectiveness (Nesic, 2007). Natural oil cannot be used in the injector well. After cooling the geothermal water, the oil becomes viscous. In some water injection wells in the Netherlands, it tends to clog the injector well, thereby requiring regular clean-ups, using HCl/solvent solutions.

## 5.2 Synthetic inhibitors

A description of the effect inhibitors have is not trivial (Nesic, 2007). The known literature uses such descriptors as 'inhibitor factors', 'inhibitor efficiency' (e.g. the NORSOK model) and 'molecular modelling'. A common approach describes the 'surface cover', or the part of the steel surface that is effectively covered by the inhibitor. The degree of protection is considered to be equal to the percentage surface coverage. The inhibition mechanism is attributed to the strong adsorption ability of the selected inhibitors on steel surface, forming a good protective layer, which isolates the surface from the aggressive environment (El-Lateef et al. 2012).

El-Lateef et al. (2012) provide a comprehensive overview of corrosion protection of steel pipelines against $CO_2$ corrosion. They describe three types of inhibitors:

- *'Inhibitors that can displace depolarizers[9] ($HCO_3^-$ ions and $H_2CO_3$ and $CO_2 \cdot H_2O$[10] molecules) from the surface of the metal.*
- *Inhibitors, which can form films of the mixed type, those are impermeable to depolarizers.*

---

[9] A depolarizer is an electroactive substance, i.e., a substance that undergoes a change of oxidation state, or the breaking or formation of chemical bonds (McNaught and Wilkinson 1997)
[10] In fact $CO_2 \cdot H_2O$ is not a molecule. There is $H_2O$ and $CO_2(aq)$ which make together $H_2CO_3^*$ (as a convention)

- *Inhibitors that can form bonds with depolarizers ($HCO_3^-$ ions and $H_2CO_3$ and $CO_2 \cdot H_2O$ molecules'.* These chemical bonds are between the hydrophilic head of the inhibitor molecule and the steel surface.

They also conclude that 'the inhibitor for $CO_2$ corrosion should be chosen on the basis of the pH and temperature, as well as the initial condition of the metal surface (the type of film and/or deposits on the surface of the metal being protected)', and that 'most corrosion inhibitors used in oilfields are organic compounds, containing nitrogen or sulfur functionalities'.

In the literature studied, few specific inhibitors are mentioned. Often, only a broad description of the nature of the inhibitor is given. Many are tannic acids (Dutch: 'looizuur') that form a protective layer on the casing steel, preventing corroding elements from reaching the steel. Tannic acid acts as a cathodic-type corrosion inhibitor (see below), retarding the cathodic process of the corrosion reactions by forming ferric tannates on the mild steel surface (Qian et al. 2013) Qian et al. further state that *'varying opinions about the effect of tannins used as inhibitors abound. Some researchers agree that tannins can react with steel to form a crazed layer of ferric tannates, which serves as an electrical insulator to delay the initial stage of rusting. The effect of tannins is strongly dependent on the process of corrosion product formation, pH, and solution concentration.*'

**Anodic inhibitors** (so called passivators) are chemical substances that act by forming a protective oxide film on the surface of the metal. This layer is passive towards corrosion. In such a way, it operates in a similar way to a protective scale, with the major difference being that a protective scale is formed from the 'native' brine. Some examples of anodic inhibitors are chromates (salts containing $CrO_4^{2-}$), soluble hydroxides, phosphates (Chilingar et al., 2008), molybdate, nitrite and orthophosphate and imidazole.

**Cathodic inhibitors** act by either slowing the cathodic reaction itself or selectively precipitating on cathodic areas (i.e. the area on the steel where the reduction takes place) to limit the diffusion of reducing species to the surface (Metrohm Autolab, 2011). Cathodic reaction rates can be reduced by employing cathodic poisons[11]. However, cathodic poisons can also increase hydrogen induced cracking since hydrogen can also be absorbed by the metal during aqueous corrosion or cathodic charging. Some examples of inorganic cathodic inhibitors are the ions of the magnesium, zinc, and nickel salts that form the insoluble hydroxides which are deposited on the cathodic site of the metal surface (Chilingar et al., 2008). Other examples are polyphosphates, phosphonates, tannins, lignins and calcium salts (Dariva and Galio, 2014).

**Mixed inhibitors** work by reducing both the cathodic and anodic reactions. They are typically film forming compounds that cause the formation of precipitates on the surface blocking both anodic and cathodic sites indirectly (Bressers, 2014).

---

[11] A 'cathodic poison' impedes the reduction reaction (proton reduction to $H_2$), for instance by forming a barrier on the electrolyte – metal interface.

## 5.3    Evaluation of corrosion inhibitors

The effectivity of inhibitors can be tested during laboratory corrosion simulation and corrosion loops. In this way an optimal inhibitor (dose) can be chosen. A current-potential curve can be obtained during the experiments to monitor corrosion with and without inhibitor (see Appendix C).

Instead of using the polarisation method described above, which requires the use of a relatively expensive potentiostat, one can also use a linear polarisation resistance measurement (LPR). The LPR however only measures in a small potential region around the open-circuit potential and only results in a corrosion resistance and sometimes the value of the open circuit potential. This can however be enough for a first indication on the effect of the inhibitor (Bressers, 2014).

## 5.4    Protective scales

Although the presence of $CO_2$ and $H_2S$ promotes corrosion it may also trigger the growth of a protective layer made of siderite ($FeCO_3$) or mackinavite ($FeS_{1-x}$), respectively, on the metal surface. The precipitation of siderite and mackinavite occurs under specific pH, temperature and concentrations of the dissolved gasses. This layer is often referred to as a passivation layer because it may shield from further corrosion. Siderite precipitation increases with higher temperatures. Nesic (2007) states that *'at room temperature, the process of precipitation is very slow and unprotective scales are usually obtained, even at very high supersaturations. Conversely, at high temperature (e.g. >60°C) precipitation proceeds rapidly and dense and very protective scales can be formed even at low supersaturation'*. Banas et al. (2007) state however that *'iron does not form corrosion resistant stable oxygen film in oxygen-free water saturated with $CO_2$ and $H_2S$'*.

With the aid of Pourbaix diagrams, Mundhenk et al. (2013) indicated the growth of siderite, which was further supported by experiments at a temperature of 80°C, 1 M $Na^+$ and $Cl^-$ concentration and 0.05 M $Fe^{2+}$ concentration. Figure 5.1 suggests that a siderite layer will be formed in a pH range from about 4 to 8 and $E_h$/mV between -0.5 and 0. A change in temperature and water chemistry (metal concentrations and salinity) will cause the barrier between the $FeCl^+$ and $FeCO_3$ to shift in the horizontal direction. To be able to determine whether a protective layer will be formed in a certain location for a specific doublet, it is recommended to perform the calculation with the parameters retrieved from the brine at the specific location.
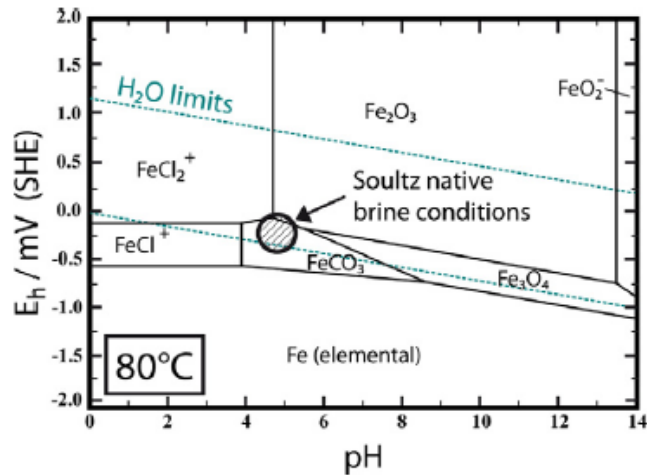
Figure 5.1 Pourbaix diagram for an Fe-C-Cl-Na-$H_2O$ system at 80°C, modelled for conditions of native Soultz geothermal brine (derived from Mundhenk et al. 2013a).

It is, however, not certain whether this passivation layer will have the quality to protect the underlying iron from further corrosion. The layer may be too thin, porous and/or deteriorate with time. A problem of the siderite layer is that a galvanic cell may occur between protected and unprotected areas of the steel that will cause further corrosion. It is, therefore, recommended to monitor the corrosion rate of the bare steel.

## 5.5      Passive and active anodic and cathodic protection

**Passive cathodic protection** safeguards the steel by putting it in electrical contact with a lower nobility material, like zinc (Figure 5.2, see also Figure 3.10). The zinc will become more positively charged and will corrode while the open-circuit potential of the iron becomes more negative (cathodic), which prevents the corrosion of iron and thereby of the steel used in the geothermal installation. Under 'normal' water conditions this would cause the evolution of hydrogen due to the reduction of water at the iron/electrolyte interface. This method is not suitable if the formation water contains significant amounts of metal ions that are more noble than iron like for instance lead, nickel or copper. In the case of the presence of lead ions metallic lead will deposit on the Fe surface near the zinc plate.
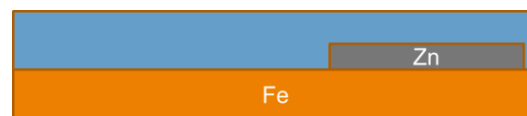


Figure 5.2 Schematic representation for the situation of passive cathodic protection (derived from Bressers, 2014). Blue = water, orange = metal e.g. casing.

In the **active cathodic protection** a dimensional stable anode (DSA) is placed close to the steel surface that needs to be protected. An external voltage is applied between the iron substrate and the DSA in order to create an electrochemical reaction (Figure 5.3). This will trigger an oxidation reaction at the DSA that will oxidize water or chloride. Both of the oxidation products, oxygen and chlorine, will very likely cause corrosion problems in the installation further along the water stream. Similar to the situation when using the passive cathodic protection it is very well possible that at the steel surface lead ions will be reduced (Bressers, 2014).

An **active anodic protection** uses a similar principle but with a dimensional stable cathode (DSK) which is placed in the electrolyte solution close to the steel surface (Figure 5.3). In this case the steel will act as the anode and oxidize, creating a passive oxide layer on the steel surface. The risk of metallic lead deposition is, however, equally present.
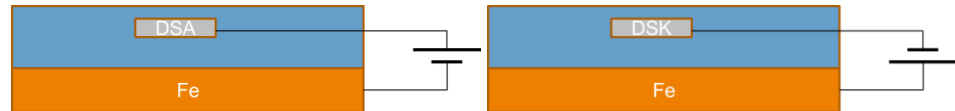


Figure 5.3 Schematic presentation for protection of the installation using active cathodic protection (left) and cathodic protection (right). (derived from Bressers, 2014). Blue = water, orange = metal e.g. casing.

## 5.6 Prevention of galvanic corrosion

Galvanic corrosion can be prevented by avoiding electrical contact of dissimilar metals in an assembly, by electrically separating the dissimilar metals with an insulating material or by physically insulating the environment from the metal surface with a coating impermeable to water (Bressers, 2014). However, complete prevention is often impossible as various metals are needed in the installation and an absolute coating cannot be obtained. The following practical measures should be considered to minimize the possibility and extent of galvanic corrosion (Zhang et al., 2011):

- Avoid combinations of dissimilar metals that are very far apart in the galvanic series.
- Avoid situations with small anodes and large cathodes.
- Isolate the coupled metals from the environment.
- Also be aware when making ground connections to the installation to avoid direct contact between two dissimilar materials through a direct connection via the grounding cables.
- Add cathodic and/or anodic inhibitors after establishing the optimal inhibitor.
- Use cathodic protection of the bimetallic couple with a rectifier or a sacrificiall anode.
- Increase the length of solution path between the two metals (mainly relevant for freshwaters).

## 5.7 Oxygen scavengers

In the case of oxygen presence, corrosion rates can also be reduced by the use of oxygen scavengers like amines, hydrazines, sulfites and (sodium-) bi-sulfites. *'These strong reducing agents are chemicals that react with the dissolved oxygen. Sulfite and bi-sulfite ions (for example Na $HSO_3$) are the best examples that form sulphates when reacting with oxygen. The redox reaction is catalyzed by either cobalt or nickel'* (corrosionpedia.com).

## 5.8 Factory coatings

Casings and production strings may be protected by a factory applied varnish coating ('japan black') during transport. This is a bituminous anti-corrosive paint. It is not removed during installation, but the layer may be damaged by chipping and scratching, either during transport or installation. Hence, it may continue to offer corrosion protection during the (early) lifetime of the well. It is not known how long this layer will remain intact, nor how well the offered protection is. It has been observed in a number of geothermal systems during inspection of the production string in the Netherlands that the string is virtually free of corrosion, while the couplings are corroded.

# 6 Corrosion monitoring and measurements

*'Pipework and vessels are always at risk of both corrosion and erosion, and continuous monitoring substantially reduces the risk of failure'* (Fuggle 2015). Several authors, for instance Fridriksson and Thorhallsson (2006) and Lopez et al. (2012) stress that monitoring of the geothermal reservoir and fluid produced is of utmost importance.

The first and foremost step towards corrosion prevention is the actual monitoring of potential corrosion (and the associated scaling). There are several ways of monitoring corrosion. Kolenberg et al. (2012) provide a good overview of current logging tools for wellbore monitoring, which, although aiming at Carbon Capture and Storage (CCS), is considered to be largely relevant for geothermal applications too. They differentiate between general leak detection, casing evaluation and cement evaluation tools. The following section on leak detection is based on this report.

## 6.1 Leak detection

Leak detection is a direct way of identifying flow in a well that should be static. he known methods are ultrasonic leak detection, surface wellhead pressure monitoring, downhole camera and temperature measurement.

Leakage above the reservoir results in inflow of relatively *low temperature* fluids (if the reservoir pressure at the leak is higher than the pressure in the tubing), or outflow of produced brine into the reservoir (if the reservoir pressure at the leak is lower than the pressure in the tubing). Hence, either the wellhead temperature of the produced water will become lower, or the flow rate less. Similarly, a change in the brine composition indicates inflow leakage from a different reservoir.
This method does not provide the location of the leak. Alternatively, when the temperature is measured using wireline tools (open wells) or pre-installed fibre-optic line (monitoring), the location can be found.

A *downhole camera* enables to view the wellbore directly, especially if the fluid is clear. A drawback of this method is that the ESP should be removed during the tripping of the camera. This method has successfully been applied in geothermal wells in Danmark for detection of scales.

The *production rate and pressure* are routinely measured at the wellhead. Depending on the reservoir pressure behind a potential leak, at a given production pressure the production rate will change (or, similarly, at a given production rate, the pressure will change). Like when monitoring the production water temperature, this method does not give the location of the leak. A *spinner log* can be used to find the actual location of the leak.

Finally, *ultrasonic leak detectors* or *noise logs* are able to find leaks through the detection of high-frequency noise due to turbulent flow. The sound is produced as gas travels from a high pressure situation to a low-pressure environment (Sizeland 2014). As the flow in geothermal wells is usually turbulent, it is currently not known whether these tools can also be useful here.

## 6.2 Casing integrity inspection logs

Bressers (2014) provides an overview of casing integrity inspection tools.
This section is largely copied from this report. Additional information was adapted
from the Kolenberg et al. (2012) report.

A *multifinger caliper* measures the internal radius of the casing in several directions
through the use of multifinger feeler arms. The amount of arms, ever increasing, is
currently up to 60. The multifinger caliper survey can measure anomalies both on
the inner and outer surfaces of the tubing or casing with an accuracy of ±0.127 cm
(Scientific Drilling product sheet).



Figure 6.1 Multifinger caliper tool (derived from http://www.sparteksystems.com).

*(Electro)magnetic thickness* logs are one of two available electromagnetic
measuring methods for corrosion monitoring. The tool is equipped with up to 18
arms on which multiple electro-magnetic induction (EM) sensors are mounted.
The sensors detect the thickness of the casing steel. Magnetic flux logs make use
of magnetic flux leakage (MFL) technology to determine the location, extent and
severity of corrosion and other metal loss defects in tubulars. Near locations of
defects such as corrosion or pitting, some of the flux may leak out of the pipe.
These leaks can be detected by the tools sensor arrays.
The magnetic thickness tool provides a measure for the thickness of the steel
casing. In combination with a multi-finger caliper, which gives a detailed image of
the casing inner diameter, a complete image of both the internal condition and the
external condition of the casing can be measured.

*Ultrasonic corrosion logs* employ a very high transducer frequency to measure
anomalies in the tubing or casing. The emitter sends out sound waves and the
detector measures the reflected response. It is able to provide information about
casing thickness, surface condition and small defects on both internal and external
casing surfaces. Apart from casing steel, an USIT (Schlumberger UltraSonic Imager
Tool) also 'sees' the cement bond but measures the steel thickness less accurately
than an EM tool.

Apart from the above mentioned casing integrity monitoring tools, Kolenberg et al.
(2012) also list *strain monitoring*: Strain is a measure of deformation. Strain in the
injection string can be monitored by the installation of a fibre-optic line.

Such a monitoring system is able to accurately measure changes in the strain, which in turn gives information about the integrity of the casing string at specific points along the entire string. The tool requires installation. It can be used in both fluid- or gas-filled un-cemented casing/tubing strings.

The major advantage of the casing inspection logs is that they monitor subsurface equipment. The disadvantages are the very high (rental) cost, and the fact that the combined effects of scaling and corrosion cannot be well distinguished when a single tool is used. A combination of multiple tools, such as caliper (measures casing inner diameter so detects scale and corrosion), EM (steel thickness, not influenced by scale) and possibly gamma ray (detects radioactive scale) enables to distinguish between various effects.

Table 6.1 provides an overview of which tools can be used in which stadium of the well life.

| | New well | Existing well | Operation | Abandon ment |
|---|---|---|---|---|
| Ultrasonic leak detector | + | + | + | -- |
| Surface wellhead pressure | ++ | ++ | ++ | + |
| Down hole camera | + | + | + | -- |
| Temperature logging | + | + | + | -- |
| Continuous temperature measurement | -- | -- | ++ | +/- |
| Multi-finger calliper | + | ++ | + | -- |
| Magnetic thickness | + | ++ | + | -- |
| Ultrasonic casing imager | + | + | + | -- |
| Strain monitoring | - | - | ++ | -- |
| CBL/VDL | ++ | ++ | ++ | -- |
| Ultrasonic imaging tool | + | + | + | -- |
| Segmented bond tool | + | + | + | -- |
| Water flow log | + | + | + | -- |
| Tracer logging | +/- | +/- | + | -- |
| Microseismics | -- | -- | + | + |
| Reservoir pressure monitoring | -- | -- | ++ | + |

| | |
|---|---|
| ++ | Primary choice for integrity assessment |
| + | Additional measurements for further assessment |
| - | Not suggested |
| -- | Unable to perform |

Table 6.1    Logging method selection (derived from Kolenberg et al. 2012).

## 6.3    Corrosion coupons

Coupons consisting of lesser[12] or similar material as the metal surface can be placed within the geothermal installation to predict general corrosion, crevice corrosion, pitting, stress corrosion cracking, embrittlement, and metallurgical structure-related corrosion. Galvanic corrosion can also be tested with such coupons. Furthermore, coupons can be used to determine the scale deposition rate.

---

[12] Lesser or more corrosion prone material means that a more conservative corrosion estimation is made.

The coupons have several limitations. An extended period of time is required to produce useful data, resulting only in average corrosion rates, and corrosion coupons can only measure corrosion in the part of the well in which they are placed (Bressers, 2014). Coupons are generally installed in the surface installation. Downhole installation is also possible but less easily inspected and/or replaced. Experimental laboratory results using coupons may be hard to translate to field experiments, especially if not all in situ conditions can be mimicked in the laboratory and / or bypass setting.

## 6.4 Electrochemical characterisation

Table 6.2 gives an overview of the suitability of electrochemical sensors for corrosion detection. Electrochemical noise measurements (ENM), electrochemical impedance spectroscopy (EIS) and linear polarization resistance (LPR) have been used extensively in downhole wireline corrosion monitoring at oil wells. Figure 6.2 shows the schematic set-up for EIS and LPR measurements (left) and electrochemical noise measurements (right). These measurements could also be performed ex-situ. In that case one has to be sure that the electrolyte resembles as much as possible the formation water. The best way would be to use formation water from a geothermal site. Care should be taken to keep the sampled fluid oxygen free. The pH of the electrolyte should be set by bubbling carbon dioxide gas through the electrolyte while measuring the pH. Of course, it should mimick the downhole situation as well. The use of these methods for the in-situ detection of lead deposition is not straight forward and is to our knowledge not published.
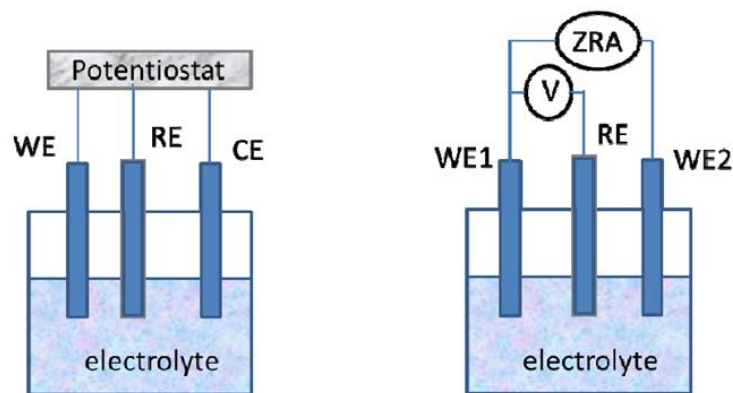


Figure 6.2 Schematic presentation of the set-up for electrochemical measurements. On the left-hand side is the set-up depicted for impedance and the linear polarization resistance measurements. On the right-hand side is the set-up for electrochemical noise measurements. WE is working electrode (material you want to investigate); RE is reference electrode, for instance a Ag/AgCl or a saturated calomel electrode (SCE) and CE is the counter electrode, which normally is a large area electrode. In the case of noise measurements two working electrodes are used of the same material.

| | LPR | EIS | ENM |
|---|---|---|---|
| Environments influence | No | Yes | Yes |
| Reference Electrode essential | Yes | Yes | No |
| Sample surface change | Yes | Yes | No |
| Easy data analysis | Yes | Yes | No |
| Result reproducible | Yes | Yes | No |
| Online data record | Yes | YES | Yes |
| Long term monitoring | No | No | Yes |

Table 6.2   Characteristics of LPR, EIS and ENM on corrosion monitoring.

## 6.5    On-site corrosion loop/skid
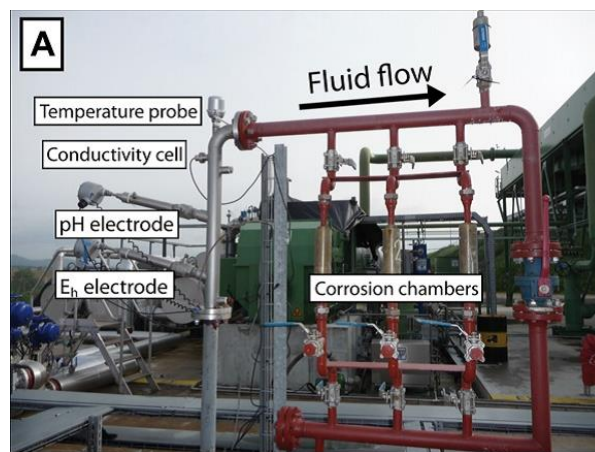


Figure 6.3 Example of an in-situ corrosion skid in the geothermal power plant at Soultz-sous-Fôrets, France (derived from Mundhenk et al., 2013a).

A corrosion loop is a section of tubing that is equipped with valves so that some of the stream is passed through a small pipe running parallel to the injection pipe at the surface of the well, thus creating a bypass (example Figure 6.3). Because the composition of this pipe is the same as the well tubing, it acts as a small-scale version of the well, which can be more easily monitored for corrosion and lead deposition (Bressers, 2014). This also offers a long-term monitoring solution and enables regular check-ups. This monitoring type is more expensive to install than the former, however less expensive than multifinger calipers. Corrosion loops can only be placed above ground. A possible setup scheme is shown in Figure 6.4. Several Dutch operators have already installed a similar loop in collaboration with Nalco.
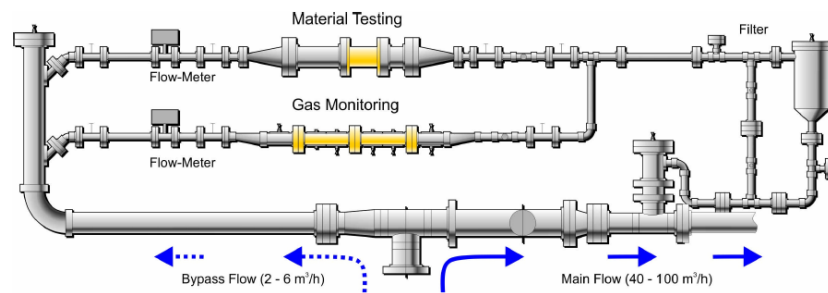
Figure 6.4 Possible setup for a corrosion loop. The flow of water is regulated by valves and is fileted before re-entering the main flow (derived from Schröder et al., 2007).

## 6.6 Laboratory simulations

The previous three examples describe monitoring techniques within the installation equipment (on site). Laboratory tests are performed off site, by recreating the geothermal environment in a laboratory. Such experiments are performed in a temperature and pressure controlled autoclave that contains the formation water from geothermal wells and the respective steel types (example Figure 6.5). Carbon dioxide is pumped into the autoclave to simulate $CO_2$ pressure and with it the pH. Most corrosion types can be recreated in such a setup. Corrosion can be characterised by inspecting the metal surface at the end of the experiment. Furthermore, electrochemical characterisations as discussed in Section 6.1.4 can be performed to in-situ monitor the corrosion processes.
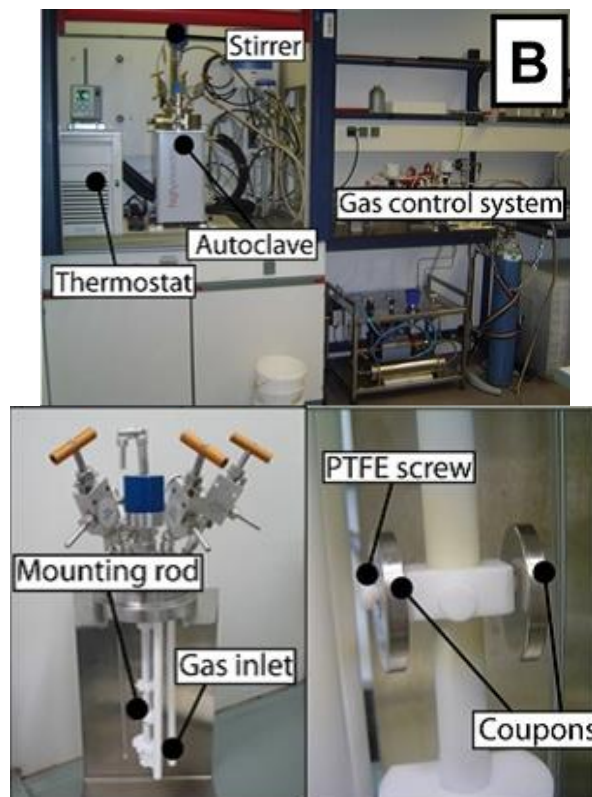


Figure 6.5 Experimental setup for autoclave experiments under geothermal conditions (derived from Mundhenk et al., 2013a).

The downside of autoclave experiments is that a continuous fluid flow-through in the order of 100-300 m³/hr, as present in geothermal doublets, is difficult to simulate. Also El-Lateef et al. (2012) state that *'corrosion rates seen in the field, in the presence of crude oil, are much lower than those obtained in laboratory conditions where crude oil was not used'*. It has also been noted that corrosion in autoclave experiments exceeds that of corrosion loops (Mundhenk, 2013). Hence, the experiments are thus only partly realistic.

Special flow loops offer a more advanced monitoring solution by circulating the fluid and alerting rates of fluid flow within the pipes (Figure 6.6). Their limitations are met as fluid renewal cannot be attained.
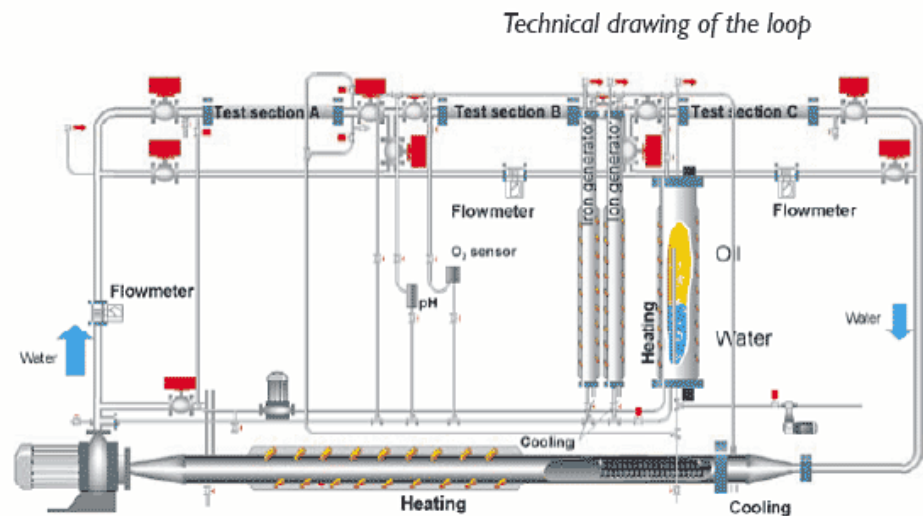


Figure 6.6 Technical design of a loop made out of hastelloy, a nickel-based alloy combining corrosion resistance with fabricability and high-temperature strength (derived from IFE website http://www.ife.no/en/ife/ife_images/petro/matkor/hastelloy-drawing.gif).

## 6.7 Manual field measurements

Manual measurements of wall thickness were carried out by Martin van der Hout of DAGO as part of the 'Industry Standard Corrosion Monitoring'. The instrument used was a portable ultrasonic Wall Thickness Gauge Model TI-25M. The measurements were carried out on a piece of horizontal production tubing, both on the lower and upper sides of the pipe. Disregarding the original thickness and hence corrosion rate, this yielded average thicknesses for the lower and upper sides of 8.67 (standard deviation 0.33) and 8.62 (0.43) mm. The measurement is very dependent on temperature. Therefore subsequent measurements can only be compared if the temperature during measuring was the same. The measurements do not provide an indication of scaling; the presence of scaling is deduced by the larger amount of noise during the measurements. Measurements taken at close distances along the production tubing (15 cm) may differ as much as 4 mm. Because the corrosion models that are in use in the Netherlands have not yet been validated or only to a limited extent, DAGO advises to measure the wall thickness at least three times, with one year periods in between. This ought, in principle, to be enough to establish a trend of wall thickness decrease with time.

Figure 6.7 Manual wall thickness measurement and disconnected piece of horizontal pipe between producer wellhead and separator (shown sideways), indicating 6mm of scale. Photo courtesy Martin van der Hout (DAGO).

# 7 Examples of corrosion in geothermal systems

The scientific literature about corrosion in deep wells is extensive. The majority is about applications in the oil and gas industry. However, the amount of publicly available publications about corrosion in geothermal wells, especially in research locations like Soultz-sous-Fôrets (France) and Groβ Schönebeck and Neustadt-Glewe (Germany) is already abundant and quickly increasing. Therefore this chapter does not pretend to give a complete overview of all relevant geothermal sites. An attempt was made to address the known literature of as many as possible relevant geothermal sites in the surrounding countries.

The literature consulted for this study was for a large part published in the Proceedings of the World Geothermal Congresses in Antalya (2005) and Bali (2010), the European Geothermal Congress in Pisa (2013), various NACE (National Association of Corrosion Engineers) conferences, and the journals Geothermics, Corrosion and Corrosion Science. www.corrosionpedia.com is a useful website for geothermal techno speak. Other corrosion studies include 'Control of corrosion and scaling in geothermal systems' (1996, European Joule program lead by BRGM (see paragraph 7.2) and 'Corrosion in geothermal plants' (2012) about the experiments conducted at the in situ laboratory Groβ Schönebeck (see paragraph 7.3.1)

Most of the publications emphasize the importance of temperature, gas and brine composition, and acidity (pH). In the Netherlands, the temperature is generally low (between 65 and 100°C). The gas collected from the Dutch geothermal wells does not contain measurable amounts of hydrogen sulfide. Instead, carbon dioxide is always present in varying amounts. The brines are always moderately to very saline, containing little sulphate (possibly reducing to hydrogen sulfide at pH 5-8 and 60-80°C). Therefore emphasis was put on collecting information from publications resulting from comparable conditions, without however a priori ignoring other publications. In order to make a valid comparison, the local geology should be addressed critically: in what way, and to which extent, are the described foreign doublets comparable to the Dutch situation in terms of temperature, gas and brine composition and acidity.

## 7.1 Experience abroad

The development of geothermal energy in the Netherlands started relatively late. After drilling the unsuccessful exploration well Asten-2 in 1987, the first successful geothermal well was Van Den Bosch-1 which was drilled as recent as 2007. Therefore, the experience gained abroad may serve as an example for the Netherlands. Especially France, Germany and Denmark, the nearest neighbours, could possibly be relevant for the Dutch situation, considering the comparable geology for a number of installations. However, about 90% of the total geothermal power in Europe is generated in Italy (expectation for 2015: 915 $MW_e$, 400 $MW_{th}$, mainly from Larderello), Iceland (830 and 310 resp.), Turkey (643 and 1250 resp.) and Hungary (3.5 and 1649, resp.) (Antics et al. 2013). For Italy, Iceland and Turkey these are high enthalpy installations and therefore in principle less relevant for the Dutch situation. Therefore, little attention will be paid to the literature from those countries in this section.

A significant part of the literature found is related to France and Germany, probably because in these two countries two well-known research facilities are located (Soultz-sous-Fôrets and Groβ Schönebeck), and because in the Paris Basin geothermal energy has already been exploited for a long time.

## 7.2 France

In France, hot water is being produced since 40 years from rocks belonging to the Middle Jurassic Dogger aquifer. Furthermore, recently a lot of experience was gained from the Soultz-sous-Fôrets triplet, located in the Rhine Valley in the Lorraine. This triplet feeds a power plant. In the remaining part of France a number of doublets is located (especially 13 in the Aquitanian Basin, mostly having very low geothermal power), but little information about those could be found in the publicly available literature – the vast majority concerns the Paris Basin and the Rhine Valley. Finally, in the French overseas territories (Guadeloupe and Martinique) two small geothermal power plants are located.

The information presented below about the Paris Basin was for a large part obtained from Lopez et al. (2010), Lopez et al. (2012) and Ungemach (2001). Information about Soultz-sous-Fôrets was obtained from Mundhenk et al. (2013a and b), Scheiber et al. (2013) and Baticci et al. (2010).

### 7.2.1 Paris basin

Fifty-five doublets have been drilled in the Paris Basin in the eighties of the last century, especially between 1980 and 1987. The first doublet, at Melun l'Almont, has been in use since 1969. Of these 55, 31 were in operation in 2008, which is about half the total amount of active doublets in France (the Aquitanian Basin coming in second). The most important problems encountered had to do with corrosion and scaling (Figure 7.1). Forty-two wells have been abandoned for technical or economic reasons. None of the doublets has encountered thermal breakthrough. Most difficulties due to scaling and corrosion have been overcome in the 1980s (Lopez et al 2012).
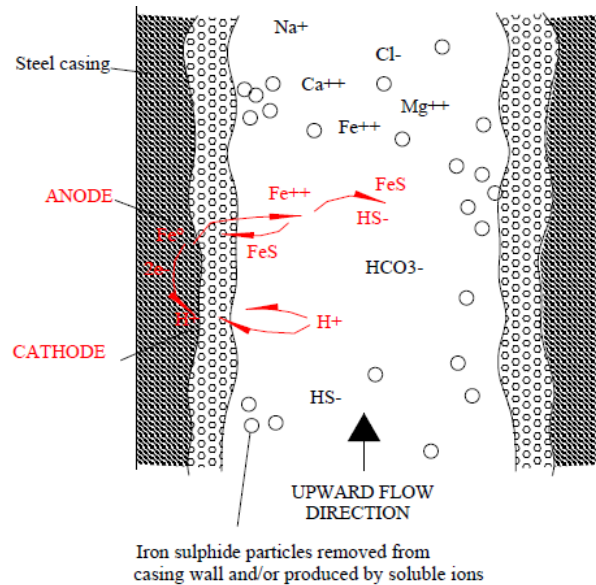
Figure 7.1 Dissolution of iron and precipitation of sulfide in the presence of hydrogen sulfide and carbon dioxide in the Paris Basin (derived from Ungemach, 2001). Microbiological corrosion by sulphate reducing bacteria occurs mainly in injection wells.

The aquifer rock is mainly limestone. The depth is about 2000 meters.
The temperature is between 55 and 80°C (gradient 3.5°C/100 meter). The salinity is between 6 and 39 g/l. The formation water contains abundant dissolved minerals, among which hydrogen sulfide (5-100 mg/l) and carbon dioxide (250-600 mg/l). The pH varies between 6.1 and 6.5. The gas to water ratio (GWR) is about 0.15. The casings are constructed using API K55 carbon steel.

After about four years of production the first corrosion (uniform and galvanic) and scaling problems occurred. This became apparent through an increase in required drawdown for maintaining the planned flow rate, an increase of the required injection pressure, and a decrease of the flow rate (Lopez et al. 2012), as well as perforated casings (in the Meaux doublet; Boissavy and Dubief, 1995). The wells were then mechanically cleaned to remove the scales, and measures were taken to prevent further corrosion. The corrosion and scaling problems were attributed to the chemical properties of the formation water, especially the large amount of hydrogen sulfide. Iron which is either released through corrosion, or naturally present in the reservoir brine, precipitates as iron sulfide, both on the casing as well as in the fluid (Figure 7.2).

In order to prevent corrosion, inhibitor is injected in the production well at casing shoe level by means of 'well bottom treatment tubing' (WBTT)[13]. At the injectors, the inhibitor is simply added at surface level. In this way, the entire trajectory is protected. The inhibitor is added constantly through a narrow injection line (Ungemach and Turon, 1988).

---

[13] WBTT is an epoxy-resin tubing, reinforced with fiber glass, which enables to apply inhibitor at bottom well level. This tubing has an outer diameter of about 40mm and a length of three meters (Boissavy and Dubief 1995). It has been used in the Meaux doublet in 1990. Later, in 1993, an improved version was implemented in the Beauval doublet. This version has an outer diameter of 19 mm. It is composed of incoloy and coated using Santoprene. This improved version has less pressure loss in the production well.

The applied inhibitors are organic compounds that contain ammonium salt and 'fatty' amines like strongly diluted sodium polyacrylate in low dose (5 ppm), which prevent particle growth like iron sulfide crystalization. The concentration is between 3 and 5 mg/l. The effectivity of the inhibitor depends on the degree to which a protective film can be formed. In general, the effectivity of the inhibitors is very large. The effectivity decreases when scaling is already present on the casings. In the latter case, it is advised to remove the scales first. In future doublets, it could be possible to use composite casing or a ceramic cover. Currently, these materials are not being used routinely because of the relative weakness of the material, the impossibility to apply it in deviated wells, and the limitation on logging wells that are completed in this way.

Lopez et al. (2010) remark that the costs of preventive measures are high, but still lower than the costs repairing and replacing corroded casings, and temporarily or permanent shutdown.

In general, it is noted that a high flow rate decreases both scaling and corrosion, while both low flow rates and temporarily ceasing production increase the corrosion risk. Degassing carbon dioxide at artesian flow rates is seen as very aggressive towards the casing.

It is concluded that the decisive factor for corrosion in the Paris Basin is the presence of hydrogen sulfide. Because this component is absent in the Dutch geothermal wells, it can be stated that a comparison of the corrosion behaviour in both environments is of limited use.

Finally it should be noted that in a joint effort all doublets contribute to the maintenance of a Dogger reservoir database. In this database a large amount of reservoir parameters is stored (notably flow rate, temperature, pressure and electricity usage). This database enables a detailed reservoir modelling. It is considered of great importance.

A recent study by Loizzo et al. (2015) goes into well integrity risk management for oil wells in the Paris Basin. Here, a risk was identified of pollution of the drinking water aquifer by well integrity failure. They conclude that 'the risk-assessment process revealed that casing corrosion caused by brine injection is the biggest driver of well-integrity risk; it also allowed tailoring effective prevention and mitigation actions. For instance, the criticality of scenarios is reduced to an acceptable level if the time between tubing failure and injection stop is kept to three months or less. Furthermore, the analysis helps define the role of periodic logging and thus reduce possible waste (i.e., actions that do not contribute to understanding, preventing, or mitigating risk.' They also state that in the Paris Basin 'the environment ministry [..] recommended a cement-bond log in every well, every 10 years to prove well integrity'. They also conclude that 'corrosion and cement evaluation logs have essential roles in charaterizing casing and cement barrier failures'. Annular pressure reading analysis helps in quickly detecting barrier failure.
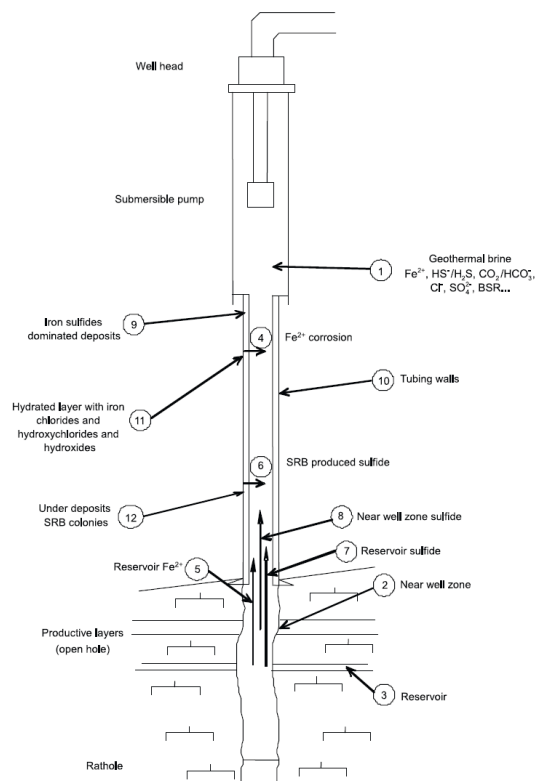
Figure 7.2 Schematic representation of well corrosion processes in a production well in the Paris Basin (derived from Lopez et al. 2010). SRB = sulphate reducing bacteria.

### 7.2.2 *Rhine valley graben (Soultz-sous-Fôrets)*

In Soultz-sous-Fôrets an ORC[14] geothermal power plant has been in operation since more than 20 years. The geothermal gradient is very high; at 800 meters depth the temperature is 120°C owing to the high heat flow of 100-120 µW/m², compared to 80 µW/m² in the surroundings (for the Netherlands, this is 56 – 70 µW/m² according to Bonté et al. 2012). The production water is extracted at larger depth from rocks belonging to the Triassic Buntsandstein and granitic basement. The temperature is 230°C. Although this temperature is not achieved in any of the Dutch doublets, Soultz is interesting for the Dutch situation anyway because of the vast amount of research since 1994 on corrosion that has being carried out at this location, especially because

- samples of the formation brine are being used for both 'weight loss' (long term) as potentio-dynamic polarisation (short term) experiments;
- Experiments are also conducted at temperatures around 70-80°C.

Near Soultz the geothermal plants of Landau and Bruchsal arefound just across the border in Germany.

---

[14] ORC: 'The Organic Rankine cycle (ORC) is named for its use of an organic, high molecular mass fluid with a liquid-vapor phase change, or boiling point, occurring at a lower temperature than the water-steam phase change. The fluid allows Rankine cycle heat recovery from lower temperature sources such as [..] geothermal heat [..].' Source: Wikipedia

The information presented below was especially taken from publications by Baticci et al. (2010), Mundhenk et al. (2013a and b), and Sanjuan (2010). Baticci et al. (2010) present an excellent chronological review of all corrosion experiments that were conducted at the Soultz location between 1997 and 2010. An important concluding remark by Baticci et al. (2010) is that, given the fact that formation water composition is one of the major influences on corrosion, a characterization of the formation water is of major importance.

The gas present in the formation water in Soultz contains a major amount of $CO_2$. This is an important observation taking into account the fact that, at temperatures between 60 and 100°C, $CO_2$ corrosion is important (e.g. Figure 4.2). According to Baticci et al. (2010) $CO_2$ amounts to 14.2 – 64% of the total gas content is, The partial pressure of this gas in the reservoir was estimated to be close to 6 bar. It is difficult to determine the exact amount of $CO_2$ (as well as the GWR) because no deep sample was taken from the wells. The analysed gas samples from the wells GPK-2 and GPK-4 were all taken at the well head during a circulation test in 2005.

In 1994 the application of corrosion inhibitor was started in the GPK-2 well. The chosen inhibitor, Mexel 432/0, in a 3-5 (in 1994-1995) and 4 ppm dose (in 1997, 8 kg/day at a flow rate of 2000 m³/d) reduced the corrosion to virtually nothing when applied at the production pump[15]. The effect of this inhibitor at temperatures 130 - 150°C is negligible (Muller et al. 2010). This is possibly of interest for the Dutch situation, as salinity, $CO_2$ and temperature are roughly within the same limits.

The first corrosion bypasses were built in 1997, with K55–C (with and without zinc coating), Uranus B6, Hastalloy and 316L stainless steel. Moderate corrosion was observed on the K55 steel. On the zinc coated K55 steel the coating had been corroded for 80%, but the steel underneath the coating remained uncorroded. The other steel grades did not suffer corrosion at all.

In 2005 the casing was inspected by Schlumberger using an acoustic USIT (UltraSonic Imaging Tool). This tool is able to detect internal and external corrosion, scaling in the pipe, deformation (buckling, ovalisation), and holes that measure over 1.2" (3 cm). This tool discovered both pitting and scaling in the wells GPK-2, -3 and -4, and ovalisation in a number of depth ranges. Because of the ovalisation, a corrosion experiment was carried out using production fluids on P110 and N80 C-steel. The measured corrosion rates were 0.4 (on P110) and 0.6 mm/year (on N80). Baticci et al. (2010) considered these rates possibly suspicious and underestimating the true rates 'because of general grease filming protection due to wellhead pack-off systems'.

Laboratory experiments on P110 steel at 80°C in 2006 showed that the concentration of hydrogen chloride plays an important role. At less than <5% HCl pitting occurs. At 2-5% HCl the corrosion rate is at maximum.

---

[15] Mexel may not be applicable in the Netherlands for environmental reasons [Erik Ham pers. comm.)

A new corrosion inhibitor 'supplied by industry' was tested in 2008 (Baticci et al. 2010) on P265GH steel (which is used in the surface installation), P110 and N80 (casing steel) (Figure 7.3 – see Appendix C for an explanation of a polarisation diagram). These steel grades were selected because their corrosion resistance is less than that of the other steel grades that are applied in Soultz, and because both casing and surface installation pipes play an important role from an economical point of view. Under laboratory conditions, a 30 ppm dose of inhibitor decreased the uniform corrosion rate strongly within a day, from several mm/year to about 0.1 mm/year, only to increase after a week to about 0.2 – 0.3 mm/year.
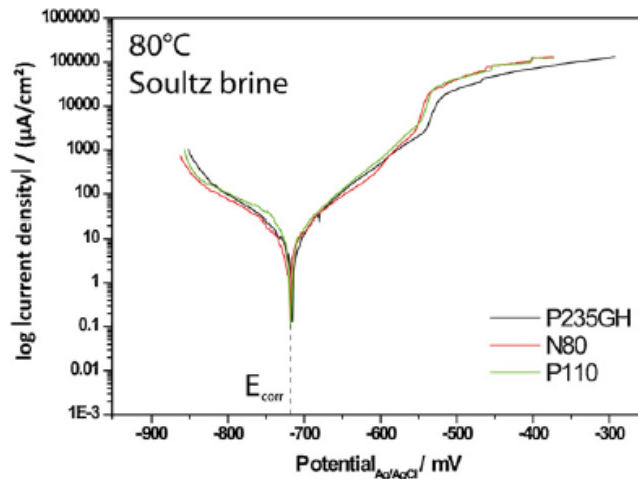


Figure 7.3 Polarisation diagram for three un-alloyed steel grades used in Soultz (derived from Mundhenk et al. 2013b). The electro-chemical behaviour of all three grades is very comparable. See Appendix C for a description of polarisation diagrams.

In 2008 a bypass consisting of three corrosion chambers between heat exchanger and injection well was installed in Soultz. This location was chosen because of the temperature range of the measurement probes, that are limited to about 120°C. This location and its temperature limit make the experiments in principle of interest to the Dutch situation. In the bypass probes for pH, temperature, conductivity and $E_h$ were positioned, as well as samples of the three steel grades mentioned earlier. Baticci et al. (2010) present a comprehensive description of the preparation of the samples (among others, the size), the bypasses (adapted to the amount of samples that should fit in at the same time), the duration of the experiment (1 week at least), and post processing (avoiding of contamination). During the experiment, which was conducted for 313, 515 and 1148 hours (approximately 13, 21 and 48 days), a protective scale was formed on all steel grade samples. The scale consisted of barite ($BaSO_4$) and celestite ($SrSO_4$). No uniform corrosion was observed, only pitting.

The number of studies into corrosion in geothermal systems in which the original formation fluid is used to determine the corrosion rate by means of both weight loss experiments and potentiodynamic polarisation, is limited. Both methods have specific advantages and disadvantages (see Mundhenk et al. 2013b table 1). An important conclusion drawn by Mundhenk et al. (2013 (2)) is that numerous studies into corrosion rates have been short term experiments, and therefore that the predictive value is limited.

Mundhenk et al. (2013b) remark that corrosion is determined by chemical factors such as $H_2$, halogenides and dissolved gas. The formation water in Soultz contains predominantly NaCl and dissolved $CO_2$ (estimated at 6 bar partial pressure), causing the pH to lie between 4.5 and 5.5. In the geothermal system a two phase mixture of liquid and gas exists. Therefore, there is a chance of uniform and local corrosion. The surface installation in Soultz operates at 20 bar pressure to prevent degassing.

Tests were conducted on a number of stainless (1.4104, 1.4404, 1.4539 and 1.4571) and unalloyed (general casing steel, comparable grades N80, P110, P235GH) steel, both in a cell as well as in a corrosion bypass at 80°C. The amount of dissolved gas (consisting of >90% $CO_2$) is reportedly high, leading to a pH ≈ 5. The TDS is about 90 g/l.

The corrosion rate, measured using electrochemical methods, of the general casing steel grades is between 0.14 and 0.18 mm/year. These steel grades were also put into a corrosion bypass for a maximum of five months. The resulting corrosion rate is similar to the one measured using the electrochemical methods. It changed little during the entire period (645 vs. 3693 hours). The observed corrosion types were uniform and pitting.

The stainless steel grades in Soultz are very susceptible to pitting corrosion, because of the chloride concentration (50 g/l), and the high temperature. The electrochemically measured corrosion rate for the stainless steel types is between 0.0055 and 0.037 mm/year. The best performing steel type (Nickle steel 2.4856) has a rate of 0.0022 mm/year. The 1.4404 and 1.4539 steel coupons that were placed in the corrosion bypass for a month did not have any visually determinable corrosion or weight loss. The 1.4104 coupon had some texture-related pitting, and a corrosion rate of 0.0028 mm/year. For these steel grades there is a large difference between the two measurement methods. The conclusion is that the stainless steel types are much less susceptible to corrosion than the mild steels, but also a factor of 1.7 to 20 more expensive.

A second study published by Mundhenk et al. (2013b) goes deeper into the variation of the corrosion rate with time, for varying cooling temperatures. Unlike the study described above, the rate was found to decrease strongly with time, probably due to the formation of a protective scale layer. The passivating effect of the siderite scale ($FeCO_3$) in a $CO_2$ containing environment is ambiguous; depending on the rate of scale formation it can be either hard and impenetrable, or porous and loose. If the rate of scale precipitation is higher than the corrosion rate, a protective scale can be formed. It can be very thin (~1 µm), but impermeable nonetheless (Nesic 2007). If the corrosion process undermines that precipitated scale, it will become porous and lacks a protective effect, despite the larger thickness (~100 µm). Higher flow rates can counteract the formation of scale, as well as corrosion. However, multiple authors state that the effect of removal or prevention of protective scales is larger, and that at higher flow rate the corrosion rate is also higher. Mundhenk et al. remark that the corrosion appears to be stronger at stagnant flow than at higher flow rates.

Figure 7.4 shows that at intermediate temperatures (80°C) the corrosion rate is higher than at 20 and 160°C. This observation, that the $CO_2$ corrosion rate is lower at higher temperatures, was also made by other authors (e.g., Figure 4.2).



Figure 7.4  Mild steel corrosion rates (in situ and autoclave, derived from Mundhenk et al. 2013).

Muller et al. (2010) describe a number of laboratory tests at high temperature (200°C) on various steel grades (P110, N80, TU42BT, and Teflon or sakaphen[16] coated steel) in a synthetic brine with Mexel inhibitor. The corrosion rates that were measured in this test are much higher than the ones reported by Mundhenk, because no protective scales are being formed due to the low iron concentration and pH, and the fact that this inhibitor is not efficient at high temperature. Instead of the protective siderite ($FeCO_3$), magnetite ($Fe_3O_4$) is formed. The results from this test are considered to be less relevant to the Dutch situation because of the high temperature.

A relevant conclusion from this study is that tests with coated steels are favourable (lower corrosion rate). Note, however, that small imperfections in the coatings can lead to local conditions that favour corrosion, especially with metallic, as opposed to organics, coating (galvanic corrosion).

## 7.3    Germany

Germany can roughly be split in three parts regarding to geothermal applications: the Molasse basin in the south, the Rhine Valley Graben in the west (which includes the Soultz-sous-Fôrets location in France), and the North German Basin (Agemar et al. 2014). The rocks encountered in the latter are to some extent comparable to those found in the Netherlands. The research project Groβ Schönebeck is also located in the North German Basin. This project was initiated in 2001 with the aim of researching processes in the geothermal loop, and to develop technology (Regenspurg et al. 2013). For the Genesys project in Hannover[17], another demonstration well was drilled by BGR and LIAG into rocks of Triassic age (Middle Buntsandstein at a depth of nearly 4000 meter) in 2009. These rocks also have an equivalent in the Netherlands.

---

[16] Sakaphen is used in the Soultz heat exchanger
[17] www.genesys-hannover.de

The goal of this project was to develop and test new concepts for direct use of geothermal heat. Unfortunately, this well was suspended very quickly after testing because of salt plugging.

7.3.1   *North German Basin (Groβ Schönebeck)*
The research facility in Groβ Schönebeck has drilled volcanic rocks and sandstones of the Rotliegend at a depth of about four kilometers, and a temperature of about 150°C. Despite the fact that neither depth nor temperature have yet been reached in Dutch doublets, the research that is being carried out in Groβ Schönebeck is considered to be relevant for the Netherlands, too. On the one hand, the rocks are in part comparable to those drilled in Koekoekspolder, Middenmeer and Heemskerk but, on the other hand, the chemical measurements were carried out at lower temperatures than the reservoir temperature. Furthermore, the procedure that was followed to obtain undisturbed samples from large depth, aiming at having undisturbed samples, was described in detail (Regenspurg et al. 2013). A 'Leutert Positive Displacement Sampler' was used to obtain fluid samples at depths of 4100 and 1800 meters under in-situ pressure and temperature circumstances. Special attention was paid to correct sampling of the gas, preventing occasional de-gassing. The observation that numerous sets of gas samples collected at a single doublet in the Netherlands have very dissimilar gas compositions (cf. Figure 3.2) indicates that the sampling procedure probably has failed. The measuring methods were specially developed to be applied to highly saline fluids. The TDS is 250 - 270 g/l. The gas contains mainly nitrogen (80-90%), methane (10-15%) and minor hydrogen (which is rather different from the Dutch situation). The pH is about 6.8.

Two corrosion processes occur in Groβ Schönebeck (Regenspurg et al. 2013). The first is anaerobic steel corrosion, which is deducted from the facts that:

- hydrogen occurs in the gas phase,
- magnetite is being formed,
- reduction of copper occurs through oxidation of casing iron,
- the concentration of dissolved iron is lowered.

The second is the formation of metal copper by reduction of dissolved $Cu^{2+}$ in association with oxidation of casing steel iron. The calculated amount of precipitated pure copper since fluid production is 93 kilos, assuming a 7 mg/l copper concentration. This has caused the total depth of the well to decrease from 4400 to 4200 meters.

Sarmiento Klapper et al. (2011) describe a corrosion test of three steel grades (super duplex UNS S32760, austenitic stainless UNS N08031 and the nickel alloy UNS N06059). These steel grades appeared to be very corrosion resistant in 24 week weight loss tests at 100 and 150°C using a synthetic GS-brine. S32760 proved to have a low resistance to pitting corrosion at high temperatures.

Alternatively, Bäβler et al. (2013) conclude from tests that (super) duplex steels S31803 and S32760 are not suitable for highly saline brines like those found in both the North German Basin or the Upper Rhine Graben because they are susceptible to localized corrosion. Other grades like austenitic N08031 and nickel alloy N06059 are concluded to be more suitable, at least up to 100°C. However, these studies used artificial brines and it is not clear whether apart from the brine also the gas composition was correctly mimicked.

7.3.2    *North German Basin (other)*

In the North German Basin, about 20 geothermal wells have been drilled (status as of 2011; Wolfgramm et al. 2011). The chemistry and composition has been described in detail for the main reservoirs, including the Rotliegend, the Triassic and the Cretaceous (Wolfgramm, Thorwart, Rauppach and Branden, 2011). At a depth of about two kilometers, Wolfgramm et al. show that the salinity the brine in non-evaporitic rocks is at least 150 g/l, or at least 250 g/l for water belonging to evaporitic formations. Schröder et al. (2007) remark that in Germany a wide range of geothermal reservoir types exists, and that therefore operators from the northern and southern parts of Germany co-operate. Seibt et al. (2000) describe the 'typical North German Basin geothermal system' to be located in sandstone reservoirs of Mesozoic (Upper Triassic and Lower Jurassic) age, 1000 – 3000 meters depth, 40 – 130°C, high salinity (250,000 ppm TDS), anoxic Na-Cl formation water, with pH 5-7. This is rather similar to the Dutch situation. They also describe the geological conditions at Neustadt-Glewe as 'typical of northern Germany' and that 'information [..] should be applicable to other northern Germany reservoirs'. Given the geological similarity of at least some of the reservoirs found in both Germany and the Netherlands, this means that Neustadt-Glewe could possibly serve as a reference for the Netherlands.

A bypass for scientific experiments was built in 2005 at the geothermal plant at Neustadt-Glewe (Schröder et al. 2007). This plant produces 97°C water at 100 m³/hr from a Triassic sandstone aquifer at a depth of about 2300 meters. The salinity is 220 g/l, the pH 5.5. The total content of dissolved gas in the formation water is 10%. The concentration of $CO_2$ in the separated gas is 73%. The online gas monitoring system of Neustadt-Glewe showed very little variation in gas composition over a period of two years (Seibt et al. 2000)[18]. The composition of the brine is typical for the Triassic Rhaetian aquifer in Northern Germany. The bypass (Figure 7.5) takes between 2 and 6 m³/hr, to be conducted through material (corrosion) testing and gas monitoring probes. Schröder et al. (2007) state that *'degassing processes promote the formation of scales.* They also conclude that *'it is fundamental to monitor the long-term development of the gas composition and content,* and that *'pressurized hot thermal water has to be sampled with care'*. They provide a detailed description of the sampling procedure using special equipment.
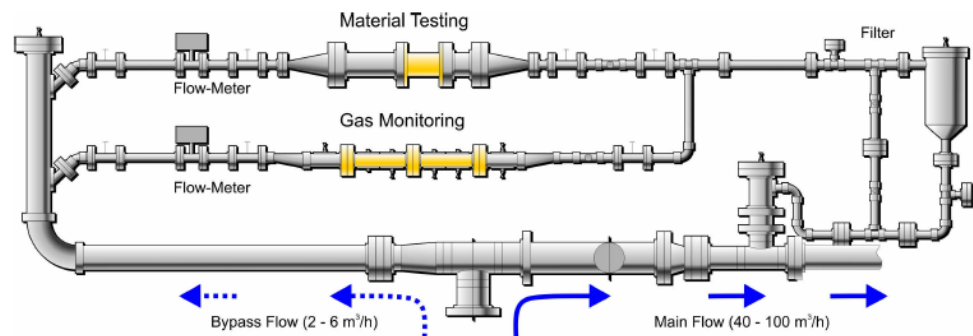


Figure 7.5  Thermal water bypass for material testing and gas monitoring at the Neustadt-Glewe plant (derived from Schröder et al 2007).

---

[18] This is in contrast to the observations made on the gas composition samples available from the Dutch doublets – see Figure 3.2

Degassing, especially at high $CO_2$ content, leads to a pH increase and the precipitation of metal and metal sulfides like PbS, at places where corrosion takes place (Figure 7.6). This appears to be similar to the situation in the Dutch geothermal doublet in Koekoekspolder. As the amount of dissolved sulfide in the brine is negligible, the reduction of sulphate to sulfide is necessary. The results of the bypass corrosion experiments show that the formation rates can be high, at 190 mg/(m²/d) on construction steel in combination with stainless steel for an experiment in the bypass.
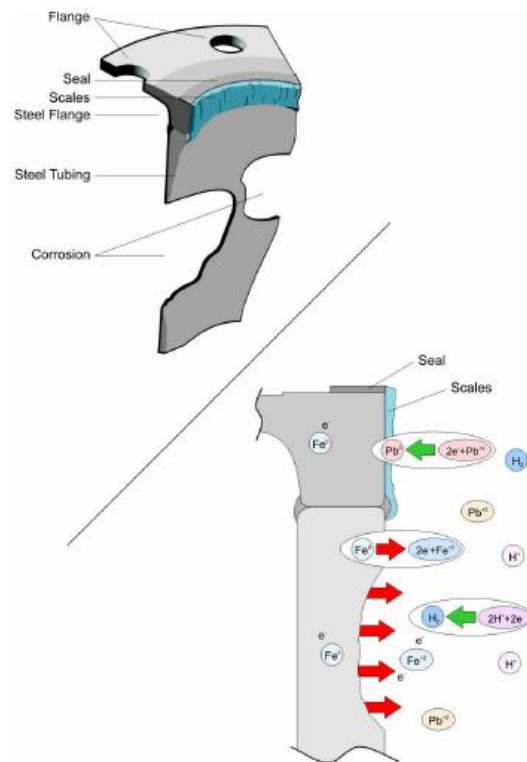


Figure 7.6  Simplified electrochemical steel corrosion at Neustadt-Glewe where iron corrodes and lead sulfide scale forms (derived from Schröder et al. 2007).

The most important conclusions from the corrosion experiments described by Schröder et al (2007) in the Neustadt-Glewe plant are that corrosion is mostly electrochemically driven, and that degassing promotes scaling. Seibt et al (2000) advise against $CO_2$ degassing in North German Basin geothermal wells. A proper material selection and plant design, adapted to the water chemistry, will help to increase the long-term stability of the geothermal installations. Schröder et al. promote that use of 45° over straight bends to prevent unintentional degassing (furthermore, this may also prevent cavitation). Glass fibre reinforced epoxy resin pipes showed no evidence of corrosion (BINE website: Geothermal Heating Plants in Operation). Due to the corrosive nature of the brine, the heat exchangers are made of titanium (DiPippo, 2005).

7.3.3    *Molasse Basin*
The Molasse Basin in Southern Germany, having a favourable geothermal gradient between 30 and 60°C/km, hosts most of the geothermal installations in Germany. The Molasse basin host predominantly carbonate reservoirs (Homuth et al. 2015). A number of literature references go into the testing of various steel grades in artificial brines that are considered to be representative for those found in the Molasse Basin. For instance, Bäβler et al (2014) report tests on S31603 (316L) and S31803 (1.4462) using a brine representing that of Unterhaching (near Munich). These are molybdenum-bearing austenitic stainless *steels* which are more resistant to general corrosion and pitting. Stober (2014) further describes the Upper Jurassic and Upper Muschelkalk rocks of the western part of the Molasse Basin to be consisting of carbonate having a TDS up to only 60 gr/kg ($\approx$ 60,000 ppm). The low TDS is confirmed by other authors like Schumacher and Schulz (2013) and Wolfgramm and Seibt (2008). Although the main constituent of the rocks (carbonate) is similar to what is encountered in the California doublet, the rocks are considered to be considerable different (natural permability vs. karst / fracture). Hence the applicability of experience in the Molasse Basin may be of limited use for the Netherlands.

7.4      **Denmark**

In Denmark operational doublets exist in Thisted (1984), Copenhagen (2005) and Sønderborg (2013). All doublets are operated by DONG (Dansk Naturgas and Dansk Olie og Naturgas). The depth and temperature ranges are roughly comparable to those encountered in the Netherlands: 1.2 – 2.6 kilometers, 48 – 74°C. The salinity is between 15 and 21%. All brines are devoid of hydrogen sulfide. The flow rates are very high (200 – 350 m³/hr). This is possibly due to the relatively shallow depth and hence high permeability. Some of the wells are closed in during the summer because of the low heat demand. The system is then protected by nitrogen blanketing to prevent corrosion. Corrosion inhibitors are only used when soft acidizing the injection well for clean-up.

The Thisted doublet has a corrosion rate of only 0.06 mm/year. The chosen corrosion allowance[19] is 3 mm. In Copenhagen the rate is 0.2 mm/year. This higher rate is probably due to the fact that the $CO_2$ content is higher: $CO_2$ 7 vol%, $N_2$ 84-88%, $CH_4$ 3-7%, GWR 0.14, pH 6.1, TDS 213-215 g/L). The extra corrosion allowance for the carbon steel chosen is therefore 5 mm. The doublet in Sønderborg has been in operation for only a short period. Therefore the corrosion rate is yet uncertain, but it appears to be like 0.2 mm/year (pers. comm.). This is in accordance with the reservoir brine and gas compositions: $CO_2$ 86-99 vol%, $N_2$ 0-13, $CH_4$ 0-1, GWR 0.16, pH 6.8, TDS 160 g/L), showing high $CO_2$. Although the $CO_2$ content of the gas is high, the pH is nearly neutral, possibly due to the low GWR.

---

[19] 'Corrosion allowance describes an extra measurement added to the thickness of the wall. This helps estimate the expected metal loss throughout the lifespan of certain equipment. Since the depth of penetration may vary from case to case, corrosion allowance has a safety factor equivalent to 2' (http://www.corrosionpedia.com).

## 7.5     Iceland

Richter et al. (2006, 2007) describe a city heating project in Reykjavik, Iceland where an extremely low corrosion rate of 1 µm/yr was measured. The reason for the low rate is the very high pH of 9.5, the low conductivity and the absence of oxygen. $H_2S$ is present in low concentration: 0.08 – 0.5 ppm. The presence of sulphur makes local corrosion a risk. At a temperature between 80 and 205°C a protective layer of iron sulphide is formed..

The corrosion rate is measured using offline methods like carbon steel coupons, of which the weight loss is measured in a bypass. Because of the low rate, the monitoring period is long. Only information about accumulated corrosion over a longer period is acquired. In spite of the low corrosion rate, corrosion monitoring is considered to be important for recognizing potential problems in an early stage.

Richter et al. investigated the possibility of using online both electrochemical (linear polarisation resistance (LPR) and electrochemical impedance spectroscopy (EIS)) and non-electrochemical (electrical resistance (ER), HA (harmonic analysis), EN (electrochemical noise) and ZRA (zero resistance ammetry)) methods.
Various probe types were used. The conclusion is that both LPR and EIS perform well in the investigated brine in the absence of oxygen. However, these methods are not ideal when the conductivity is low. The methods are time consuming and error prone. LPR was hampered by scaling on the electrodes. Non-electrochemical methods like differential ER was more valuable in the presence of oxygen. The EN measurements indicate that local corrosion occurred, but also that uniform corrosion is dominant. The Pitting Factor was measured with EN and showed promising results for measuring-localized corrosion on-line.

In the Iceland Deep Drilling Project (IDDP), 320-450°C steam is being produced (Karlsdottir et al. 2014). The steam is highly corrosive when the steam condenses because of the presence of $CO_2$ (732 mg/kg), $H_2S$ (339), HCl (93) and HF (5), resulting in a pH between 2.6 and 3.5. Because of the high flow velocity (70-100 m/s, mass flow up to 50 kg/s), erosion and erosion corrosion is a severe issue. This situation bears little resemblance to the Dutch situation.

The corrosion rate was measured in a bypass with various diameters, constructed of various steel grades (austenitic stainless UNS N08028 and UNS S31254, duplex stainless UNS S32708, carbon steel P265GH ASTM grade A-1, and a ceramic coated carbon steel), in order to be able to measure the erosion at varying flow rates. The thickness of the steel after erosion/corrosion was determined acoustically using a Krautkamer Ultrasonic Thickness Gauge model DM4 (works for steel, not for ceramic material), and by running a digital caliper. The steam is saturated with silica. In the tubings abundant silica scale was encountered after testing.
Most erosion took place at the ends of bends in the bypasses. In the carbon steel pipes both uniform and pitting corrosion was observed. The ceramic liner showed cracking.

For the high enthalpy wells on Iceland, the Iceland Geological Survey (ISOR) recommends to use K55 or L80 steel for both casing and liners, whereas Cr-steel may be necessary for the uppermost 100 meters, given the presence of HCl and $H_2S$ (Fridriksson and Thórhallsson).

Careful selection of alloys may well prevent most corrosion problems. Because of the high chloride concentration, a titanium-alloy is recommended for the heat exchanger. ISOR points at the unique composition of the brine, which makes it difficult to present a unique solution for corrosion problems, and also strongly recommends to monitor both reservoir and fluid composition.

# 8 Classification of geothermal systems

Only very few attempts have been made to classify geothermal systems, either as a whole, or specifically aiming at corrosion risk. Falcone (2013) states that *'currently, no universally recognised standards exist for classifying and reporting geothermal resources'*. For the few proposed systems, no follow-up was found in the literature, which, in itself, is rather telling.

GeothermEx, Inc. proposed a possible scheme for the United States relatively recently at the request of the US Department of Energy (DOE) and the Geothermal Energy Association (GEA), (Sanyal 2005, see Figure 8.1). This scheme classifies geothermal systems into seven classes, mainly on the basis of temperature. Other factors influencing the classification are a) the steam fraction in the fluid phase, b) the type of power generation, c) production mechanism, d) factors controlling productivity other than temperature and e) 'unusual' operation problems such as scaling and corrosion. A single class is reserved for 'non-electrical grade' systems at less than 100°C. Hence, on basis of temperature all systems in the Netherlands would classify in the same class when this system is used. For the non-electrical grade class 1, no 'unusual development or operational problems' are listed.
The conclusion is that this proposed system is of little or no use for assessing corrosion risks in the Dutch situation.
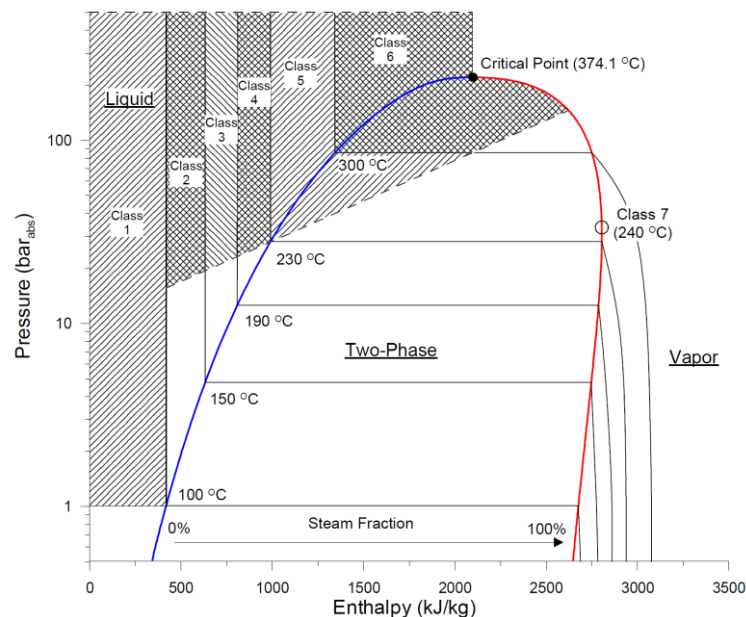


Figure 8.1 Classification scheme on pressure-enthalpy-temperature diagram for water. (derived from Sanyal, 2005).

In an earlier stage, a proposal for a 'geothermal corrosivity classification system' was put forward by Ellis (1981, 1985) based on key corrosive species, wellhead temperature, and similarities of corrosion behaviour using data from 45 worldwide geothermal resources. Logically, this system goes much deeper into temperature,

TDS, total key corrosive species (TKS[20], further defined in Ellis II and Conover 1981), and the various types of corrosion described in chapter 1. Ellis (1985) states however that *'this classification system does not eliminate the need for site specific evaluation of corrosion problems; but does allow some generalization about materials performance and design requirements'*. Seven classes are defined using seven defining parameters:

- resource phase (liquid, vapour);
- total key corrosive species (TKS);
- amount of chloride;
- pH of the unflashed fluid;
- pH of the flashed fluid;
- gas content of the steam phase;
- plant inlet temperature.

TABLE 1. CORROSIVITY CLASSIFICATION OF 45 WORLDWIDE GEOTHERMAL RESOURCES[a]  (Con't)

| | CLASS Va | CLASS Vb | CLASS VI |
|---|---|---|---|
| **DEFINING PARAMETERS** | | | |
| Resource Phase Domination | Liquid | Liquid | Steam |
| Total Key Species (TKS) (ppm) | <5,000 | <5,000 | Not Applicable |
| Amount of Chloride | 3 to 72% of TKS | 3 to 72% of TKS | <1 ppm in steam |
| pH (Unflashed fluid) | 6.5 to 7.5 | ≥7.9 | Not Applicable |
| pH (Flashed fluid) | Not Applicable | Not Applicable | Not Applicable |
| Vol Percent Gas in Steam | Not Applicable | Not Applicable | <5 |
| Plant Inlet Temperature (°C) | 49 to 105 | 49 to 105 | 120 to 200 |
| **OBSERVED CORROSION OF CARBON STEEL** in nonaerated geothermal environment. | 0.2[b] to 0.4 mm/yr uniform corrosion with pitting up to 2 mm/yr[c]<br><br>Variation of $H_2S$ from 0.03 to 5 ppm has little effect.[c] | <0.04 mm/yr uniform corrosion (median of 21 data points = 0.003 mm/yr) with pitting zero to 0.5 mm/yr (median of 20 data points = 0.09 mm/yr). | 0.13 to 0.25 mm/yr uniform corrosion typical in steam.<br><br>Little or no pitting. |
| **GENERALIZED CORROSION BEHAVIOR OF OTHER ALLOYS** in nonaerated environments unless indicated otherwise. | SSC hazard.<br><br>Copper and cupronickel unsuitable.<br><br>T316 generally suitable.<br><br>Performance of brasses and bronzes unknown.<br><br>Aluminum alloys unacceptable. | SSC hazard.<br><br>Copper and cupronickel unacceptable.<br><br>Leaded Red Brass acceptable[d].<br><br>13% zinc brass dealloyed.<br><br>T316 generally suitable.<br><br>Aluminum alloys unacceptable. | Corrosion-fatigue of 12 Cr turbine blades twice as severe as in boiler quality steam.<br><br>More blade problems when turbine inlet steam is superheated.<br><br>Aerated condensate corrosive to carbon steel and some stainless grades.<br><br>Aluminum alloys unacceptable. |
| **REFERENCE SITES** | Iceland - 10 Sites<br><br>Klamath Falls, OR | Diamond Ring, SD<br><br>Edgemont, SD<br><br>Marlin, TX<br><br>Pagosa Springs, CO<br><br>Philip, SD | Italy - Boraciferous Region - 10 Sites<br><br>The Geysers, CA |

[a]From Ellis and Conover 1981 unless otherwise stated.
[b]Radian Corporation - unpublished data.
[c]Anliker and Ellis 1981a
[d]Anliker and Ellis 1981b

Figure 8.2 Ellis II (1981) corrosivity classes V and VI.

For the low enthalpy systems found in the Netherlands, the two classes that come closest to the Dutch situation when considering temperature are Ellis II' Va and Vb shown in Figure 8.2. However, those both have low TKS as well as high pH (>6.5). Since both the $CO_2$ content and the salinity, which are not explicitly listed, are considered to have a major influence on the corrosion risk, the conclusion is that the general classes defined by Ellis II have very limited significance for the Dutch situation. Furthermore, Ellis II and Conover (1981) state that *'a quantitative prediction of their corrosive effects is complicated by the following factors. Different*

---

[20] 'Geothermal fluids contain several chemical species that have a significant effect on the corrosion of metallic construction materials. These key species, which were identified from corrosion literature and data on chemical composition of fluids from liquid-dominated geothermal resources, are as follows: oxygen, hydrogen ion (pH), chloride ion, hydrogen sulfide, carbon dioxide species, ammonia species and sulfate ion'. (Ellis II and Conover 1981).

*materials respond to the same fluid component in different ways and to different degrees. The interaction of two or more chemical species may give results different from those obtained with the individual species. The importance of a species depends on the form of attack (uniform corrosion, pitting, crevice corrosion, stress corrosion cracking, or corrosion fatigue).*' Hence, given these early observations by Ellis II and the conclusions drawn from the $CO_2$ corrosion models, it can easily be concluded that a corrosion classification system that is simply defined by imposing static limits on TKS will not work.

# 9 Conclusions and recommendations

In this chapter conclusions about the specific findings are presented first. Next, the project objectives are considered.

## 9.1 Conclusions

### 9.1.1 *Types of corrosion*

The major corrosion types are uniform corrosion, localized corrosion (pitting, crevice and filiform), (mechanical) erosion corrosion and environmentally induced cracking (including stress corrosion cracking). Especially uniform and pitting / crevice corrosion are expected in Dutch doublets.

The expected corrosion type in the subsurface installation is uniform corrosion on commonly applied low grade steel casings (L80, K55, etc). Higher grade carbon and / or stainless steels are more corrosion resistant but also more expensive. The expected corrosion type in the surface installation is pitting corrosion on higher alloy steels. Crevice corrosion is expected where crevices occur along the pipes, like around couplings.

### 9.1.2 *Corrosion potential*

Ther interplay of formation water chemistry, gas composition, pH, temperature, steel grade and scaling / corrosion is very complex.

The main corrosive species are the dissolved gases $O_2$, $H_2S$ and $CO_2$. $O_2$ is in principle avoidable in the installation by using oxygen scavengers or nitrogen blanketing. $H_2S$ is not encountered in current Dutch geothermal reservoirs. $CO_2$ occurs in all Dutch doublets. The main metallic corrosive species are the less noble metals like titanium, lead and copper.

Abundant available data of the brine and gas composition, collected from both the oil & gas and geothermal industry shows that the variation in formation water composition may be extreme, even at short distance, horizontally (between wells, typically kilometers) or vertically (samples taken at different depth within a well). Care should be taken not too hastily apply conclusions drawn from one doublet to another one, even if present in the same reservoir. There is much uncertainty in the gas composition measurements, especially concerning the $CO_2$ content. There is a very strong link between $CO_2$ content of the dissolved gas and the corrosion potential.

The main corrosion risks are $CO_2$ corrosion in the production well, galvanic corrosion, and lead and copper scaling in the injection well, which may also lead to corrosion by exchange of casing iron by less noble metals.

A high pH reduces the corrosion risk in limestone reservoirs. Degassing increases the pH, thereby reducing the $CO_2$ corrosion risk but at the same time increasing the scaling risk.

*9.1.3 Corrosion models*

There is abundant literature about $CO_2$ corrosion modelling in oil and gas wells, as well as (freeware) software modelling tools, both empirical and mechanistic. The predictive force of these models is limited, given the complexity of the processes involved. The spread of the corrosion rates predicted by the various models is large. Despite the limited predictive force on a practical scale, these tools do provide insight in the importance of different factors like pH, $CO_2$ partial pressure and temperature. As these tools were developed for the oil and gas industry and were not tested on geothermal wells, the calculated corrosion rates can at best be used indicatively.

The (empirical) NORSOK model shows that a temperature reduction from about 100°C to about 50°C increases the corrosion rate. The highest corrosion rate lies in the 50-70°C range. An increase of the $CO_2$ partial pressure increases the corrosion rate.

Empirical models cannot be used for extrapolation by definition. They are based on interpolation of sample data, and regressions on sample data relationships. The corrosion rate in geothermal installations having one or more parameters outside the sample range used for the construction of the model can therefore not be determined. Calculated corrosion rates can only be used indicatively.

Mechanistic models can be used for extrapolation and to gain insight in the underlying chemical processes. They are complex to build, they rely heavily on field data input and they may fail in their conceptual model setup.

9.1.4 *Corrosion rates*

Corrosion rates are difficult to model with currently available software tools. Indicative general / uniform corrosion rates strongly depend on the pH and partial $CO_2$ pressures and therefore measurements of the $CO_2$ content of the gas. The quality of the currently available gas composition measurements is unknown as many are performed on surface samples. High $CO_2$ partial pressures and hence high corrosion rates cannot be excluded. However, studies on doublets abroad show that the corrosion rate can be significantly reduced by using inhibitors. Corrosion rate measurements are still hardly available and seldomly measured in situ. Crevice corrosion may lead to very quick failure (as has been observed in more than one Dutch doublet).

9.1.5 *Inhibition*

Naturally occurring oil serves as natural inhibitor in some installations. Different classes of chemical inhibitors are those that displace depolarizers from the metal surface, those that form films that are impermeable to depolarizers, and those that form bonds with depolarizers. Synthetic chemical corrosion inhibitors like tannic acids should be added along the entire well trajectory, starting at bottom hole, in order to offer complete protection. Care should be taken to ensure the dose is adequate to protect the whole installation. This is an practical and interative process.

9.1.6    *Monitoring*

Many literature sources stress the need for measuring and monitoring.

Corrosion monitoring data are not yet available for the Netherlands. Therefore, no conclusions can be drawn regarding the optimal monitoring frequency and duration, other than by using examples from abroad. These however may well be limited in relevance. This is a severe drawback.

Abundant literature is available about corrosion monitoring in bypasses and in the laboratory. Often, laboratory experiments do not match corrosion rates measured in the field. This emphasizes the complexity of the process, and the need for field measurements.

9.1.7    *Experience abroad*

Experience with corrosion prevention abroad shows that successful mitigation of corrosion starts with long-lasting monitoring in the surface system and the laboratory.

The selection and dosing of the best inhibitor is often a matter of trial-and-error. Different inhibitors perform under different conditions (brine, temperature range, steel).

The corrosion rate may change quickly in the course of time due to the formation of protective scales, especially in the first days or weeks. Scales may either be protective, or not, depending on the formation process. This behaviour can change in time.

Good results have been achieved in France using fiberglass and coated completions, in combination with downhole inhibitor addition.

While degassing may be beneficial from a financial point of view, it changes the brine composition, possibly leading to unexpected results in the injection well (corrosion, scaling). Some German authors therefore advise against degassing.

9.1.8    *Project objectives*

With the combined effort of TNO and the stakeholders during the IPC-corrosion project, we can now address the key questions posed at the beginning of the study:

1) Can corrosion of unprotected steel be expected?

Corrosion can be expected in Dutch geothermal doublets based on the physical and chemical conditions encountered (e.g. temperature, pH, dissolved solid concentrations). Dutch Rotliegend reservoirs contain both $CO_2$ and dissolved metals and therefore may have a substantial corrosion risk. Dutch Jurassic and Cretaceous reservoirs contain $CO_2$ and sometimes some oil, and have an intermediate corrosion risk. Dutch Carboniferous reservoirs have a high pH and hence are less prone to corrosion. Calculations using the Electronic Corrosion Engineer and the NORSOK model using 'average' doublet data indicate that the corrosion risk may be severe. As no measured corrosion rate data are available and corrosion modelling software can only be used in an indicative way, these conclusions are theoretical.

2) Is it reasonable to expect that conditions exist where corrosion in geothermal wells is limited by natural protection mechanisms like oil films or iron carbonate scaling?

Naturally occurring oil can serve as inhibitor. Protective scales, such as Fe-carbonate, can be expected in some Dutch wells. Their efficiency depends on their growth rate, thickness, permeability and the flow conditions. For each well, those conditions are different.

3) At which locations in a geothermal well can the corrosion rate be expected to be relatively high and / or low?

If a $CO_2$ containing brine is degassed, the risk of scaling in the injection well is limited due to the increased pH. The $CO_2$ corrosion rate increases with increasing $CO_2$ partial pressure, so corrosion can be most severe downhole in the production well. However, the formation of a protective scale can at the same time prevent corrosion. Top of line corrosion can also be severe but this can be prevented by maintaining a nitrogen blanket. The application of (expensive) high grade steel in the surface system may prevent or limit corrosion.

4) In which ways can the corrosion rate be lowered, either by design, or by the application of inhibition?

The corrosion rate can be lowered in both ways. A variety of synthetic corrosion inhibitors (e.g. cathodic and anodic inhibitors, oxygen scavengers) can be used to lower or altogether eliminate the corrosion potential. In order to offer complete protection, inhibitors should be added downhole in the production well via an injection tubing (which should preferably be installed during the completion of the well). The use of corrosion resistant materials in the installation, such as fibreglass and coated pipes, could in principle reduce the risk of corrosion. An optimal choice of couplings may reduce crevice and/or erosion corrosion. If steel grades with different potential are applied adjacently, isolators should be installed.

5) If corrosion should be expected, which monitoring techniques are available / effective / achievable / applicable?

As first indication of possible corrosion, corrosion can be assessed by monitoring the production rate, pressure and temperature at the well-head, and their change in time. During production pauses and maintenance of the ESP, downhole camera and casing integrity inspection logs can be applied to verify the degree of corrosion. However, these latter methods are relatively expensive. On technical and financial grounds it is unnecessary and undesirable that they are executed on a high frequency basis.

Laboratory experiments (e.g. in autoclaves or flow-through reactors) can be conducted for understanding corrosion mechanisms, as well as for verifying prevention methods. As corrosion intensity can be different under continuous flow of unaltered gas and water composition, an on-site testing facility (bypass) would be the preferred option for both monitoring and inhibitor testing. The on-site testing facility offers a long-term corrosion monitoring solution and can provide a cheaper monitoring approach.

## 9.2 Recommendations

All doublets should be monitored. This includes the gas and formation water compositions, pH, temperature, OCP, flow rate, production and injection temperature and pump pressure(s). Monitoring can take place in bypasses and / or subsurface.

Because the corrosion behaviour of the subsurface system may not always be unambiguously reflected in the surface system, inspection of the subsurface system is recommended as long as the corrosion rates in the subsurface system are unknown or poorly understood.

Measurements and monitoring data should be stored in a joint database.

In order to be able to compare measurements from (different) doublets, made by different consultants under varying conditions, a standard sampling procedure is imperative. API RP 45 (for oil field waters) may serve as an example, if properly adapted to the geothermal practice.

Inhibitors should be applied downhole in the production well to provide optimal protection. The optimal choice of chemistry and dose should be determined experimentally.

# 10 References

Agemar T., Weber J and Schulz R. (2014). Deep geothermal energy production in Germany. Energies 2014-7, p4397-4416.

Alt-Epping P., Wabera H.N., Diamonda L.W. and Eichinger L. (2013). Reactive transport modelling of the geothermal system at Bad Blumau, Austria: implications of the combined extraction of heat and $CO_2$. Geothermics 45(2013) p18-30.

American Petroleum Institute (API) (1998). Analysis of oilfield waters. API recommend practice RP 45. 3rd edition, august 1998. 72p

American Petroleum Institute (API) (2003). Sampling petroleum reservoir fluids. API recommended practice RP 44, 2nd edition, april 2003. 64p

Antics M., Bertani R. and Sanner B. (2013). Summary of EGC 2013 country update reports on geothermal energy in Europe. EGC 2013 conference, 3-7 June 2013, Pisa, Italy. 18p.

Banas J., Lelek-Borkowska. U., Mazurkiewicz B. and Solarski W. (2007). Effect of $CO_2$ and $H_2S$ on the composition and stability of passive film on iron alloys in geothermal water. Electrochimica Acta 52(18), p5704-5714.

Bäβler R., Boduch A. and Sobetzki J. (2014). Corrosion Resistance of High-alloyed Materials in Flowing Artificial Geothermal Water. NACE Corrosion 2014 paper 3825, 8p.

Bäβler R., Sobetzki J. and Sarmiento Klapper H. (2013). Corrosion resistance of high-alloyed materials in artificial geothermal fluids. NACE corrosion conference 2013 paper 2327. 8p

Baticci F., Genter A., Huttenloch P. and Zorn R. (2010). Corrosion and Scaling Detection in the Soultz EGS Power Plant, Upper Rhine Graben, France. Proceedings World Geothermal Congress 2010, Bali, Indonesia, 25-29 april 2010. 11p.

Birner J., Wolfgramm M. and Seibt A. (2013). Inhibitoren – Vom Laborversuch zum erfolgreichen Einsatz. Beitrag "Der Geothermiekongress 2013" Essen, 12.-14. November 2013. 11p.

Blasco-Tamarit E., Igual-Munoz A., Garcia-Anton J., Garcia-Garcia D., Effect of temperature on the corrosion resistance and pitting behaviour of alloy 31 in LiBr solutions, Corros. Sci. 50 (2008) 1848–1857.

Bonté D., Van Wees, J-D. and Verweij J.M. (2012). Subsurface temperature of the onshore Netherlands: new temperature dataset and modelling. Netherlands Journal of Geosciences 91(4), p465-490.

Boissavy C. and Dubief R. (1995). New technologies in the geothermal well of Meaux. World Geothermal Congress 1995, Firenze, Italy, May 18-31 1995. p2219-2222.

Børeng R., Schmidt T., Vikane O., Tau L.A., Dybdahl B., Dale, T.I. and Thowsen, O. (2003). Downhole measurement of pH in oil & gas applications by use of a wireline tool. SPE 82199, 12p.

Bressers P.M.M.C. and Wilschut F. (2014). Lead deposition in geothermal installations. TNO internal report.

Brondel D., Edwards R., Hayman A., Hill, D. Mehta and S. Semerad T. (1994). Corrosion in the oil industry. Oilfield review, april 1994, p1-12.

Carroll J.J., Slupsky J.D. and Mather A.E. (1991). The solubility of carbon dioxide in water at low pressure. J. Phys. Chem. Ref. Data 20(6), p1201-1209

Chapgaon S.A. (2013). Corrosion and Materials in the Oil and Gas Industries - Chapter 11: Material Selection in Oil and Gas Environments. CRC Press, p273–298.

Chawla, S.L. and Gupta, R.K. (1993). Materials selection for corrosion control. ASM International, digital printing december 2010.

Chilingar, G.V., Mourhatch R. and Al-Qahtani G.D. (2008) The fundamentals of corrosion and scaling for petroleum and environmental engineers. Gulf publishing company, Houston, Texas. 276p.

Dariva, C.G. and Galio, A.F. (2014). Corrosion Inhibitors – Principles, Mechanisms and Applications, Developments in Corrosion Protection, Dr. M. Aliofkhazraei (Ed.), ISBN: 978-953-51-1223-5, InTech, DOI: 10.5772/57255. Available from: http://www.intechopen.com

DiPippo, R. (2005). Geothermal power plants: principles, applications, case studies. Butterworth-Heinemann: Elsevier, Oxford, England, 2012, 600p.

Drijver B. (2014). Corrosie en scaling bij geothermie systemen. IF Technology B.V. Report, 46p.

Duan Z., Sun R., Zhu C. and Chou I. (2006). An improved model for the calculation of $CO_2$ solubility in aqueous solutions containing $Na^+$, $K^+$, $Ca^{2+}$, $Mg^{2+}$, $Cl^-$, and $SO_4^{2-}$. Marine Chemistry 98(2006), p131-139.

Dugstad A., Lunde L. and Videm K. (1994). Parametric study of CO2 corrosion of carbon steel, Corrosion/94, paper no. 14 (Houston, TX: NACE International, 1994)

Dugstad A., Clause S. and Morland B. (2011) Transport of dense phase $CO_2$ in C-steel pipelines – when is corrosion an issue? NACE paper 11070

El-Lateef H.M., Abbasov V.M., Aliyeva L.I. and Ismayilov T.A. (2012). Corrosion protection of steel pipelines against $CO_2$ corrosion – a review. Chemistry Journal 02(02), p52-63.

Ellis II P.F. (1981). A geothermal corrosivity classification system. Geothermal resources council, TRANSACTIONS vol 5, october 1981, p463-466.

Ellis II P.F. and Conover M.F. (1981). Materials selection guidelines for geothermal energy utilization systems, prepared for US DoE Division of Geothermal Energy. DOE/RA/27026-1., 596p.

Ellis II P.F. (1985). Companion study guide to short course on geothermal corrosion and mitigation in low temperature geothermal heating systems prepared for the Geo-Heat Center Oregon Institute of Technology Klamath Falls, OR. DCN 85-212-040-01 34p.

Falcone G. (2013). Status of geothermal resource classification and key stakeholders.

Fridriksson T. and Thórhallsson S. (2006). Geothermal utilization: scaling and corrosion. 36p. Proceeding Iceida Workshop, Managua, Nicaragua, June 26-30, (2006).

Frankel G.S. (2003) Pitting Corrosion, In: Metals Handbook, (Eds) S.D. Cramer, B.S. Covino, Vol. 13A, ASM International.

Fuggle T. (2015). Continuous corrosion and erosion monitoring in geothermal power facilities. Proceedings World Geothermal Congress 2015, Melbourne, Australia, 19-25 April 2015. 5p.

Ginzel R.K. and Kanters W.A. (2002). Pipeline corrosion and cracking and the associated calibration considerations for same side sizing applications. Journal of Non-destructive testing (NDT.net) 7(7).

GPC IP, KWR, Ministry of Economic Affairs and Productschap Tuinbouw (2015). Report assessment of injectivity problems in geothermal greenhouse heating wells. Concept report 15 January 2015. 39p.

Gräfen H. and Kuron D. (1996). Pitting corrosion of stainless steels. Materials and Corrosion 47(1), 16-26.

Hartog F.A. and Jonkers G. (2002) Lead Deposits in Dutch Natural Gas Systems. In: A.P. Schmidt and R.D. Schuiling (Eds), Shell Research and Technology Center (Inst. of Earth Sciences, Utrecht U.), SPE Production & Facilities 17(2), p122-128.

Heitz, E. (1991). Chemo-mechanical effects of flow on corrosion. Proceedings of the symposium on flow-induced corrosion, fundamental studies and industry experience. Kennelley, Hausler and Silverman (eds.), NACE, Houston, p1-29.

Homuth S., Götz A.E. and Sass I. (2015). Physical properties of the geothermal carbonate reservoirs of the Molasse Basin, Germany – outcrop analogue vs. reservoir data. Proceedings World Geothermal Congress 2015, Melbourne, Australia, 19-25 april 2015.

IFE (2009). Guidelines for prediction of $CO_2$ corrosion in oil and gas production systems. IFE/KRE-2009/003

International Association of Oil and Gas Producers (IOGP) (2012). Petroleum and natural gas industries – Well integrity – Part 2: Well integrity for the operational phases. OGP Draft 116530-2 of 2012-11-29. 94p.

Jones L.W. (1988). Corrosion and water technology for petroleum producers. Tulsa, oklahoma, USA, OGCI publications. 202p.

Kampman N., Bickle M., Wigley M. and Dubacq B (2014). Fluid flow and $CO_2$-fluid-mineral interactions during $CO_2$-storage in sedimentary basins. Chemical Geology 369, p22-50

Kane R.D. and Cayard M.S. (1998). Roles of $H_2S$ in the behaviour of engineering alloys: a review of literature and experience. Corrosion 98 paper 264. 28p.

Karlsdottir S.N. (2014). On-site erosion–corrosion testing in superheated geothermal steam. Geothermics 51(2014), p170-181.

Klapper H.S., Bäßler R., Sobetzki J. Weidauer K. Stürzbecher D. (2013). Corrosion resistance of different steel grades in the geothermal fluid of Molasse Basin. Materials and Corrosion 64-9

Kolenberg Y., van Heekeren H., Boersma K. and Gutierrez-Neri, M. (2012). Evaluation of current logging tools and industry practices for material selection and repairs. CATO-2 Deliverable WP3.4-D15, 76p.

Laplaige P., Lemale J., Decottegnie S., Desplan A., Goyeneche O. and Delobelle G. (2005). Geothermal resources in France – current situation and prospects. Proceedings of the World Geothermal Congress 2005, Antalya, Turkey, 24-29 April 2005. 13p.

Libowitz G.C. and Whittingham M.S. (eds) (1979). Materials Science in Energy Technology, Chapter 5 'Materials for Geothermal Energy Utilization'.

Lichtner, P.C., 2007. FLOTRAN Users Manual: Two-Phase Non-isothermal Coupled Thermal–Hydrologic–Chemical (THC) Reactive Flow and Transport Code, Version 2. Los Alamos National Laboratory, Los Alamos, NM.

Loizzo, M., Bois A.P., Etcheverry P. and Lunn M.G. (2015). An evidence-based approach to well-integrity risk management. SPE 170867, SPE Annual Conference and Exhibition, Amsterdam 2014, 12p.

Lopez S., Hamm V., Le Brun M, Schaper L., Boissier F., Cotiche C. and Giuglaris E. (2010). 40 Years of Dogger aquifer management in Ile-de-France, Paris Basin, France. Geothermics 39(2010), p339-356.

Lopez S., Hamm V. and Goyeneche O. (2012) Optimal and sustainable use of the Dogger aquifer geothermal resource: long-term management and new technologies. Proceedings of SIMS 2012, the 53rd Scandinavian Simulation and Modelling Society Conference, Reykjavik, Iceland. 17p.

Mahler A. (Dansk Fjernvarmes Geotermiselskab) 2014. Danish experiences with operation of deep geothermal district heating plants. Presentation Norddeutsche Geothermietagung, Hannover.

Mahler A. and Magtengaard J. (2010). Country update report for Denmark. Proceedings World Geothermal Congress 2010, Bali, Indonesia 25-29 april 2010, 9p.

Mahler A., Røgen B., Ditlefsen C., Nielsen L.H. and Vangkilde-Petersen T. (2013). Geothermal energy use, country update for Denmark. EGC 2013 conference, 3-7 June 2013, Pisa, Italy. 12p.

Metrohm Autolab b.v. (2011). Corrosion inhibitors. Autolab application note COR05 – Corrosion – Part 5. 2p.

Muller J., Bilkova K., Genter A. and Seiersten M. (2010). Laboratory results of corrosion tests for EGS Soultz geothermal wells. Proceedings World Geothermal Congress 2010, Bali, Indonesia 25-29 april 2010. 12p.

Mundhenk N., Huttenloch P., Kohl T., Steger H. and Zorn R. (2012). Laboratory and in-situ corrosion studies in geothermal environments. GRC Transactions 36(2012), p1101-1106

Mundhenk N., Huttenloch P., Sanjuan B., R., Kohl, T., Steger, H. and Zorn, R. (2013a). Corrosion and scaling as interrelated phenomena in an operating geothermal power plant. Corrosion Science 70, p17-28.

Mundhenk N., Huttenloch P., Kohl T., Steger H. and Zorn R. (2013b) Metal corrosion in geothermal brine environments of the upper Rhine graben - Laboratory and on-site studies. Geothermics 46(2013) p14-21.

Mundhenk N., Huttenloch, P., Baessler, R., Kohl, T., Steger, H. and Zorn, R. (2014). Electrochemical study of the corrosion of different alloys exposed to deaerated 80 C geothermal brines containing $CO_2$. Corrosion Science 84, p180-188.

NACE (1999). TPC5 Corrosion control in petroleum production. 350p.

NACE (2002). Sulfide Stress Cracking. NACE MR0175-2002

Nesic S. (2007). Key issues related to modelling of internal corrosion of oil and gas pipelines – A review. Corrosion Science 49, 4308–4338.

Nesic S., Solvi G.T. and Enerhaug J. (1995). Comparison of the rotating cylinder and pipe flow tests for flow-sensitive carbon dioxide corrosion.Corrosion Science 51(10), p773-787.

NORSOK (2005) Standard M-506. $CO_2$ corrosion rate calculation model

Nyborg R. (2010) $CO_2$ corrosion models for oil and gas production systems

Olsen S. (2003). $CO_2$ corrosion prediction by use of the NORSOK M-506 model. Guidelines and limitations. Corrosion 2003 paper 03623, 11p.

Pohjanne P., Carpén L., Hakkarainen T. and Kinnunen P. (2008). A method to predict pitting corrosion of stainless steels in evaporitive conditions. Journal of constructional steel research, 64(11), 1325-1331.

Popoola L.T., Grema A.S., Latinwo G.K., Gutti B and Balogun A.S. (2013). Corrosion problems during oil and gas production and its mitigation. International Journal of Industrial Chemistry, 4(35), 15p.

Postlethwaite, J. and Nesic, S. (2000). Erosion-corrosion in single and multiphase flow. In: Uhlig's Corrosion Handbook, 2nd edition.

Pourbaix M. (1974). Atlas of electrochemical equilibria in aqueous solutions, National Assosiation of corrosion engineers, Houston (USA), 2nd edition.

Qian B., Hou B. and Zheng M. (2013). The inhibition effect of tannic acid on mild steel corrosion in seawater wet/dry cyclic conditions. Corrosion Science 72(2013) p1-9.

Regenspurg S., Feldbusch Helmholtz E. and Saadat A. (2013). Corrosion Processes at the Geothermal Site Groß Schönebeck (North German Basin). NACE Corrosion 2013 conference and expo paper 2606. 15p.

Regenspurg S., Wiersberg T., Brandt W., Huenges E., Saadat A., Schmidt K and Zimmermann, G. (2010). Geochemical properties of saline geothermal fluids from the in-situ geothermal laboratory Groß Schönebeck (Germany). Chemie der Erde – Geochemistry 70, suppl. 3, 2010. p3-12.

Roberge P.R. (2000). Handbook of corrosion engineering. McGraw-Hill ISBN 007-076516-2; 1140p.

Richter S., Hilbert L.R. and Thorarinsdottir R.I. (2006) On-line corrosion monitoring in geothermal district heating systems. I. General corrosion rates. Corrosion Science 48(2006), p1770-1778.

Richter S., Thorarinsdottir R.I. and Jonsdottir F. (2007). On-line corrosion monitoring in geothermal district heating systems. II. Localized corrosion. Corrosion Science 49(2007), p1907-1917.

Roberts C. (2008). Water pipe leakage from erosion corrosion. Subrogator Magazine.

Scientific Drilling – product sheet

Sander R. (2014). Compilation of Henry's law constants, version 3.99. Atmospheric chemistry and physic discussions 14, 29615–30521, 2014, 907p.

Sanjuan B., Millot R., Dezayes Ch. and Brach M. (2010). Main characteristics of the deep geothermal brine (5 km) at Soultz-sous-Forêts (France) determined using geochemical and tracer test data, CR. Geosci. 342(2010) p546–559.

Sanyal S.K. (2005). Classification of geothermal systems – a possible scheme. Proceedings 30th workshop on geothermal reservoir engineering, Stanford University. 8p.

Salmiento Klapper H., Bäßler R., Saadat A. and Asteman H. (2011). Evaluation of suitability of some high-alloyed materials for geothermal applications. NACE Corrosion 2011 Conference & Expo paper 11172.

Scheiber J., Seibt A., Birner J., Genter A. and Moeckes W. (2013). Application of a scaling inhibitor system at the geothermal power plant in Soultz-sous-Forêts: Laboratory and on-site studies. EGC 2013 conference, 3-7 June 2013, Pisa, Italy. 10p.

Schmidt A.P. (2000). Naturally occurring radioactive materials in the gas and oil industry. Origin, transport and deposition of stable lead and 210Pb from dutch gas reservoirs. PhD Thesis, Utrecht University.

Schmidt A.P., Hartog F.A., Van Os B.J.H. and Schuiling R.D. (2000). Production of 210Pb from a Slochteren Sandstone gas reservoir. Applied Geochemistry 15(9), pp1317-1329.

Schillmoller C.M. (1989). Selection of corrosion-resistant alloy tubulars for offshore applications. 21st Annual offshore technology conference, Houston, Tx, USA, May 1-4, 1989. 11p

Schumacher S. and Schulz R. (2013). Effectiveness of acidizing geothermal wells in the South German Molasse Basin. Geothermal Energy 1 p1-11.

Schröder H., Teschner M., Köhler M., Seibt A., Krüger M., Friedrich H.-J. and Wolfgramm M. (2007). Long term reliability of geothermal plants – Examples from Germany. Proceedings European Geothermal Congress 2007 Unterhaching, Germany, 30 May-1 June 2007. 5p.

Seibt A., Hoth P. and Naumann D. (2000). Gas solubility in formation waters of the North German Basin – implications for geothermal energy recovery. Proceedings World Geothermal Congress 2000 Beppu - Morioka, Japan, May 28 - June 10, 2000. 6p.

Sizeland E. (2014). Ultrasonic devices improve gas leak detection in challenging environments. World Oil october 2014 p133-135.

Stober I. (2014). Hydrochemical properties of deep carbonate aquifers in the SW German Molasse basin. EGW 2014 3rd European Geothermal Workshop, Karlsruhe, Germany, 15-16 October 2014. 4p.

Sully J.R. and Taylor D.W. (1987). Electrochemical Methods of Corrosion Testing, Metals Hand Book. Vol 13.

Tanupabrungsun T., Young D., Brown B and Nešić S. (2012). Construction and verification of pourbaix diagrams for $CO_2$ corrosion of mild steel valid up to 250°C. NACE corrosion 2012 Conference and Expo, paper C2012-0001418, 16p.

Ungemach P. and Turon R. (1988). Geothermal well damage in the Paris Basin: A review of existing and suggested workover inhibition procedures. SPE paper 17165, SPE Formation Damage Control Symposium, Bakersfield, CA, Feb. 8-9, 1988.

Ungemach P. (2001). Handling of corrosion and scaling shortcomings in low enthalpy geothermal environments. European Summer School on. Geothermal Energy Applications, Oradea, Romania, p113-127.

Ungemach P., Antics M. and Papachristou M. (2005). Sustainable geothermal reservoir management. Proceedings of the World Geothermal Congress 2005, Antalya, Turkey, 24-29 April 2005. 12p.

Verweij, J.M. (2006) Carbon dioxide in natural gas accumulations in onshore and offshore Netherlands. TNO Report (www.nlog.nl), 07.2006.

Waard C. de (-).http://cdewaard.home.xs4all.nl/#CO2. Accessed 2015-01-27.

A. D. McNaught and A. Wilkinson (eds.) (1997). The IUPAC Compendium of Chemical Terminology, 2nd ed. Blackwell Scientific Publications, Oxford

Wolfgramm M. and Seibt A. (2008). Zusammensetzung von Tiefenwässern in Deutschland und ihre Relevanz für geothermische Anlagen. GtV-Tagung Karlsruhe 2008, p503–516.

Wolfgramm M., Thorwart K., Rauppach K. and Brandes J. (2011). Zusammensetzung, Herkunft und Genese geothermaler Tiefengrundwässer im Norddeutschen Becken (NDB) und deren Relevanz für die geothermische Nutzung. Z. geol. Wiss. 39 Heft 3-4 p173-193.

Wolfgramm M., Rauppach K. and Thorwart K. (2011). Mineralneubildungen und Partikeltransport in Thermalwasserkreislauf geothermischer Anlagen Deutschlands. (New mineral formations and transport of particles in the thermal water loop of geothermal plants in Germany). Z. geol. Wiss. 39.

Zhang X. and Kermen E (2013). Specifications and design criteria for innovative corrosion monitoring and (downhole) sensor systems, including sensitivity analysis, CATO-2 Deliverable WP3.4-D16, 2013

Zhang X.G. (2011). Galvanic corrosion. in: Uhlig's Corrosion Handbook, Third Edition, Edited by R. Winston Revie, John Wiley & Sons, Inc.

# 11     List of abbreviations

| | |
|---|---|
| CCS | carbon capture and storage |
| DSA | dimensional stable anode |
| DSK | dimensional stable kathode |
| EIS | electrochemical impedance spectroscopy |
| EN | electrochemical noise |
| EOR | enhanced oil recovery |
| Ep | pitting potential |
| Er | repassivation potential / electrical resistance |
| ESP | electric submersible pump |
| GWR | gas water ratio |
| HA | harmonic analysis |
| LPR | linear polarisation resistance |
| M | molair |
| MFL | magnetic flux leakage |
| OCP | open circuit potential |
| wt% | weight percent |
| pCO2 | partial $CO_2$ pressure |
| pH | measure of the acidity or basicity of an aqueous solution |
| ppm | parts per million |
| PREN | pitting resistance equivalent number |
| SEM | scanning electron microscope |
| SHE | standard hydrogen electrode |
| SCC | stress corrosion cracking |
| TD | total depth |
| TDS | total dissolved solids |
| TKS | total key species |
| ZRA | zero resistance ammeter |

*Corrosion in Dutch geothermal systemsCorrosion in Dutch geothermal systems*

# A    Pourbaix diagrams

This appendix was copied from TNO report R11416 'Lead deposition in geothermal installations' by P.M.M.C. Bressers and F. Wilschut.

Pourbaix diagrams, also known as a potential/pH diagrams, show the possible stable equilibrium phases of a specific aqueous electrochemical system at a set temperature (mostly at 25°C). In other words, for a given mixture of chemical compounds (e.g., iron in water, or iron and carbon dioxyde in water), at a given temperature, it predicts the stable phases (solid or in solution), for varying pH and electric potential.

Predominant ion boundaries are represented by lines. Each line corresponds to an equilibrium reaction. As such, a Pourbaix diagram can be read much like a standard phase diagram with a different set of axes. Similarly to phase diagrams, they are completely based on thermodynamics and therefore do not give information about reaction rates or kinetic effects.

All Pourbaix diagrams used in this report are drawn up for aqueous solutions at 25°C[21] showing the potentials with respect to the standard hydrogen electrode (NHE). In all diagrams two diagonal (dashed) lines marked (a) and (b) delineate the area in which water is thermodynamically stable. The area below the line marked (a) is where water will be reduced and hydrogen gas will be formed. Depending on the pH of the electrolyte the corresponding reaction can be written as:

$$2\text{H}^+ + 2e^- \leftrightarrow \text{H}_2(\text{g}) \tag{1}$$

or

$$2\text{H}_2\text{O} + 2e^- \leftrightarrow 2\text{OH}^- + \text{H}_2(\text{g}) \tag{2}$$

The corresponding equilibrium potential for these reactions can be written as:

$$E_0 = 0.000 - 0.591pH - 0.0295\log(p_{H_2}) \quad (\text{V}) \tag{3}$$

The area above the line marked (b) in the Pourbaix diagram is where water will be oxidized and oxygen gas will be formed:

$$2\text{H}_2\text{O} \leftrightarrow \text{O}_2 + 4\text{H}^+ + 4e^- \tag{4}$$

Since this is an equilibrium, it also indicates the strength of oxygen as an oxidizing agent. The corresponding potential for this equilibrium is:

$$E_0 = 1.228 - 0.0591pH + 0.0147\log(p_{O_2}) \quad (\text{V}) \tag{5}$$

As an example, Figure A.1 shows the Pourbaix diagram of iron (Fe) in water at 25°C. Iron is chosen as an example since it is a main component of any Dutch

---

[21] 25°C, or 298K, is the reference temperature for which Pourbaix diagrams are directly available. Specific Pourbaix diagrams for other temperatures can be generated with specialized software.

geothermal installation. Besides the already mentioned (a) and (b) lines indicating the water stability there are several other equilibrium lines visible. The diagram shows that metal iron is not a stable phase over the complete pH range from −2 to +16. In an acidic environment (pH < 7) iron will oxidize to form $Fe^{2+}$ (lines numbered 23) while at more alkaline conditions the hydroxide $Fe(OH)_2$ is formed (line marked 12). Above pH 14 (irrelevant for the Dutch situation) $HFeO_3^-$ can be found.

The diagram also indicates which phases are solid in **bold**, and which are dissolved in the aqueous solution in normal font. At lower pH the stable phase $Fe^{2+}$ will be dissolved in the solution, while at higher pH the iron hydroxide phase will form a (passive) film on the iron substrate.

The diagram also shows, on the vertical axis, that when a potential is applied to the system, either by an external power supply or through the presence of other electrochemical active species, other iron phases can be in equilibrium. At low pH and at higher potentials the $Fe^{2+}$ will oxidize further to $Fe^{3+}$ and at higher pH $Fe(OH)_2$ can be oxidized to $Fe(OH)_3$.
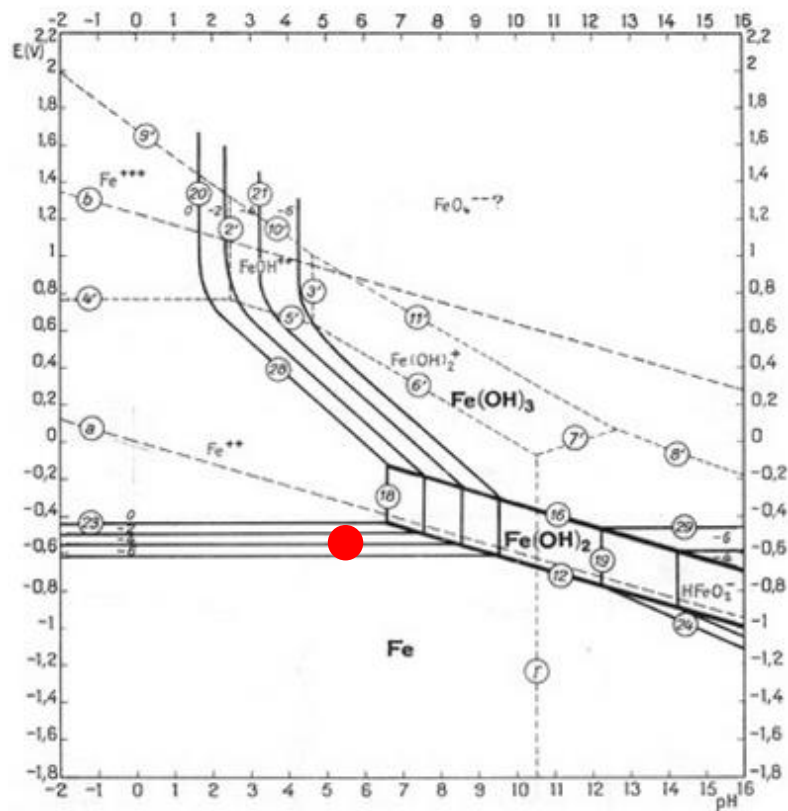


Figure A.1 Pourbaix diagram for the system iron-water, at 25°C.

The red dot in the Pourbaix diagram indicates the situation for iron in a brine (at 25°C) with a pH between 5 and 6. In this case we assume absence of an external power supply. The diagram shows that in this pH region the iron metal phase is instable as it is below the reduction potential of water. In other words, due to the reduction of water (equation 1) the iron can be oxidized (lines 23):

$$Fe \rightarrow Fe^{2+} + 2e^- \tag{6}$$

*Corrosion in Dutch geothermal systemsCorrosion in Dutch geothermal systems*

In the diagram this equilibrium potential is indicated by reaction 23 and four parallel lines marked 0, −2, −4 and −6. This number indicated refers to the logarithmic concentration of $Fe^{2+}$ in the solution. The parallel lines show the change in equilibrium potential upon the concentration of $Fe^{2+}$ in the electrolyte. The potential corresponding to the line for a concentration of 1 M of $Fe^{2+}$ (marked with the value 0) is referred to as the standard equilibrium potential which is −0.44V versus NHE.

In the presence of $CO_2$, which occurs in most Dutch doublets, the Pourbaix diagram looks slightly different (Figure A.2); instead of iron hydroxide $Fe(OH)_2$, iron carbonate siderite ($FeCO_3$) is formed at negative potential and high pH.
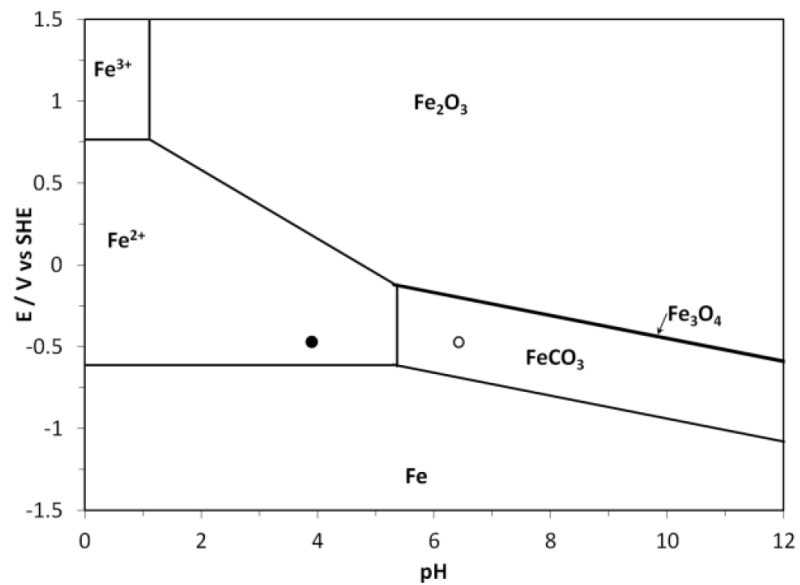


Figure A.2 Pourbaix diagram for $Fe-CO_2-H_2O$ system at 80°C, 10ppm $Fe^{2+}$, 10 ppm $Fe^{3+}$, 1 bar $H_2$, 1 bar $O_2$ (Tanupabrungsun et al. 2012).

*Corrosion in Dutch geothermal systemsCorrosion in Dutch geothermal systems*

# B    Nernst equation

The Nernst equation (and the relevant standard equilibrium potential determined from the Pourbaix diagram) is used to calculate the equilibrium potential or half-cell potential at a given concentration and temperature, which is the driving force for electrochemical reactions:

$$E = E^0 + \frac{RT}{nF}\ln(a_{ox}) \qquad (7)$$

In which:

- $E$     half-cell or equilibrium potential at the temperature of interest;
- $E^o$    standard equilibrium potential;
- $R$     universal gas constant: $R = 8.314 J/(K*mol)$;
- $T$     absolute temperature (K);
- $a$     chemical activity/concentration for the relevant species (mol/l);
- $F$     Faraday constant: $F = 96485 C/mol$;
- $n$     number of electrons transferred in the half-reaction.

As an example we look again at the iron case described above and calculate the half-cell potential at a temperature of 80°C (353K) and an $Fe^{2+}$ concentration of 0.2g/l which is the maximum concentration as observed for the Slochteren formation water (Table 1). As shown in the previous paragraph the standard equilibrium potential determined from the Pourbaix diagram of ion in the relevant pH range is −0.44V vs NHE for the reaction shown in Equation 6. Since two electrons are involved in this reaction n equals 2. The concentration of the oxidized species ($Fe^{2+}$) can be calculated using the molecular weight of iron (55.8g/mol). The 0.2g/l corresponds to 3.6e-3mol/l. Since in this case the reduced species is the solid state iron we can neglect it's concentration and re-write the Nernst equation to:

$$E = E^0 + \frac{RT}{nF}\ln(a_{ox}) \qquad (8)$$

Using the above values the equilibrium potential at 80°C and 0.2g/l $Fe^{2+}$ is calculated to be −0.526V vs NHE.

# C Tafel plots

Tafel plots can be used to estimate corrosion rates. Using Tafel plots (also named i-V or current-potential diagrams) can routinely be constructed in an experimental setting of an electrolyte (e.g. casing metal) in a brine by applying a potential difference and measuring the electric current. Tafel plots have a relation with Pourbaix diagrams, because they share the open circuit potential axis – vertical in the Pourbaix diagram, horizontal in the Tafel plot.

The basic principle is that an electrolyte in a brine in rest, i.e., the <u>net</u> electrical current is 0, has an equilibrium potential which is not 0. In this state the anodic current (which dissolves the metal) is equal to the cathodic current. When the potential is changed, either to more positive or more negative potentials, the net current will not be 0 anymore.
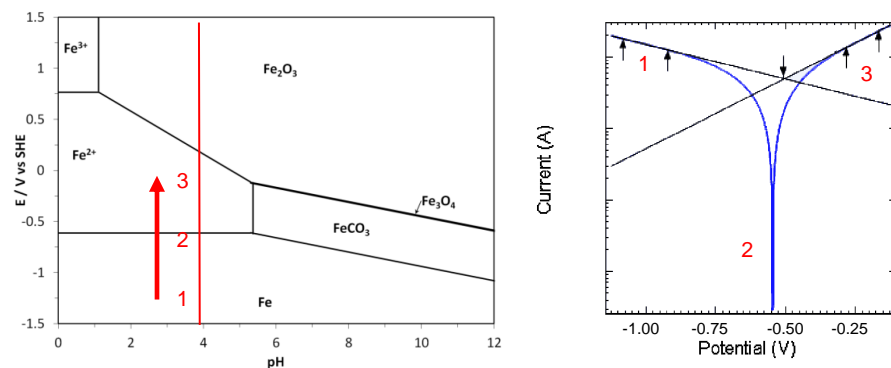


Figure C.1 Relation between Pourbaix diagram and Tafel plot (Pourbaix diagram adapted from Tanupabrungsun, Tafel plot adapted from Metrohm Autolab B.V. application note 'Measurement of corrosion rates'). Note the logarithmic scale for the current.

Moving along a constant pH trajectory upwards in the Fe-$CO_2$-$H_2O$ Pourbaix diagram (red line) means moving from left to right in the Tafel plot along the blue line. The technical description below was adapted from the website for the Dissemination of IT for the Promotion of Materials Science (DoITPoMS) that is maintained by the University of Cambridge (www.doitpoms.ac.uk).

- (1) Metal Fe is stable on this location in the Pourbaix diagram (having an open circuit potential of -1 V), , so metal ions in solution would deposited on the metal. The metal acts as a cathode (electron donor). This corresponds to the cathodic (left) branch of the Tafel plot.
- (2) Both the metal Fe and its ions $Fe^{2+}$ are equally stable at equilibrium (about -0.6 V). Corrosion and deposition reactions run at the same rate. The net current is zero. The Tafel plot forms an asymptote.
- (3) $Fe^{2+}$ ions are stable relative to the metal Fe above the horizontal Fe – $Fe^{2+}$ equilibrium line,. Therefore the metal acts as anode (electron acceptor) and corrodes.

When the corrosion current has been measured experimentally for various potentials and both were plotted in the diagram, it is possible to construct the two tangent lines shown at locations 1 and 3 in the Tafel plot (between the arrows).

The intersection of the two lines determines the corrosion current. The corrosion current flow can be converted to mass flow using Faraday's Law when realizing that the strength of electric current is directly proportional to the amount of electrons removed from metal Fe. For each two electrons, a single $Fe^{2+}$ ion is removed from the metal.